The Role of MicroRNAs in Endothelial Progenitor Cell Function

John Behbahani

Thesis submitted to the Faculty of Graduate and Postdoctoral Studies
in partial fulfillment of the requirements for a degree of Doctor of Philosophy
in Cellular and Molecular Medicine

Department of Cellular and Molecular Medicine
Faculty of Medicine,
University of Ottawa

© John Behbahani, Ottawa, Canada 2016

ABSTRACT

Cultures of peripheral blood mononuclear cells (MNCs) give rise to at least two different variants of endothelial progenitor cells (EPCs), early and late outgrowth EPCs. We investigated whether microRNAs in early and late EPCs could serve as markers of internal processes that can be exploited to distinguish cell identity and functional capacity. We hypothesized that as MNCs give rise to early and late EPCs, there is a gradual change in total microRNA profile, reflecting a total change in processes within the predominant cell population. Using a candidate microRNA array, early and late EPCs showed vastly different microRNA expression profiles. MiR-146a expression increased progressively as early EPCs emerged around 5-7 days ($p<0.05$). Through targeting TRAF6 and IRAK1, miR-146a conferred inflammatory tolerance in early EPCs, likely contributing to their purported ability to suppress inflammation. MiR-146a knock down (KD) in endotoxin-stimulated early EPCs reduced anti-inflammatory cytokine IL-1RA ($p<0.001$), and increased expression of pro-inflammatory cytokines IL-1β ($p<0.001$) and IL-8 ($p<0.01$). Interestingly, the microRNA expression profile of late EPCs was highly congruent to mature endothelial cells, with 100-fold greater miR-126 expression than monocytes and early EPCs ($p<0.01$). MiR-126KD in late EPCs abolished matrigel-network formation ($p<0.05$); while overexpression (OE) in early EPC augmented network formation ($p<0.05$) and chemotactic migration ($p<0.001$). We also found that the melanoma cell adhesion molecule or MCAM (CD146) identified late EPC precursors. Only $MCAM^{+}$MNCs from adult blood (<5% of total MNCs) yielded late EPC-like colonies. Robust miR-126 expression in these cells predicted the generation of late EPCs. Overall, our results suggest that miR-146a in early EPCs likely contributes to repair by suppressing inflammation during cardiovascular injury; while in late EPCs, miR-126 directly promotes angiogenesis and vascular repair. Finally, we highlight a unique method for the efficient generation of late EPCs by using MCAM selection and screening for miR-126.

ABBREVIATIONS AND DEFINITIONS

AcLDL	Acetylated low-density lipoprotein
BrdU	Bromodeoxyuridine, 5-bromo-2'-deoxyuridine
Cardiac patient	Patient with/recovering cardiovascular complications; ie: Myocardial infarct
CCASP3	Cleaved caspase-3
CD206	Mannose receptor
CD209	Dendritic cell-specific intercellular adhesion molecule-3-grabbing non-integrin
DAPI	4',6-diamidino-2-phenylindole
DC	Dendritic cell
DMSO	Dimethyl sulfoxide
Early EPC or simply “EPC”	Early outgrowth endothelial progenitor cell, circulating angiogenic cell (CAC)
EBM	Endothelial basal media
ECFC	Endothelial colony forming cell, aka late EPC
EGM	Endothelial growth media
ELCC	Endothelial-like colony forming cells (and all similar cells like CFU-Hills and late EPCs)
eNOS	Endothelial nitric oxide synthase
EPC	Endothelial progenitor cell
ERK	Extracellular signal-regulated kinase
FAM-	Fluorescein fluorophore
FGL2	Fibrinogen-like protein 2
HEK	Human Embryonic Kidney 293T Cells

HELA	HeLa adenocarcinoma cell line
HPF	High power field
HUVEC	Human umbilical vascular endothelial cells
IGF1	Insulin-like growth factor 1
IL-1/IL1-RA	Interleukin-1/Interleukin 1 receptor antagonist
IL-8	Interleukin 8
IL4	Interleukin 4
IRAK1	Interleukin-1 receptor-associated kinase 1
KD/OE	Knockdown (via microRNA inhibitor)/Overexpress (via mimic)
KDR	Kinase insert domain
Late EPC	Late outgrowth endothelial progenitor cell
LPS	Lipopolysaccharide, an endotoxin
MACs	Magnetic-activated cell sorting
MCAM	Melanoma cell adhesion molecule
MNC	Mononuclear Cell(s)
MRE	MicroRNA response element
NFKB	Nuclear factor kappa-light-chain-enhancer of activated B cells
NFKB/p50	Nuclear factor NF-kappa-B p105 subunit
NFKB/p65	Nuclear factor NF-kappa-B p65 subunit/ Transcription factor p65
NO	Nitric oxide
O.D.	Optical density, absorbance
PBS	Phosphate buffered saline

PI3KR2/p85b	PI3K regulatory subunit 2/p85 beta subunit
RasGAP	p120-Ras GTPase activating protein
SDF1	Stromal cell-derived factor 1
SPRED-1	Sprouty-related, EVH1 domain-containing protein 1
TLR	Toll-like receptor
TRAF6	TNF receptor-associated factor 6
VEGF	Vascular endothelial growth factor
VEGFR2	Vascular endothelial growth factor receptor 2

ACKNOWLEDGEMENTS

First off, I would like to thank Dr. Duncan Stewart. Despite having one of the busiest schedules of anyone I know, Dr. Stewart always took the time, even for a rushed 10-minute meeting, to provide insight and direction for my work. For this genuine effort, I am truly grateful. I learned a lot about how to "be in the zone" from Dr. Stewart. Most importantly, I am grateful for the opportunity to learn under the guidance of such a prolific scientist.

Next, I would thank Dr. David Courtman. Throughout my years as a graduate student I have had numerous one-on-one chats with Dr. Courtman, both in and outside of the laboratory. It is pretty clear that he's more than just knowledgeable about science. Once you get past the outer shell, he's a remarkably genuine and kind-hearted person. I am thankful for his sincerity, valuable knowledge and perspective.

Most importantly, I would like to thank my friends who have been central to my enjoyment and well-being during for grad school. I've often said that it is the company of good friends that make long journeys worthwhile; and this was certainly a journey that needed friends. Throughout grad school I've met and worked with some of the brightest and interesting group of people, including EH, LC, AP, MSA, WC, JV, AB, WF, WC, WW, TD, BZ, HG, SR, FB, CAJ, CSG, MS, SA, SK, MF, NB, ABU and SAP. I will never forget any of them.

Finally, I would like to give my heartfelt thanks to my family and our dog Bandit. They have always provided me with encouragement and motivation to keep moving forward. In science it really just boils down to "moving forward". If you get caught up in failures you'll stagnate, and with stagnation comes absence of discovery. Science is discovery, so keep moving forward.

TABLE OF CONTENTS

LIST OF TABLES

LIST OF FIGURES

LIST OF APPENDICES

CHAPTER I - INTRODUCTION

1.1 The Endothelium

The arterial wall is layered into three sections: the tunica intima, tunica media and the tunica adventitia. These layers refer to the innermost layer (which is exposed to circulation), the middle and the outermost layers, respectively. The tunica intima consists of the endothelium and the internal elastic lamina. The internal elastic lamina plays a major role in determining vessel elasticity. For instance, in conditions such as atherosclerosis, calcification of the internal elastic lamina contributes to the hardening of the arteries (1). The tunica media consists of a smooth muscle layer which functions to moderate arterial tone. Relaxation and constriction of the smooth muscle layer is influenced by crosstalk between the endothelial layer and local factors. Adjacent to the smooth muscle layer there is an external layering of elastic lamina (the external elastic lamina). Similar to the internal elastic lamina, the external elastic lamina also contributes to the elastic properties of the artery. Finally, the tunic adventitia consists primarily of the connective tissues (including collagen, fibronectin and cells like fibroblasts, for example), which are involved in vessel insulation, tissue repair and physical support.

The endothelium is a monolayer of endothelial cells, which line the innermost layer of blood vessels in the circulatory system and the lymphatic system. As such, the endothelium directly interacts with blood and lymph, as well as the cells, which circulate within these systems. The endothelium serves a key role in vascular tone, blood fluidity and platelet aggregation (2). Additionally, the endothelium is a major actor in the regulation of immunology, angiogenesis, and inflammation. The endothelial cells which constitute the endothelium control blood flow by regulating vascular tone through the synthesis and release of both relaxing (vasodilating) and contracting (vasoconstricting) factors such as nitric oxide, lipoxygenases, endothelin, adenosine, purines etc. (2).

Of these factors, nitric oxide (NO), which is produced nitric oxide synthase (NOS) enzymes, is a very well-known chemical compound that serves many important biological functions from maintaining vascular integrity by inhibiting platelet aggregation (2-4) to leukocyte-endothelium adhesion and vascular smooth muscle cell proliferation (5-7). Dysfunction of the endothelium that can disturb the release (or absorption) of such vasoactive components could result in cardiovascular pathology or the perpetuation of cardiovascular disease. Therapeutic approaches to remedy endothelial dysfunction at this level include applications of cell therapy, which can facilitates vasodilation while supressing inflammation (in cases of cardiovascular injury, for instance). This, in turn, promotes circulation (and distribution of reparative factors) into sites of injury or ischemia, thereby improving recovery and health.

1.2 Angiogenesis

Angiogenesis is the highly regulated process of the formation of microvascular networks from pre-existing vessels. Both blood and lymphatic vessels undergo angiogenesis to form extensive networks, which are essential to normal physiological processes involving the transport of cells, gases, fluids, micro and macromolecules. As such, angiogenesis plays a pivotal role in cardiovascular recovery or tissue repair following injury or chronic illness. Inducers of angiogenesis include angiopoietins, stromal cell-derived factor 1, tumor necrosis factor-alpha, interleukins, and members of the vascular endothelial growth factor (VEGF) family. As such, angiogenesis continues to be an important putative target for therapy (8). As a highly regulated process, angiogenesis is typically under a tight balance of pro- and antiangiogenic agents; usually turned on only for brief periods and then completely inhibited (9).

Endothelial cell migration is essential to angiogenesis. The motility of endothelial cells requires the activation of numerous signalling pathways resulting from chemotaxis (cell migration toward a gradient of soluble chemoattractants), mechanotaxis (directional migration generated by mechanical forces), or hepatotaxis (migration towards a gradient of immobilized ligands), eventually affecting cytoskeletal remodelling (10). The end result is endothelial cell motility that is achieved through cell extension and contraction (which resembles a cell pushing its rear towards the front and progressing forward). This process is essential in the formation of new blood vessels during vascularization and the extension of existing vessels during angiogenesis; because during this process endothelial cells must migrate (under the influence of VEGF) onto a matrix of collagen and hyaluronan to fuse with angioblasts in the formation of blood islands which later remodel into tubular structures, vascular plexus and ultimately new blood vessels (11). However, in addition to migration, endothelial cell proliferation is also a critical feature during these processes. As a vessel grows, the emerging endothelial cells begin to proliferate into emerging tubules, but this process is dependent on their adhesion onto the existing scaffolding matrix. It has been demonstrated that proliferation can be co-coordinately affected by both growth factor and integrin signalling pathways. During vessel growth, the release of factors like VEGF has been shown to enhance proliferation and the expression of several integrins that are involved in angiogenesis including $\alpha_v\beta_3$, $\alpha_v\beta_5$, and $\alpha_5\beta_1$ integrins (11-13). The $\alpha_5\beta_1$ integrin is essential in endothelial cell anchorage onto fibronectin; as noted in section 1.1, fibronectin is one of the chief scaffolding glycoproteins in blood vessels. Conversely, in the absence of VEGF endothelial cells have been shown to undergo apoptosis, resulting in the regression of blood vessels (14).

1.3 Endothelial progenitor cells

Repair of damaged endothelium was previously thought to occur mainly through local mitosis of

healthy neighboring endothelial cells (15). However, this view has since been changed to include the repair of endothelium by circulating endothelial progenitor cells (EPCs) in addition to local endothelial cells (16, 17). Since their discovery in 1997 by Asahara et al., EPCs have emerged as a "hot topic" among both clinicians and researchers because of their therapeutic potential (17). EPCs have been shown to be effective in facilitating neoangiogenesis and vascular repair in numerous studies on cardiovascular injury, including atherosclerosis, post-myocardial infarction and even re-endothelialization of vascular grafts (18-23). It has been shown that *in vivo*, these circulating progenitor cells originate in the bone marrow and are mobilized in response to cardiovascular injury, growth factors or in response to stimuli such as ceramide-1-phosphate and NADPH oxidase Nox2 (24, 25). EPCs circulate within the mononuclear cell (MNC) fraction of peripheral blood and home to injured sites where some cells are incorporated into new blood vessels *in situ* and thereby facilitate the formation of new blood vessels; or they facilitate the extension of existing vessels (Figure 1), forming structural components of growing vasculature (26, 27). Circulating EPCs have been defined by surface markers, such as CD34, CD133 and KDR (17, 18); however, as yet there is no consensus concerning what markers define a subset of "true" endothelial cell precursors.

In vitro, EPCs are generated from mononuclear cells and exist in two distinct varieties. For the first type, unselected peripheral blood mononuclear cells (PBMCs or MNCs) are cultured for 5-7 days on an appropriate matrix (i.e. fibronectin) in the presence of endothelial growth factors (i.e. VEGF, IGF, EGF, etc.), resulting in a population of highly angiogenic cells exhibiting classical "early EPC" rod-like morphology, and these are termed early outgrowth EPCs or circulating angiogenic cells (CACs). These early EPCs still express monocyte markers, such as CD14 and CD45, but also show some endothelial characteristics by expressing CD31, lectin binding and uptake of acetylated low density lipoprotein (LDL) (28). Early EPCs are non-

proliferating and fade gradually during prolonged culture. However, after 2 weeks of mononuclear cell culture, clusters of highly proliferative cells appear with cobble-stone morphology and these cells are termed late-outgrowth EPCs, endothelial colony forming cells (ECFCs) or blood-outgrowth endothelial cells. These cells rapidly overgrow culture and replace early EPCs over time (29). Late EPCs (short for late outgrowth EPCs), in addition to having robust endothelial morphology, have high expression of endothelial markers CD31, VE-cadherin and KDR. These two types of culture-derived "EPCs" contribute to vascular repair and regeneration *in vitro* and *in vivo*, but appear to do so by very different mechanisms (30). Early EPCs act mainly through paracrine mechanisms, such as releasing of pro-angiogenic cytokines; whereas late outgrowth EPCs are believed to promote repair of the endothelium through direct integration into damaged vasculature (28, 30). To date, it is widely accepted that both cell populations arise from the MNC fraction of peripheral adult blood, but the relationship between these two types of EPCs is very unclear. Specifically, it is not known whether late outgrowth EPCs arise from mononuclear cell cultures by an infrequent transdifferentiation event or from a very rare subset of distinct endothelial precursor cells that exists within the general mononuclear (early EPC) cell population that are "pre-programmed" to give rise to endothelial cells. Therefore, we were interested in comparing the profiles of a major new class of epigenetic regulators of gene expression (namely microRNAs) in mononuclear cell populations at different stages of EPC specification to gain new insights into the mechanisms underlying the activity and function of early EPCs and late outgrowth EPCs.

1.4 EPCs in cardiovascular injury and repair

In vivo studies which have focused on the use of EPCs for treatment of ischemic injury (in small animals) have provided considerable evidence of their therapeutic potential. In a rodent model of hind limb ischemia,

human circulating EPCs have been shown to improve perfusion and neovascularization (i.e. formation of new blood vessels where previously none existed) (31). Numerous models of myocardial ischemia in animals have shown that angiogenesis and arteriogenesis (the increase of existing vessel diameters) are significantly improved following the mobilization of EPCs from the bone marrow, promoting the recovery of both left ventricular ejection fraction and myocardial perfusion (20, 32-35). These effects have also been shown through the direct administration of bone marrow-derived MNCs. In the ischemic limb model, intramuscular injection of MNCs derived from bone marrow increased exercise tolerance, limb flow and the total increase in the number of capillaries as well as augmentation of both small and large vessel formation, including enhancement of collateral development (36-38). It is likely that MNCs are particularly responsive to ischemia as it has been demonstrated that even the hypoxic culture of MNCs significantly improves the effect of cell delivery to the ischemic limb (36). In both rat and pig models of myocardial ischemia, implantation of these cells has also been shown to improve myocardial angiogenesis and subsequently, perfusion (39-42). Combined, these findings have formed part of the premise for numerous clinical trials for myocardial infarction and ischemia.

1.5 Clinical relevance of EPCs for therapy

Today, there is a large body of preclinical evidence supporting the therapeutic potential of bone marrow-derived cells in stimulating neovascularization (43). It has been shown that tissue ischemia releases chemokines (such as vascular endothelial growth factor and stromal-cell derived factor 1), which correlate with increased mobilization of circulating EPCs from the bone marrow and their engraftment into ischemic tissue where they are believed to participate in neovascularization (20, 32, 44-51). Additionally, EPCs also secrete stromal-cell derived

factor 1 (SDF-1), a factor involved in recruiting CXCR4 positive stem and progenitor cells to injured tissue (49, 52).

Though the preclinical evidence pointing to the neovascularization ability of EPCs is robust, the interpretation of all the relevant studies on the effects of these cells is complicated by the use of various cell types, doses and disease models (32, 46, 51, 53). Nonetheless, both culture-derived early and late EPCs have shown considerable ability to promote neovascularization (32, 46, 54). Crucially, a number of studies have confirmed that fully differentiated mature endothelial cells, though phenotypically similar to late EPCs, lack the ability to induce neovascularization to the same therapeutic effect (32, 46, 55). These findings suggest that although late EPCs strongly resemble mature endothelial cells, they must retain critical progenitor cell properties that are essential for their regenerative activities. However, their relationship to the monocyte-like early EPCs is unclear, and at present there is no consensus on markers that can be used for the selection of the exact MNCs, which are destined to become therapeutic early or late EPCs (from the initial population of circulating MNCs).

The homing of EPCs to the sites of ischemic injury has been largely attributed to the SDF-1/CXCR4 agonist-receptor system, which is intimately involved in governing the trafficking of circulating EPCs from the bone marrow to ischemic tissue (50, 56, 57). *In vitro* and *in vivo* studies have shown that SDF-1 (a factor released during ischemic injury) stimulates EPC chemotaxis (58, 59) through the activation of the CXCR4 receptor (60). Protease-activated receptor-1 (PAR-1) agonists have been shown to increase the angiogenic capabilities of EPCs by upregulating SDF-1 and CXCR4 (52); and conversely, impairment of CXCR4 signalling with neutralizing antibodies against CXCR4 in healthy human EPCs and heterozygous knockout mice has negated this effect (61). NO and caveolin have also been shown to regulate CXCR4 expression and activity. Both are also involved in angiogenesis through the enzyme endothelial nitric oxide synthase, or eNOS (62, 63). ENOS is produced by

vascular endothelial cells and is critical in regulating vascular tone; and in cardiovascular repair, by promoting leukocyte adhesion and endothelial cell proliferation (64). Given that eNOS plays a pivotal role in angiogenesis and endothelial health, this system is likely involved in the reparative activity of EPCs. At least one study has shown that treatments such as Wortmannin, which target inhibitors of the VEGF-PI3K/Akt-eNOS pathway, promote EPC-mediated recovery following coronary artery ligation in mice (65). Other naturally occurring biological factors have also been identified, such as microRNAs, which may similarly promote the VEGF/eNOS pathway by also targeting pathway inhibitors like PI3K (66).

1.6 Indirect mechanism of action of EPCs

The proangiogenic activity of EPCs is achieved, in part, through paracrine mechanisms that involve the secretion of growth factors such as insulin-like growth factor-1 (IGF-1), hepatocyte growth factor (HGF), VEGF, NO and SDF-1 (49, 67). It is likely that these factors facilitate repair of damaged tissue by stimulating adjacent cells, but these alone are unlikely to explain all the regenerative actions of EPCs. It is also possible that other mechanisms such as engraftment and differentiation in new endothelial cells or immune modulatory interactions with inflammatory cells play an important role as well (67-69). At the very least, our lab has demonstrated that the mechanism of action of early EPCs in preventing the establishment of pulmonary arterial hypertension in a rat model was in part mediated through an immune-regulatory mechanism (70). It is also possible that other factors are released by EPCs such as microRNAs, which are responsible for what guides/generates late EPCs (*in vitro*) from an unknown and rare circulating cell and this could play a role in their ability to stimulate neovascularization and endothelial repair *in vivo*. In recent years, both microparticles and the much smaller exosomes have been

implicated in mediating the biological transfer of cell excretions (71). Where exosome are known primarily for transport of smaller components like microRNAs, microparticles harbor a broader spectrum of potentially useful bioactive substances including cytokines, signaling proteins, mRNAs and importantly, microRNAs (71, 72). A key difference in the transfer of microRNAs in exosomes versus microparticles is that within microparticles, microRNAs are encased and protected within the RNA-induced silencing complex (RISC); whereas in the latter, they are not (71).

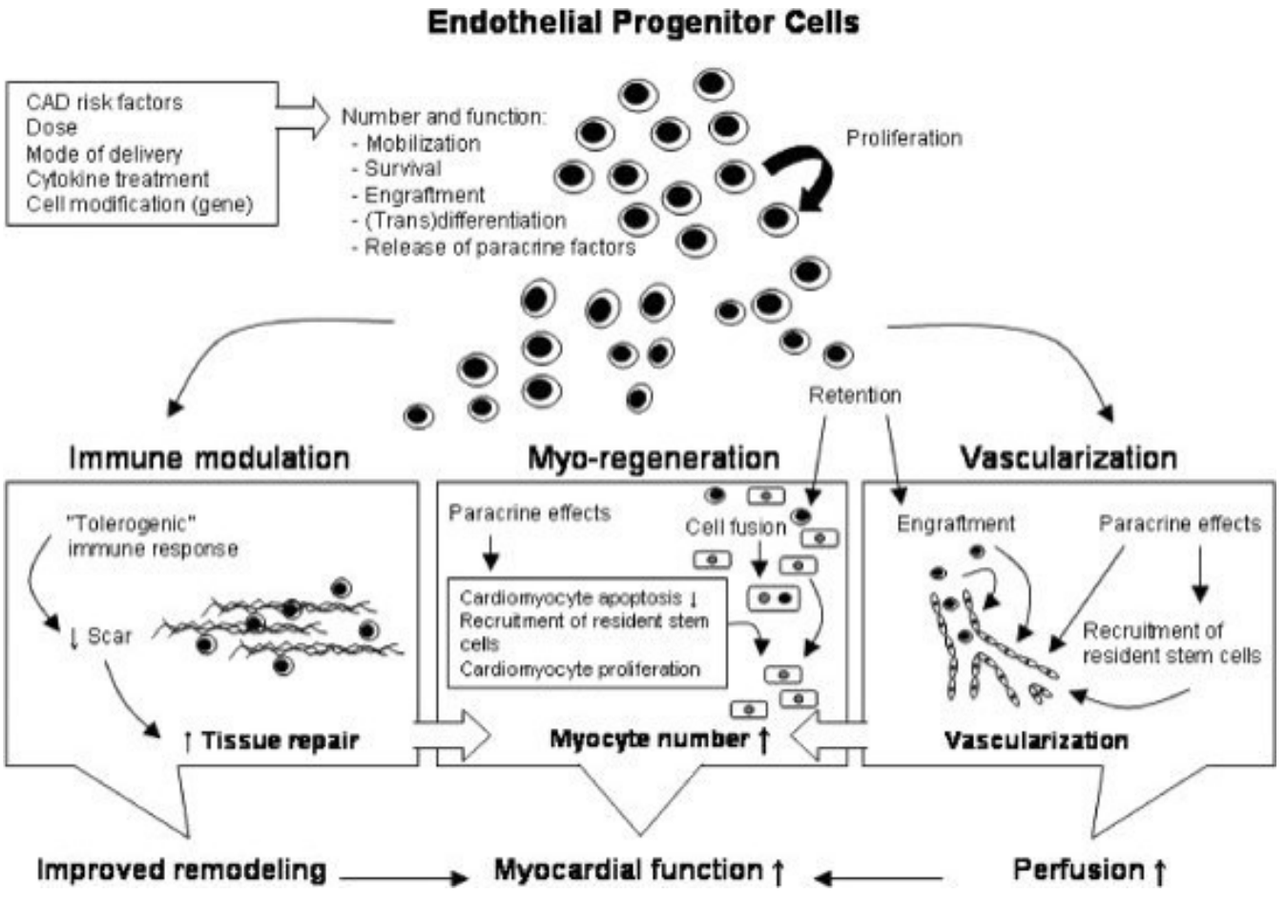

Figure 1: Mechanism theory of EPC facilitated repair and regeneration

Repair of cardiovascular injury using EPCs is believed to occur through three chief mechanisms: Immune modulation, facilitation of tissue regeneration and neovascularization. After homing to sites of injury, early EPCs stimulate neovascularization through paracrine stimulation or incorporation into neovessels. Scarring from injury could be reduced by the ability of EPCs to modulate immune response to injury. Obtained with permission from Ward et al. (2007).

1.7 MicroRNAs

MicroRNAs (miRNAs or miRs) are short 20-24 nucleotide long ribonucleic acids (RNA) that are typically found in eukaryotic cells which post-transcriptionally regulate the expression of a target gene. MicroRNAs were first discovered in *Caenorhabditis elegans* in 1993 as single-stranded regulators of mRNA, and are now identified as important controllers of angiogenesis (73-76). As with protein-coding genes, type II RNA polymerase generally transcribes microRNAs, subjecting them to both positive and negative regulation at the transcriptional level (77). In general, microRNAs are transcribed as separate non-coding units, though many consist of polycistronic clusters which contain multiple microRNA transcripts that initially emerge as primary microRNAs. Endoribonucleases Drosha/DGCR8 processes these primary microRNA transcripts in the nucleus prior to export (via exportin-5) to the cytoplasm as a pre-microRNAs. A second endoribonuclease Dicer then processes the pre-microRNAs, cleaving the looped end, producing mature single stranded microRNAs (77). Some microRNAs are coded in introns and arise from the processing of excised introns of protein-coding genes (78). Typically microRNAs emerge as two strands, a guide and a passenger strand. MicroRNA passenger strands are labeled with a star (*) indicating the less predominant microRNA strand; but if the abundance of both strands is uncertain, each microRNA strand is just denoted with a -5p or -3p as specifically indicating the 5' or 3' arm of the surviving microRNA duplex (79). The guide strands of microRNAs confer most of the regulatory functions and are protected in an RNA-induced silencing complex, while the passengers are not, and are usually degraded quickly, serving minimal regulatory functions (79, 80). In plants, microRNAs possess perfect complementarity through classical Watson-Crick base- pairing with the target mRNA 3'UTR region, resulting in mRNA cleavage and destruction (81, 82). In animals however, microRNAs have imperfect complementarity with target mRNA 3'UTR, causing mRNA blockade and

subsequent inhibition of translation (83). This imperfect complementarity allows a single microRNA to have multiple targets, increasing potential pathway interactions and their complexity for study. As such, microRNAs are assigned "predicted" targets based on computational algorithms, and then the sequences are confirmed using biochemistry techniques for validation such as reporter assays. In general, the probability of a microRNA-target interaction is greatest when the complementarity is evolutionary conserved (meaning there is consistency in complementarity across several species); and when the sequence length of the microRNA/mRNA complementarity is longer as designated by a #mer number (8 being highest). Additionally, microRNAs can be exported out of the cell to affect neighboring cells or other cells through circulation (74). As such, they can be found both in the interstitium and plasma (75). It has been estimated that there are greater than 3000 different human microRNAs which regulate the expression of ~60% of all proteins (84), thereby governing a wide variety of cell processes including growth, survival, differentiation and senescence (85). In endothelial cells, microRNAs play an important role in regulating genes involved in angiogenesis. A good example is miR-126, which promotes angiogenesis by regulating downstream mediators of VEGF signalling, while other microRNAs (i.e. miR- 221/222) have shown inhibitory effects on angiogenesis (66, 86). As such, these molecules are of great interest for future therapeutics and for understanding gene expression in somatic and stem cells.

1.8 MicroRNAs and immune regulation

Myeloid-derived cell populations such as monocytes, granulocytes, dendritic cells and macrophages recognize unique signaling molecules associated with pathogens and released by damaged/activated tissues (87-90). These signaling molecules are recognized by surface or intracellular receptors of immune cells such as

Nod-like or Toll-like receptors (TLR). Once bound, they initiate a cascade of intracellular events leading to the production and release of proinflammatory cytokines, reactive oxygen/ nitrogen species, chemokines,

MicroRNA	Targets	Effects
miR-9	NF-κB1	Negative regulator of TLR4 signaling
miR-19	TLR2	Decreases TLR2-mediated inflammation
miR-21	PDCD4, IL-12 p35	Negative regulator of TLR4 signaling
miR-27b	PPAR-γ	Enhances response to LPS
miR105	TLR2	Decreases TLR2-mediated inflammation
miR-106a	IL-10	Decreases IL-10
miR125b	TNF-α; IRF4	Diminishes inflammation; enhances macrophage activation
miR-145	TIRP	Inhibits TLR signaling
miR-146a	TRAF6, IRAK1, IRAK2	Negative regulator of TLR signaling
miR-155	AID; MyD88; TAB2; Pellino-1; IKKε; SHIP-1; SOCS1; C/EBP-β	Enhances inflammation; negative feedback regulation
miR-223	IKKα; Pknox1	Proinflammatory activation of macrophages
Let-7i, let-7e	TLR4	Downregulate inflammatory signaling

Table 1: MicroRNAs in innate immunity.

Select list of microRNAs with immune-mediating targets and noted effects. Adapted from Liu et al. (2013).

antimicrobial peptides and promote enhanced phagocytic activity (88-90). Stimulation of these pattern recognition receptors is required for efficient activation of T lymphocytes and development of specialized adaptive immunity for clearance of infection and cell debris (91). Inappropriate inflammatory activation or chronic activation can lead to host tissue damage and pathology (92). Maintenance of homeostasis of the immune system, with an appropriate balance of response and resolution of inflammation is therefore essential for host health and survival. As such,

inflammatory pathways are subjected to both positive and negative regulatory control that fine-tunes an optimal immune response (80, 89, 93).

One important pathway, which we focused on in this thesis, was the canonical TLR4/NFKB signalling pathway. The TLR4 receptor has a variety of known ligands including polysaccharides, viral proteins, and heat shock proteins. However, the most well known TLR4 ligand is endotoxin or lipopolysaccharide (LPS). The TLR4 receptor is responsible for activating the innate immune system through two pathways: the MyD88 (myeloid differentiation primary-response protein 88)-dependent and MyD88-independent pathways. Both of these TLR signalling pathways culminate in activation the nuclear factor-kappaB (NFKB) transcription factor, which controls the gene expression of numerous inflammatory cytokines. Upon TLR activation, MyD88 interacts with the death domains of members of the IL-1 receptor-associated kinase (IRAK) family, causing phosphorylation of IRAK4 and IRAK1, which dissociate from MyD88, interacting with TRAF6 (a E3 ubiquitin ligase) and causing lys63-linked polyubiquitation of TRAF6 itself and NEMO (94, 95). The ubiquitinated NEMO and TRAF6 recruit a protein complex that activates two distinct pathways involving the IKK complex and the mitogen-activated protein kinase (MAPK/ERK/JNK, p38) pathway (96). Activation of the IKK complex results in the phosphorylation of the IKB and its ubiquitination and proteasmal degradation, freeing NFKB/Rel complexes. Post-translational modifications such as phosphorylation, acetylation and glycosylation further activate the NFKB/Rel complexes, causing translocation to the nucleus where they induce target gene expression (either alone or in concert with other transcription factors)(97). The presence of NFKBp50/NFKBp65 within the nucleus thereby indicates the activation of the TLR4/NFKB inflammatory pathway. Alternatively, in the noncanonical NFKB pathway, there are inactive NFKB/Rel complexes in the cell cytoplasm and signalling through other receptors like CD40 and BR3 (B-cell activating factor 3) activate the kinase NIK (NFKB-inducing kinase), which then activates the IKK complexes that phosphorylate C-terminal residues in NFKBp100 which leads to its

ubiquitation and ultimately proteasomal processing to NFKB2/p52 (98). This creates the transcriptionally competent NFKBp52/RelB complexes, which then translocate into the nucleus to induce target gene expression.

There is growing evidence to suggest that microRNAs act as important regulators of immune-development and response (92, 99-103). Several studies suggest that microRNAs may be important biomarkers of uncontrolled inflammation and related pathology (99-102). To this end, a growing list is emerging of microRNAs that act as important regulators of immune response and adaptive immunity, including macrophage polarization with implications on wound repair and tumor progression; a summary of microRNAs involved in innate and adaptive immunity are provided in Table 1 and Table 2 (104).

Numerous microRNAs have been implicated in activated immune cells. For instance, miR-146a has been implicated in inflammatory response to both bacterial and viral infections (105, 106). Lipopolysaccharide stimulated human monocytes rapidly upregulate miR-146a via TLR4 receptor signaling, which acts as in a

MicroRNA	Targets	Effects [increase/decrease]
miR-10	Ncor2; Bcl6	Treg [increase]
miR-17-92	Bim; PTEN	CD4 T-cell proliferation [increase]
miR-29b	T-bet; IFN-γ	Th1 [decrease]
miR-146a	IRAK1; TRAF6; Stat1	TCR signaling [decrease]; Treg [increase]
miR-155	c-Maf	Th1 [increase]; Th17 [increase]; Treg survival [increase]; Th2 [decrease]
miR-181a	SHP1, 2; DUSP5, 6	TCR Signaling [increase]
miR-182	Foxo1	CD4 T-cell expansion [increase]
miR-301a	PIAS3	Th17 [increase]
miR-326	Ets	Th17 [increase]
miR-150	c-Myb	B1 cell expansion [decrease]
miR-155	PU.1; SHIP-1; AID	Antibody secretion [increase]; class-switch recombination [increase]
miR-181		B-cell expansion [increase]

Table 2: MicroRNAs in adaptive immunity.

Select list of microRNAs with immune-mediating targets, and noted effects. Adapted from Liu et al. (2013).

negative feedback loop to depress TLR signaling by targeting tumor necrosis factor receptor-associated factor 6 (TRAF6) and interleukin receptor-associated kinase (IRAK1) (107, 108). As such, miR-146a upregulation is suspected as an essential component of endotoxin tolerance in innate immune response, while decreased induction may be associated with prolonged inflammation (109). In macrophages, miR-146a acts as a negative regulator of vascular stomatitis virus-induced type 1 interferon response (106). Mice with miR-146a deficiency in their T regulatory (Treg) cells, as well as miR-146a knockouts, develop hypersensitive macrophage response to LPS-stimulation and life-long autoimmune disorders (110, 111). Treg cells with deficiencies in miR-146a undergo breakdown of immunologic tolerance as manifested by lethal IFN-gamma-dependent immune-mediated lesions (110). It has been speculated that this is the result of augmented activation and expression of signal transducer and activator of transcription 1 (Stat1), a purported target of miR-146a (80, 110).

1.9 MicroRNAs in cardiovascular health, repair and endothelial progenitor cell function

Since their discovery, microRNAs have been studied closely over the past decade for exploratory research into their physiological roles. To date, numerous microRNAs have been implicated in roles, which greatly impact cardiovascular pathology and hold potential for endothelial progenitor cells in repair.

There is a growing body of evidence implicating miR-221 and miR-222 in coronary artery disease (CAD). Zhang et al. observed reduced expression of miR-221/222 in patients with CAD who were treated with the lipid-lowering drug, atorvastatin (112). Atorvastatin was also reported to markedly increase the numbers of circulating early EPC in patients while lowering miR-221/222 (113). This correlated observation was later confirmed by a separate group as it was shown miR-221 significantly reduces proliferation of bone marrow-derived EPCs (114).

Using computational target prediction software, it was identified that miR-221 directly targets PAK1 a regulator of cell motility and proliferation in EPCs under hypoxic conditions, further linking miR-221 to suppression of early EPC proliferation (114). In contrast, a study comparing healthy and diabetic patients found that miR-130a expression directly correlated to EPC proliferation (115). Meng et al. reported that the expression of Runt-Related Transcription Factor 3, RUNX3 (an important regulator of transcription) is under repressive control by miR-130a. This group showed that suppression of miR-130a in EPCs resulted in increased RUNX3 mRNA and protein expression in treated cells, reducing the formation of colonies significantly (115). Another documented microRNA implicated in EPC proliferation is miR-126. In zebrafish, Fish et al. first identified miR-126 as an activator of the vascular endothelial growth factor (VEGF)/eNOS signalling by direct targeting of PIK3R2 and SPRED-1, both of which serve as repressors of this critical angiogenic pathway (66). The role of miR-126 in EPC function is still poorly understood, however numerous reports have suggested an important role in the regulation of proliferation. Key findings in studies on miR-126 in human EPCs have primarily focused on diabetes and preeclampsia. Meng at al. identified that in diabetic patients with comparatively dysfunctional late EPCs, overexpression of miR-126 (targeting SPRED-1) resulted in improved colony formation in addition to augmenting proliferation and migration, while decreasing apoptosis (116). Similarly, in preeclampsia, late EPC number and function is typically diminished compared to healthy controls (117). Yan et al. reported significantly lower miR-126 in late EPCs from preeclampsia patients and that in these cells, overexpression of miR-126 (targeting PIK3R2) increased proliferation, differentiation, migration and colony formation by regulating PI3K-AKT signalling (117).

The 3'UTR region of SDF-1 mRNA contains a predicted microRNA response element (MRE) for miR-126 (118). Under healthy *in vivo* conditions, endothelial cells express robust miR-126 compared to other microRNAs, but this robust expression is diminished under ischemic conditions or injury (119). *In vitro* suppression of miR-126 has a reciprocal effect on the expression and function of SDF-1 in endothelial cells,

which is a factor that is actively secreted by injured endothelial cells. Reportedly, increased SDF-1 in injured endothelial cells causes increased mobilization of progenitor cells towards the non-lineage and stem cell progenitor states (Sca-1+/Lin-), facilitating the repair of damaged cardiovascular tissue (119). The homing of EPCs towards sites of injury is also thought to be mediated by changes in Rac1/2 expression, which is a pleiotropic regulator of cell cycle, differentiation, motility, cell-cell adhesion as typically utilized during normal endothelial repair (120). Shen et al. demonstrated that the expression of Rac1/2 is directly affected by SDF-1α through an unknown mechanism, which may indicate another important link between EPCs and SDF-1 in cardiovascular repair (120). In the spleen, it has been reported that the recruitment of EPCs is achieved through the SDF-1/ CXC chemokine receptor 4 (CXCR4) axis (121). This axis is implicated in VEGF-mediated mobilization of bone marrow-derived cells during repair (122). Rolland-Turner et al. demonstrated that CXCR4 expression negatively correlates with miR-150 expression in early EPCs, causing a reduction in reparative potential (123). However, this group found that treatment with nucleoside adenosine reduced miR-150 expression, thus augmenting CXCR4 and enhancing early EPC migration (123). Similarly, ischemia reduces miR-150 expression in early EPCs, thereby increasing CXCR4 and cell homing to ischemic sites (124). Predictive computational analysis from numerous databases including targetscan.org, and miRbase.org identify CXCR4 as a direct target of miR-150, and thus supports these findings (125). Collectively, these studies suggest that under healthy normal physiological conditions, mature endothelial cells have robust expression of miR-126 which under normal conditions silences SDF-1 and enhances angiogenesis through the VEGF/eNOS pathway (by targeting PIK3R2 and SPRED-1); while early EPCs have higher expression of miR-150 which targets and suppresses CXCR4. However the expression of these microRNAs changes upon injury. Upon cardiovascular injury or ischemia, miR-126 and miR-150 expression is reduced in endothelial cells and early EPCs (respectively). This effect increases SDF-1 in injured endothelial cells and CXCR4 in early EPCs,

promoting mobilization and recruitment of early EPCs to the site of cardiovascular injury, promoting repair (123-125).

The role of microRNA in the interaction of injured endothelium with circulating EPCs is believed to be mediated, in part, by microparticles. Deregibus et al. have recently reported that microvesicles released by EPCs are indeed internalized by injured endothelial cells, and this in turn accounts for the horizontal transfer of various RNAs, promoting angiogenesis (126). Microparticles released by EPCs have been shown to improve angiogenesis in resident renal cells (126). Activation of angiogenesis in human pancreatic islet endothelium has been reported using microparticles containing proangiogenic miR-126 (127). It has been suggested that direct targeting of SPRED-1 by miR-126 in late EPCs affects RAS/ERK signaling and in turn, affects late EPC proliferation. As such, EPC function may also be regulated through Ras/ERK signaling under the control of miR-126 (128, 129).

1.10 Overview of thesis

Despite a growing body of evidence supporting the efficacy of early and late EPCs in promoting angiogenesis and vascular repair, there is no consensus concerning whether early EPCs and late outgrowth EPCs are in fact related cell types, and if so, in what way. For example, do late outgrowth cells arise from early EPCs by a rare differentiation event, or are late EPCs derived from a rare committed precursor cell type that exists within the initial mononuclear cell pool? The elucidation of such questions will allow for better ways to harness the therapeutic potential of these cells and allow for the development of more efficient approaches for the generation of otherwise cumbersome adult late outgrowth EPCs for therapeutic applications (and allowing for more

mechanistic studies on the role of these cells in promoting angiogenesis). Since microRNAs are now established as having profound roles in controlling numerous processes related to cell function, we sought to investigate the functional roles of microRNAs in early and late EPC outgrowth, particularly on how microRNAs influence early and late EPC development and function. We postulated that microRNAs could provide valuable insight into the relationship between early and late EPCs and the processes occurring within these cell types, which reflects their therapeutic nature.

Chapter 3 Overview

Rationale:

This chapter is divided into two parts. In part one we measured *change* in microRNA expression profiles using a candidate microRNA array of thirteen relevant microRNAs as circulating MNCs *gradually* gave rise to early and late EPCs. Measuring microRNA profiles at multiple time points allowed us to correlate the gradual change in profile during differentiation of early and late EPC. In part two, we performed an unbiased global gene and microRNA array between early EPCs and late EPCs, providing a greater breadth of insight into absolute differences between these cell types.

Part 1 hypothesis:

As MNCs give rise to early and late EPCs, there is a gradual change in total microRNA expression profile which reflects a total shift in predominant cell population and the processes occurring within the remaining cell types.

Part 2 hypothesis:

Early and late EPCs will express distinct microRNA expression profiles that reflect differences in biological activity and may provide new insights into the relationships between these cell types and the

mechanisms underlying the origins of late EPCs from MNCs and early EPCs.

Chapter 4 Overview

Rationale:

Our results from the expression profiling study uncovered a number of key findings. Firstly, in early EPCs the predominant microRNA species expressed was miR-146a, a regulator of intracellular inflammatory response. Since it is believed that early EPCs have an indirect therapeutic mode of action partially mediated through immune modulatory mechanisms (70, 130), we postulated miR-146a is involved in the anti-inflammatory therapeutic nature of early EPCs. Our rationale considered the evidence that miR-146a regulates TLR4 signaling response in numerous myeloid-differentiated cells like macrophages and dendritic cells. As such, we queried whether miR-146a functioned in a similar manner in early EPCs.

Hypothesis:

MiR-146a represents a key regulator of the immune modulatory activity of early EPCs by terminating the pro-inflammatory response to sustained cytokine stimulation and reducing NFKB activation.

Chapter 5 Overview

Rationale:

A second finding from the expression profiling study was that late EPCs express a unique microRNA expression profile compared to MNCs and early EPCs, which strongly resembles that of

mature endothelial cells (having very high expression of miR-126). As noted earlier, miR-126 has been shown in numerous studies to confer pro-angiogenic activity. Since late EPCs are thought to mediate vascular repair through direct integration into the endothelium and engraftment, we postulated that miR-126 plays a key role in the specification of an endothelial phenotype.

Hypothesis:

The high expression levels of miR-126 in late EPCs is indicative of endothelial differentiation and confers direct angiogenic activity. Moreover, to the extent that late EPCs may arise from early EPCs, over expression of miR-126 in early EPCs will promote endothelial differentiation and angiogenic potential.

CHAPTER II: MATERIAL AND METHODS

a) Tissue processing, early and late EPC culture

Leaukapheresis (the product of isolated blood leukocytes using apheresis) is rich in white blood cells which contain monocytes, and these are what are believed to become EPCs. In all experiments, early and late EPCs were generated from human adult leukapheresis that was conducted using a Cobe Spectra (Gambro BCT, Denver CO), which was taken from the adult peripheral blood of healthy participants and prepared as described (131). Up to 3-12 billion leukocytes enriched with monocytes (10-25% total) were generated using this process. For culture, leukapheresis product was washed and diluted four fold in PBS and ficoll density gradient centrifugation was used to consolidate a monocyte-enriched buffy coat layer (Ficoll Histopaque 1077, Sigma), which was isolated and used for cell culture purposes. For our candidate array, processed MNCs were plated at a density of $0.5x10^6$ cells/cm^2 at 1, 3, 5, 7, and 9 days for early EPCs on human fibronectin (Roche Applied Science, Indianapolis, IN)-coated flasks (Figure 2). For later experiments, only day 5 early EPCs were used. Cell culture medium consisted of endothelial cell basal medium supplemented with 20% human serum and endothelium growth factors with antibiotics (EGM2-MV, Cambrex, cat. No. CC-3202 –instead of FBS from the kit, we used human serum from Wisent Cat. No. 022-210). After three days, non-adherent cells were removed with old media and fresh culture medium was supplied. Change of medium occurred every other day. Morphology was assessed daily using phase light microscopy. Late EPCs are cultured for >21 days (on non-fibronectin-coated flasks). An exhaustive list of materials can be found in the supplemental chapter. A time-lapsed video showing the generation of EPCs can be found in the following links: https://goo.gl/kRZbaM and https://goo.gl/ilpS4f

b) Early and late EPC characterization using immunofluorescence

For characterizing EPCs, the generated early and late EPCs were characterized to confirm uptake of fluorescein-labeled Ulex europaeus (UEA-1) lectin-binding (Vector, FL 1101) as well as 1,1'-dioctadecyl-3,3,3',3'-tetramethyl indocarbocyanine perchlorate-labeled acetylated low- density lipoprotein (AcLDL, Life Technologies L-3484) uptake as described (*114*). Briefly, cells were grown on 2 chamber coverslips (Nunc Lab-Tek II slides, 154526) that were pre-coated with fibronectin. For permeabilization and intracellular imaging, cells were permeabilized using 0.1% Triton-X100, and then fixed using fresh 2% paraformaldehyde (PFA). Afterwards, the slides were mounted following manufacturer's protocol using Vectashield-dapi media (Vector labs H-1200). This mounting media contained DAPI (4',6-diamidino-2-phenylindole). Dried, mounted slides were then imaged using fluorescence microscopy (Nikon C1, Champigny-sur-Marne, France).

c) Characterization of early and late EPC markers using flow cytometry

In addition to immunofluorescence for characterization, we performed flow cytometric analysis using an Attune acoustic focusing cytometer (Applied Biosystems) on early and late EPCs. Analysis was done using Flowjo Single Cell analysis software (version 10). For every $1.5x10^6$ cells, the following amount of antibodies were used for study: 10µL monocytic marker CD14 (cat. 555398), 5µl pan-leukocyte receptor CD45 (cat. 555483), 10µl melanoma cell adhesion marker CD146 (cat. 562135), 10µl mature endothelial marker CD31 (cat. 555482), 15µl vascular endothelial growth factor receptor, CD309/VEGFR2 (cat. 560494) and 10µl of appropriate isotype controls to establish gating parameters. Isotype controls were all PE-conjugated (BD Pharmigen) and selected to reflect the candidate IgG subclass. For early EPCs, we confirmed $CD14^+$, $CD45^+$, $CD31^+$ as well as lectin binding and AcLDL uptake; and for late EPCs, $CD14^-$, $CD45^-$, $CD31^+$, $CD146^+$, lectin binding and AcLDL uptake as well. All antibodies used were monoclonal, PE-conjugated and purchased from BD Pharmigen. We

followed methodologies as described (*115*). Briefly, prepared cells harvested using TrypLE (Invitrogen, Burlington, ON) and washed and placed into flow cytometry test tubes (BD Pharmigen, WG27) at a density of 1-5x10^5 cells per assay tube containing 100 μL flow buffer (PBS with 5% FBS). If were to be used within 2 days, they were fixed using a 4% formaldehyde solution for 10 minutes at 37ºC. The primary antibodies were applied and incubated following manufacturer's instructions. After incubation, cells were washed again, centrifuged and re-suspended in 2-3 mL flow buffer. After incubation, cells were washed again and re-suspended in 3 mL flow buffer prior to analysis on flow cytometer.

d) Total RNA extraction

To extract our RNA for study, prepared cells were quantified and separated (6.5 million) for total RNA extraction using manufacturer's protocol for the mirVana miRNA isolation system (Ambion, Austin, TX, USA) as described (132). Briefly, 2-5x10^6 early or late EPCs were detached from the cell culture flask using 600 μL denaturing lysis buffer (cell scraper used to scrape off remaining cells). Cell lysates were then mixed with miRNA homogenate additive, followed by an acid-phenol chloroform extraction. Following 10,000g centrifugation at 4 ºC, the aqueous phase was transferred into a new tube and mixed with one third the volume of 100% pure ethanol, and then passed through an RNA purification column. The resultant suspension was then washed 3 times with wash buffer, and the total RNA was eluted into 100 μL of preheated (95 ºC) elution solution. Extracted RNA was then frozen in elution solution at -80 ºC until study.

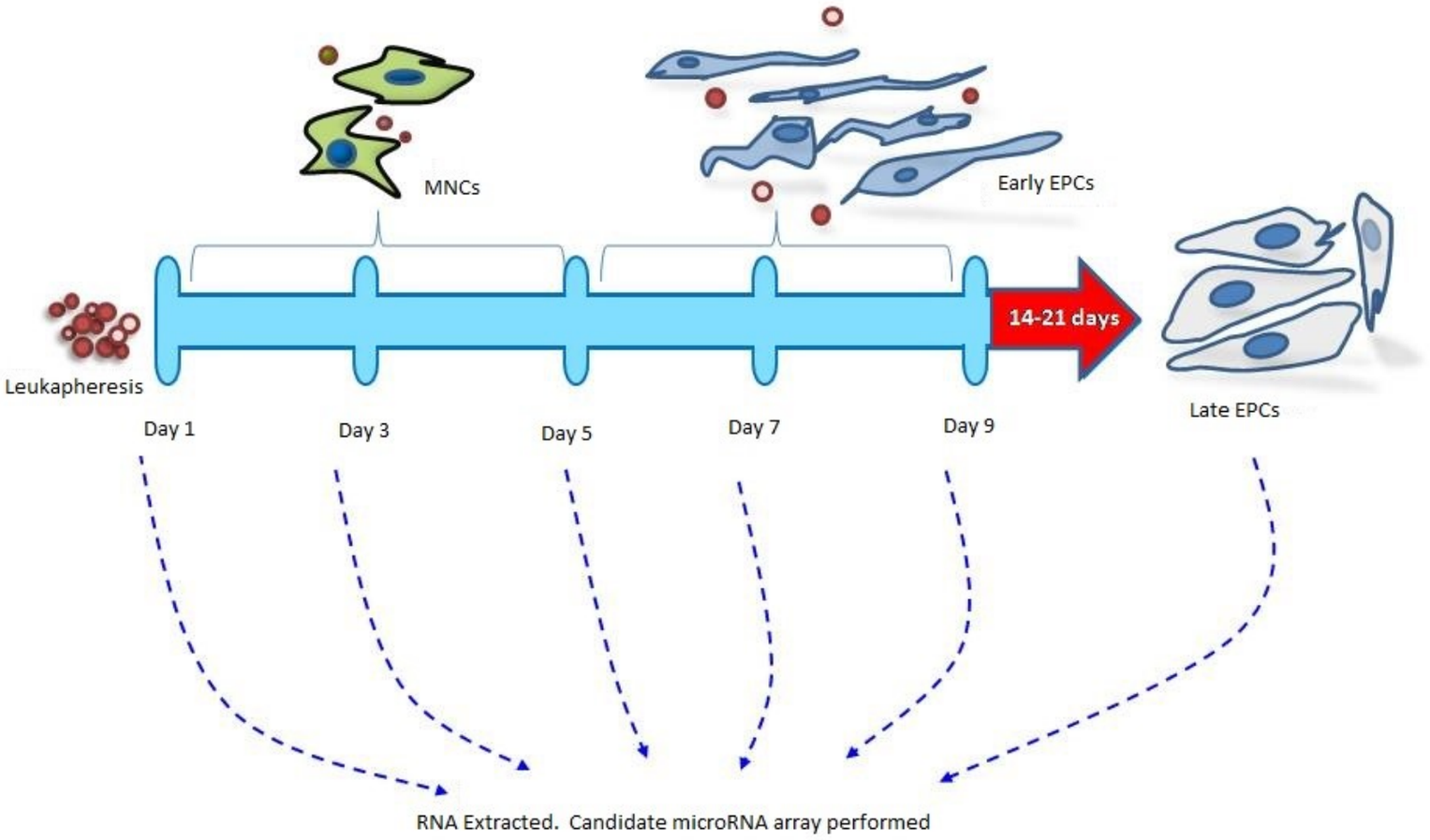

Figure 2: Cell culture timeline for each participant sample in the microRNA candidate array

Several flasks of cells were grown concurrently and lysed successively using the timeline shown. At each time point, RNA was extracted and analyzed for 13 candidate microRNAs. Time required for generation of late EPCs varied per participant but remained within 14-21 days in culture.

e) Reverse Transcription

For performing qRT-PCR, the TaqMan microRNA reverse Transcription Kit (Applied Biosystems Inc.) was used following manufacturer's protocol for reverse transcription (RT). Each reaction contained 0.15 μL

miRBase ID	Primer ID	Species	Sequence
hsa-miR-34a-5p	000426	Human/Mouse/Rat/	UGGCAGUGUCUUAGCUGGUUGU
hsa-miR-92a-3p	000431	Human/various	UAUUGCACUUGUCCCGGCCUGU
hsa-miR-126-3p	002228	Human/Mouse/Rat	UCGUACCGUGAGUAAUAAUGCG
hsa-mir-130a-3p	000454	Human/Mouse/Rat	CAGUGCAAUGUUAAAAGGGCAU
hsa-miR-132-3p	000457	Human/Mouse/Rat	UAACAGUCUACAGCCAUGGUCG
hsa-mir-146a-5p	000468	Human/Mouse/Rat	UGAGAACUGAAUUCCAUGGGUU
hsa-miR-155-5p	002623	Human/various	UUAAUGCUAAUCGUGAUAGGGGU
hsa-miR-424-5p	000604	Human/various	CAGCAGCAAUUCAUGUUUUGAA
hsa-miR-221-3p	000524	Human/Mouse/Rat	AGCUACAUUGUCUGCUGGGUUUC
hsa-miR-217-5p	002337	Human/various	UACUGCAUCAGGAACUGAUUGGA
hsa-miR-222-3p	002276	Human/Mouse/Rat	AGCUACAUCUGGCUACUGGGU
hsa-miR-503-5p	001048	Human/various	UAGCAGCGGGAACAGUUCUGCAG
hsa-miR-210-3p	000512	Human/Mouse/Rat/	CUGUGCGUGUGACAGCGGCUGA

Table 3: Primer IDs and sequences

MicroRNA sequences verified using miRBase.org database release 18-21. MicroRNAs species labelled "various" identify primer sequences applicable to a wider species range.

of 100 mM dNTP, 1.5μL of 10x RT buffer, 3μL of selected microRNA primer (Table 3), 1μL of Multiscribe™ reverse transcriptase, 20 ng of total RNA and nuclease-free H_2O (to adjust each reaction volume to 15μL). The RT cycle steps were 16 ºC for 30 minutes, 42ºC for 30 minutes, 85 ºC for 5 minutes.

f) Real-Time PCR

Real time PCR assays components were purchased from Applied Biosystems Inc. and were performed according to manufacturer's instructions. Each reaction was adjusted to a total volume of 20 μL containing: 2 μL of reverse transcription product 10 μL of 2x TaqMan universal PCR mastermix, 1 μL of 20x TaqMan microRNA assay primer and ddH_2O to adjust volume. Real time PCR was performed on a Bio-Rad CFX96™ Real Time PCR Detection System using the following stages: stage 1, 95 ºC for 10 minutes, stage 2, 95 ºC for 15 seconds and 60 ºC for 1 minute (repeated stage 2 for 40 cycles). The obtained Ct values were analyzed using the Livak ddCt, or $2^{(\Delta\Delta Ct)}$ method to obtain the relative expression levels of each microRNA (133). Expression values were normalized to the mean of the endogenous references RNU6B (U6) and RNU48 (U48). It should be noted that we tested three small nucleolar microRNAs for normalization, which included RNU44 (Appendix J), but subsequently removed RNU44 from all analysis due to its higher Cq.

g) Assessment of RNA purity and integrity for comprehensive global arrays

In addition to our candidate microRNA array, we conducted global gene and microRNA arrays using the Affymetrix GeneChip® Human Gene 2.0 ST and Affymetrix GeneChip® miRNA 3.0 arrays, following the manufacturer's instructions as described (134). Early and late EPCs were grown using the same process and

procedures as described. Total RNA was collected from early EPCs on days 1, 3, 5, 7, and 9 and late EPCs (per healthy participant). Following extraction, RNA purity was assessed using a nanodrop^{TM} spectrophotometer (with a minimum cutoff of 2-2.15 for 260/280). Total RNA was extracted from early and late EPCs of three males and three females (Figure 3) using the previously described procedure. We measured RNA integrity using an Agilent 2100 Bioanalyzer (Agilent Technologies) as described (135) and using a minimum RIN (RNA integrity number) of 7.0. After RNA quality and integrity was confirmed, the samples were prepared for arrays. For the global arrays, we only compared day 5 EPCs and late EPCs (as our results from our candidate array showed that day 5 was the optimal time point for early EPC predominance). The RNA for the unused days was stored for later experiments.

A

Prepared RNA Samples

Sample Number
260/280|260/230
RIN

Participant	Day 1	Day 3	Day 5	Day 7	Day 9	Late EPC
ENA124	1 2.09/2.02 8.6	2 2.08/2.13 9.1	3 2.07/1.84 8.90	4 2.08/2.02 7.10	5 2.07/1.89 8.30	6 2.10/1.99 9.40
ENA125	7 2.08/2.03 9.10	8 2.10/1.85 7.60	9 2.13/2.08 8.80	10 2.06/2.05 8.70	11 2.08/2.07 8.50	12 2.10/2.16 7.50
ENA126	13 2.09/2.02 8.90	14 2.09/2.09 7.50	15 2.07/2.03 9.20	16 2.02/1.64 N/A	17 2.00/1.25 N/A	18 2.05/2.13 9.80
ENA133	19 2.11/2.15 9.10	20 2.07/2.08 9.10	21 2.09/2.13 9.30	22 2.07/1.91 8.50	23 2.05/2.05 9.10	24 2.04/1.94 9.50
ENA134	25 2.09/1.63 8.30	26 2.08/1.99 8.50	27 2.09/2.09 9.50	28 2.07/1.75 7.40	29 2.05/1.82 5.00	30 2.08/2.21 9.50
ENA135	31 2.10/2.09 9.20	32 2.10/2.19 7.90	33 2.09/2.15 9.10	34 2.07/1.91 6.30	35 2.05/1.97 7.90	36 2.12/2.21 9.70

B

Patient ID	Affymetrix ID	Sex	Age	Date
ENA124	5756	Male	47	05-May-12
ENA125	5757	Female	24	06-Jun-12
ENA126	5758	Male	44	12-Jun-12
ENA133	5759	Female	53	09-Apr-12
ENA134	5760	Female	58	26-Apr-12
ENA135	5761	Male	61	June 6 2012

Day 5 Cells correspond to "early EPCs"
Late - Correspond to "late EPCs"

Figure 3: Tabulation of RNA and participant information for microarray

(A) RNA integrity and 260/280 values for RNA used in microarray. (B) Participant information for samples used in arrays.

h) Flashtag™ Biotin microRNA labeling

To prepare RNA samples for array, total RNA samples were labeled using reagents supplied in the Affymetrix Flashtag™ Biotin labeling kit (Affymetrix 901910) following manufacturer's protocol as described by Auer et al. (136). Samples where adjusted for volume consistency (8μL) prior to the addition of spike-in controls at a ratio of 4:1. Manufacturer supplied ATP mix was diluted in 1mM Tris at a dilution factor of 1:500 for total RNA. Poly-A-tail master mix was added at a ratio of 1.5 (of 10X Reaction Buffer and 25mM $MnCl_2$) to 1 (Diluted ATP Mix and PAP Enzyme). 5 mL of the prepared poly-A-tail master mix was added to 10 μL RNA/Spike-ins, totalling a volume of 15 μL. Afterwards the samples were heated to 37 ºC for 15 minutes and then placed on ice for 5 minutes. 5x Flashtag™ biotin ligation mix was then added in addition to T4 DNA ligase. Samples were incubated at RT for 20 minutes prior to the addition of stop solution (as supplied in the kit). The prepared samples were then run on the Affymetrix GeneChip® using the Human Gene 2.0 ST array platform.

i) TLR stimulation of early EPCs

For TLR4 stimulation of early EPCs, early EPCs were grown to day 5 (as discussed in our array studies) and treated with Escherichia coli lipopolysaccharides or LPS (Sigma, L6529-1MG) at a concentration of 100 ng/mL, 20 ng/mL of IL-4 (Peprotech, 200-04), or media as control for 24 hours as described (70). Noticeable changes in morphology (specifically, loss of elongated shape and size) occurred within 24 hours. Following 24 hours, media was changed and cells were imaged using a standard upright microscope (Nikon C1, Champigny-sur-Marne, France). Protein and/or RNA extraction was then performed using the methods described.

j) Protein extraction and Western blotting

Protein extraction and Western blotting was performed as previously described (131). Briefly, treated early EPCs were lifted from flask using TrypLE express (Life Technologies, 12605036) and spun at 300 g for 7 minutes. Cell pellet was lysed using Ripa buffer (Millipore, 20-188) supplemented with cOmplete protease inhibitors cocktail Tablet (Roche, 04693116001) as recommended in manufacturer's protocol. Resultant cell suspension was sonicated for 15 seconds, then centrifuged at 4 ºC degrees at 10,000g for 15 minutes. The supernatant was collected for western blotting. NuPAGE 4-12% bis-tris gel using MOPS buffer (Life Technologies, NP0321PK2) was used for electrophoresis, then transferred to PVDF membrane and probed with the specified antibodies. Antibodies against NFKB p105/p50 at 1:1000-3000 (Rb mAb,Cell Signaling, 3035S), eNOSIII at 1:100 (Rb pAb, Millipore, 07-520), TRAF6 at 1:5000 (Rb mAb Abcam, AB33915), IRAK1 1:2000 (Rb mAb, Cell Signalling, 4359s) and Erk1/2 at 1:5000 (Rb mAb, Cell Signalling 9102S) and β-actin antibody at 1:10000 (Ms mAb Sigma-Aldrich, A2228-200UL) were used. IRDye infrared secondary antibodies were used for detection of the above targets (Li-COR Odessy Infrared Imaging System, Li-Cor Biosciences, Guelph, ON). Unless otherwise stated, 20 μg of whole cell lysate was used per blot. Representative Western blots for loading control and comparisons of basal expression are included in Appendix K.

k) ELISA: Bromodeoxyuridine (BrdU) detection for proliferation

BrdU detection was performed using the CHEMICON BrdU detection kit (Millipore 2750) following the manufacturer's protocol as described (137). In brief, cells plated on a 96 well plate were seeded at $0.5x10^6$ cells/cm^2 until day 5 for early EPCs. Cells were then treated with microRNA mimic for over

expression (OE), scramble-miR or microRNA inhibitor for knockdown (KD). Following treatment, cells were treated with 1X BrdU for 24 hours. Afterwards, cells were washed three times, permeabilized, then fixed for 30 minutes at room temperature (RT). Subsequently, cells were washed three more times. BrdU detection antibody was added for 1 hour at RT, washed, and then peroxidase conjugate was added (as directed) for 30 minutes at RT, followed by another set of washes. TMB peroxidase substrate was added before BrdU was detected using PolarStar Omega optical density plate reader to measure absorbance at 450/550nm (BMG labtech, Germany). The detected BrdU was then compared to the scramble-miR transfected group.

l) ELISA: Cleaved caspase 3 measure for apoptosis

Cleaved caspase 3 activity assay was performed using human cleaved caspase-3 (Asp175) fluorescence-based immunoassay (R&D Systems KCB835) for apoptosis using manufacturer's protocol as described (138). In brief, cells were grown on a 96 well plate, seeded at $0.5x10^6$ cells/cm^2 until day 5 for early EPCs. Cells were then treated with microRNA mimic (OE) or microRNA inhibitor (KD). For treatment, the 96 well plate was centrifuged at 300 g at 4 degrees for 3 minutes. Cells were fixed with 4% PFA at RT for 20 minutes. Resultant cells were washed, quenched using supplied quenching buffer, and washed again using 1X wash buffer and 1X quenching buffer prior to 1 hour of blocking as per manufacturer protocol. Cells were incubated overnight with cleaved caspase 3 antibody. The following day, cells were washed, and secondary antibody was applied for 2 hours at RT. For control, GAPDH was used as supplied in the kit. Cells were washed a final time before addition of fluorescence substrates. The resultant plate was read using a PolarStar Omega multi-mode plate reader (BMG labtech, Germany); cleaved caspase 3 was recorded at 600 nm (excitation at 540 nm) and GAPDH was recorded at 450 nm (excitation at 360 nm). Resultant CCASP3 readings were normalized to GAPDH, and for analysis results were then normalized to scramble-miR transfected cells. Late EPCs were done

in a similar manner but grown to P3 (passage).

m) Quantitative analysis of cell adhesion using captured images

Following typical acquisition of cell images using standard microscopy, cells were enumerated using Image J software. Captured fields were randomly chosen per group and were counted in a blinded manner using various parameters: cell length, cell shape and symmetry as discussed in assessments of morphology (section (t)).

n) Detection of nuclear NFKBp65 activation by immunofluorescence

Early EPCs were grown to day 5 in 2 chamber coverslips (Nunc Lab- Tek II slides, 154526). On day 5, early EPCs were treated with miR-146a inhibitor or scramble-miR using the same methods previously mentioned. One extra slide of early EPCs was treated with LPS alone (100 ng/mL, overnight) for control. The next day, media was changed and the miR-146a inhibitor-treated cells were treated with LPS (100 ng/mL, overnight). Following treatment, cells were fixed using 4% PFA for 15 minutes at RT. Slides were blocked in 1X PBS/5% normal serum/0.3% Triton™ X-100 for 1 hour at RT followed by PBS washes. Primary antibody NFKBp65 (cell signalling 8242S) was used at 1:1000 overnight. The next day, slides were washed three times in PBS, and incubated in Alexa Fluor 488-conjugated secondary antibody (Life technologies, 1024116) for 1 hour at RT prior to washing and mounting. Images were captured using fluorescence microscopy (Nikon C1, Champigny-sur-Marne, France).

o) Assessing transfection of microRNA inhibitor using immunofluorescence and flow cytometry

To confirm total percent uptake and transfection efficiency, early EPCs were grown to day 5 in 75 cm^2 flasks and on 2 chamber coverslips (Nunc Lab- Tek II slides, 154526). Briefly, on day 5, early EPCs were transfected with 5'6-FAM-labeled miR-146a-5p inhibitor (at 5 pmol/1.75 cm^2 oligonucleotide) per 1.41 μL of total volume using Lipofectamine 2000 (Life Technologies, 11668027). Oligonucleotide details are provided in Table 4. The next day, media was replaced with fresh EGM-2MV media. Cells grown in flasks were used for flow cytometry. To visualize distribution and uptake of fluorescent-labelled oligonucleotides using immunofluorescence, cells were grown on 2 chamber coverslips as described earlier. Cells were permeabilized (if needed) using 0.1% Triton-X100, fixed using fresh 2% paraformaldehyde (PFA), and mounted following manufacturer's protocol using Vectashield-dapi media (Vector labs H-1200). Dried, mounted slides were imaged using fluorescence microscopy (Nikon C1, Champigny-sur-Marne, France).

Mature miR ID Mimic/Inhibitor	**Stem-loop accession #/Supplier**	**Mature miRNA ID**	**Stem-accession/description**
hsa-miR-146a-5p mimic	MI0000449/Life Technologies MC10722 (cat.4464066)	UGAGAACU GAAUUCCA UGGGUU	MI0000477/CGAUGUGUAUCCUCAG CUUUGAGAACUGAAUUCCAUGGG UUGUGUCAGUGUCAGACCUCUGA AAUUCAGUUCUUCAGCUGGGAUA UCUCUGUCAUCGU
hsa-miR-146a-5p inhibitor	MIMAT0000449/Life Technologies MH10722 (cat. 4464084)		
FAM-hsa-miR-146a-5p	MIMAT0000449/Exiqon (500150)		/5'6-FAM/ACCCATGGAATTCAGTTCTC

Table 4: Oligonucleotide and stem-accession details for miR-146a

p) MRE sequence confirmation using luciferase-reporter construct

We used luciferase-reporter assays to confirm that our microRNA oligonucleotides accurately complement the 3'UTRs of our computationally-predicted mRNA targets, thereby confirming our proposed pathway interactions. Using the manufacturer's recommended protocol, a LightSwitch 3'UTR plasmid for TRAF6 (Switchgear genomics, S813016) was co-transfected in HEK293T cell line with miR-146a mimic, scramble, or media using DharmaFECT DUO (Cedarlane, T-2010-02). Further information on TRAF6 reference genome used for sequence design can be found in Appendix C. Briefly, HEK293T cells were grown to 80% confluency using DMEM media (10%FBS) in white 96 well TC plates (the black 96 well plates can cause inaccurate luminometer measurements). Each transfected well-contained 3.3μL (30 ng/μL) of supplied GoClone reporter, and 50 nM microRNA mimic and was transfected overnight. The next day, cells were treated with the supplied Lightswitch Assay reagent (SwitchGear genomics, LS010) and read for 2 seconds using a PolarStar Omega luminometer (BMG labtech, Germany). This was performed to further confirm oligonucleotide sequence complementarity, after having confirmed uptake and cytoplasmic distribution.

q) Bio-Plex Pro Human Cytokine Array

To assess the effect of miR-146a manipulation on cytokine production in early EPCs, we used the Bio-plex Pro Human Cytokine 27-plex system which is based on fluorescently dyed magnetic microspheres (beads) using XMAP multiplex technology (Bio-Rad, M500KCAF0Y), following the manufacturer's protocol (139). The following detection targets where used: IL-1beta, IL-1ra, IL-2, IL-4, IL-5, IL-6, IL-7, IL-8, IL-9, IL-10, IL-12 (p70), IL-13, IL-15, IL-17, Basic FGF, Eotaxin, G-CSF, GM-CSF, IFN-gamma, IP-10, MCP-1 (MCAF), MIP-

1alpha, MIP-1beta, PDGF-BB, RANTES, TNF-alpha and VEGF. Manufacturer supplied standards (using 1:4 dilution) and controls were used. Acquisition and analysis was performed on a Bio-Rad Bio-plex 200 Luminex machine using the Bio-Plex manager software version 6.1 which contained the appropriate acquisition modalities (Bio-Rad laboratories, CA).

r) Validating MRE sequence with miR-126 knockdown using reporter assay

As described for MRE sequence confirmation in (p), a LightSwitch 3'UTR plasmid for SPRED-1 (Switchgear genomics, S811430) was co-transfected in HEK293T cells with miR-126 inhibitor, scramble-miR, or media using DharmaFECT DUO (Cedarlane, T-2010-02) following the manufacturer's protocol (140). Further details on the SPRED-1 reference genome we used for vector design can be found in Appendix C. Briefly, HEK293T cells were grown to ~80% confluency in white 96 well TC plate. Each transfected well-contained 3.3 μL of (30 ng/μL) GoClone reporter, 100 nM microRNA inhibitor following manufacturer's protocol and was transfected overnight. The next day, cells were treated with Lightswitch Assay reagent (SwitchGear genomics, LS010) and read for 2 seconds using a PolarStar Omega luminometer (BMG labtech, Germany). Sequences for miR-126 mimics and inhibitors are provided in Table 5.

Mature miR ID Mimic/Inhibitor	miRBase accession #/Supplier	Mature miRNA ID	Stem-accession/sequence
hsa-miR-126-3p mimic	MIMAT0000445/Life Technologies MC12841 (cat.4464066)	UCGUACCGUGAGUAAUAAUGCG	MI0000471/CGCUGGCGACGGGACAUUAUUACUUUUGGUACGCGCUGUGACACUUCAAACUCGUACCGUGAGUAAUAAUGCGCCGUCCACGGCA
Has-miR-126-3p inhibitor	MIMAT0000445/Life Technologies MH12841 (cat. 4464084)		
FAM-hsa-miR-126-3p Inhibitor	MIMAT0000445/Exiqon (500150)		/5'6-FAM/CATTATTACTCACGGTACG

Table 5: Oligonucleotide and stem-accession details for miR-126

s) Transfection and Detection of intracellular microRNA mimics by immunofluorescence

Early EPCs were grown to day 5 in 75 cm^2 flasks and on 2 chamber coverslips (Nunc Lab- Tek II slides, 154526). On day 5, early EPCs were transfected using 5'6-FAM-labeled microRNA 126-3p inhibitor (5 pmol/1.75 cm^2 oligo) per 1.4 μL of final total volume and Lipofectamine 2000 (Life Technologies, 11668027). The next day, media was replaced with fresh EGM-2MV media. Cells were subsequently fixed using fresh 2% paraformaldehyde (PFA) and mounted using Vectashield-dapi media (Vector labs H-1200). Dried, mounted slides were imaged using fluorescence microscopy (Zeiss LSM 510 META/AxioVert200).

t) Assessments of early EPC morphology following over expression of miR-126

Following transfection of early EPCs with miR-126 mimic, we assessed change in morphology using a standard upright microscope (Nikon C1, Champigny-sur-Marne, France) imaged over 6 hour intervals. Subsequently, images were analysed for change in shape, size and number *in silico* (ImageJ). This computational analysis considered composition of cell dimensions with respect to the aspect ratio of cell longitudinal: transverse axis as well as the circularity ($f=4\pi A/P^2$) and elongation ($f=i_2/i_1)^{0.5}$ shape factors. Cells, which were at least twice as long as they were wide in dimension, were deemed "rod-shaped".

u) Matrigel-based tube formation assay

Early EPCs grown to day 5 or late EPCs were given microRNA treatment overnight and plated on BD BioCoat Matrigel Basement Membrane coated 6-well plates (BD BioSciences) at 75,000 cells per well using manufacturer's protocol (141). Unlike late EPCs, healthy early EPCs do not form matrigel networks when cultured alone on matrigel, therefore these cells are normally co-cultured with HUVECs for this assay. HUVECs where grown to ~80% confluence on T75 corning flasks using only EGM-2 media supplemented with 20% human serum (Lonza, cat. CC-2517 and Wisent Cat. No. 022-210). Early EPCs were co-cultured with HUVECs at 1:1; while late EPCs were cultured alone for all matrigel assays. Cells were suspended in 2 mL medium supplemented with 100 ng/mL recombinant VEGF (R&D Systems) and grown for 24 hours. Images were taken at 1.5, 5, 12, 15, and 24 hours; and after analysis it was deemed that 12 hours provided the clearest distinction between treatment groups. Following data acquisition, analysis was done at the 12 hour

mark using Angiogenesis Analyzer for ImageJ (http://image.bio.methods.free.fr/ImageJ/?Angiogenesis-Analyzer-for-ImageJ). Since there is normal uncontrollable variability for each experimental run due to cell distribution and typical experimental error, ImageJ software settings were set based on the control groups per each experimental run. To minimize extraneous variability for comparisons, experiments with early EPCs were normalized to untreated early EPCs co-cultured with HUVECs; while for late EPCs, results were normalized to untreated late EPCs grown on matrigel alone.

v) Boyden chamber migration assay

Chemotactic migration capacity of early EPCs was assessed using a modified Boyden chamber (Figure 4) migration assay a previously described by Kuliszewski et al with modification (141). Early EPCs were starved of serum for 1 hour and re-suspended in EBM-2 + 0.5% BSA at $5x10^5$ cells/mL. 500 μL of this prepared cell suspension, containing $2.5x10^5$ cells was placed within cell culture inserts (Becton Dickinson, 8 μm pores), then placed within companion plates containing 500 μL EBM-2 + 0.5% BSA containing VEGF and SDF-1 (100 ng/mL, of both). Selection of 8 μm pore sizes made active chemoattraction assessable as early EPCs were measured at 15-20 μm in diameter, requiring active migration through smaller pores. After 2 hours of migration at 37 ^oC, inserts were removed; the underside membrane was fixed and stained for DAPI for nuclear staining. Migrated cells were counted by DAPI staining using a florescent inverted light microscope (Nikon Eclipse TS100). Four random fields were captured per high-power field (HPF) and counted blindly at 100x magnification (i.e.: cells were counted without operator knowledge of the treatment groups).

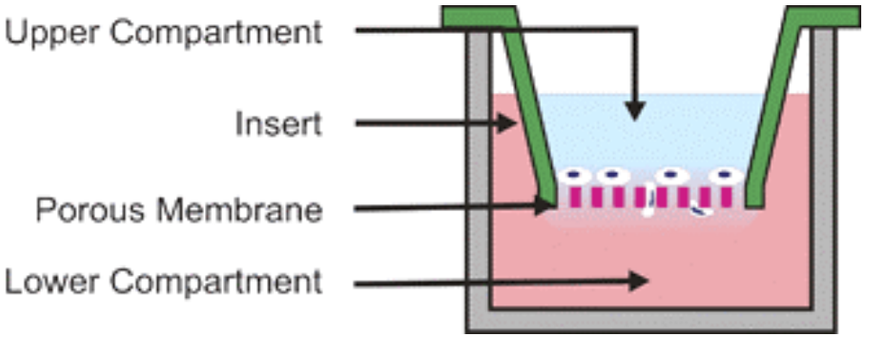

Figure 4: Simplified cell migration chamber

Obtained with permission from Keenan et al. (2008).

w) Research ethics and statistical analysis

The Ottawa Heart Institute Research Ethics Committee approved all protocols performed on human tissue from donors, with the participants providing written informed consent. The studies presented are in conformity with the Declaration of Helsinki for use of human tissue and adhere to the National Council on Ethics in Human Research guidelines.

Unless otherwise indicated, mean ± SEM values are reported in the graphs throughout this thesis (presumed normal distribution). A scramble-miR was used to compare non-specific transfection effects while untreated control groups were used to compare treatments. For most paired comparisons, a student's T test was performed (paired, when appropriate); otherwise a one-way ANOVA was used using either a Dunnett's test or a Tukey's post-hoc test as indicated in the figure captions. Statistical software employed for analysis was Graphpad Prism version 6.0. Array analysis was performed using a Pearson correlation with non-parametric significance of analysis of microarrays (SAM) technique via R-package (Stanford University). Statistical significance was considered as $p<0.05$.

CHAPTER III – EXPRESSION PROFILING PART 1: Candidate MicroRNA Array During EPC Outgrowth

3.2.1 Introduction

Over the past decade, there has been a growing amount of experimental evidence in support of the efficacy of EPCs in cardiovascular therapy (142, 143). In the majority of cases, therapeutic applications of EPCs have focused primarily on early EPCs, which are thought to induce revascularization primarily through paracrine mechanisms (49, 55, 144-146). In contrast, late outgrowth EPCs appear to act largely by engraftment and transdifferentiation (147). However, compared to early EPCs, late EPCs have not been tested in clinical trials and less is known about their therapeutic nature. Moreover, the challenges associated with the generation of late outgrowth EPCs, in addition to a continued lack of consensus regarding the existence of possible precursor cells that give rise to late EPCs; have proven to be major limitations to their study.

In vivo, circulating EPCs are believed to originate from the bone marrow, mobilizing in response to an injury to facilitate vascular repair and angiogenesis (148-150). *In vitro*, early EPCs are generated from adult peripheral blood-derived monocytes during short-term (3-5 days) culture in an endothelial growth medium. These cells retain monocyte markers (CD14 and CD45), variably express some endothelial markers (i.e. KDR and Tie2), can bind lectin and take up AcLDL (28). By contrast, late EPCs possess greater endothelial-like morphology, but lack classical monocytic characters such as CD14 and can also bind lectin and uptake AcLDL (146). However, it is not known whether late EPCs represent a unique cell lineage predestined to become endothelial-like cells and are distinct from early EPCs or if they arise secondarily from early outgrowth cells by a differentiation process. But what is certain is that early EPCs are clearly culture modified mononuclear cells, and may share some similarities with other monocyte-derived cells, such as macrophages or dendritic cells (27, 151).

As post-transcriptional regulators of gene expression, microRNAs likely play an important role in regulating gene expression and driving phenotypic changes in cells. Since microRNAs regulate the expression of large numbers of related genes, we sought to define the profiles of microRNA expression within early and late outgrowth EPCs to establish the extent to which these were shared and how these profiles change during the processes leading to the outgrowth of early and late EPCs. This work will form a basis for the rest of the thesis by defining the unique microRNA signatures for the two EPC subtypes and providing insights into the potential mechanisms that govern both their derivation and function.

3.1.2 Hypothesis and Aim

Hypothesis: As MNCs give rise to early and late EPCs; there is a gradual change in total microRNA expression profile, which reflects a shift in the predominant cell population and the processes occurring within the remaining cell types.

Aim: To compare differences and similarities in microRNA expression profiles between mononuclear cells, early and late EPCs during outgrowth.

3.1.3 Results

a) Generating and characterizing MNCs, early and late EPCs

A key requirement for this initial study was the identification of an optimal time window for establishing an early EPC phenotype during mononuclear cell culture. The time required for generating early EPCs from human circulating mononuclear cell cultures varies in different reports from 3 to 10 days. However, we identified that within the first three days in culture, the majority of cells have not taken on the classical early EPC rod-shaped morphology. By day 5 in culture, nearly 80% of studied cells, across all participants, exhibited typical early EPC morphology (Figure 5). This observation became further confirmed when we noted that the establishment of rod-shaped morphology in early EPCs reflected the appearance of other EPC characteristics as noted below.

b) Classical early and late EPC characterization

A typical (or classical) feature of early and late EPCs is lectin-binding ability. Both early and late EPCs bound Ulex lectin (an endothelial selective lectin) in abundance. Additionally, DiI-labelled AcLDL uptake was similar in both cell types (Figure 6). It should be noted that due to lack of proliferation in early EPCs, rendered images appear less confluent than late EPCs. For clarity, low power and high power magnification is provided in Figure 6 to show total fluorescence and cell distribution.

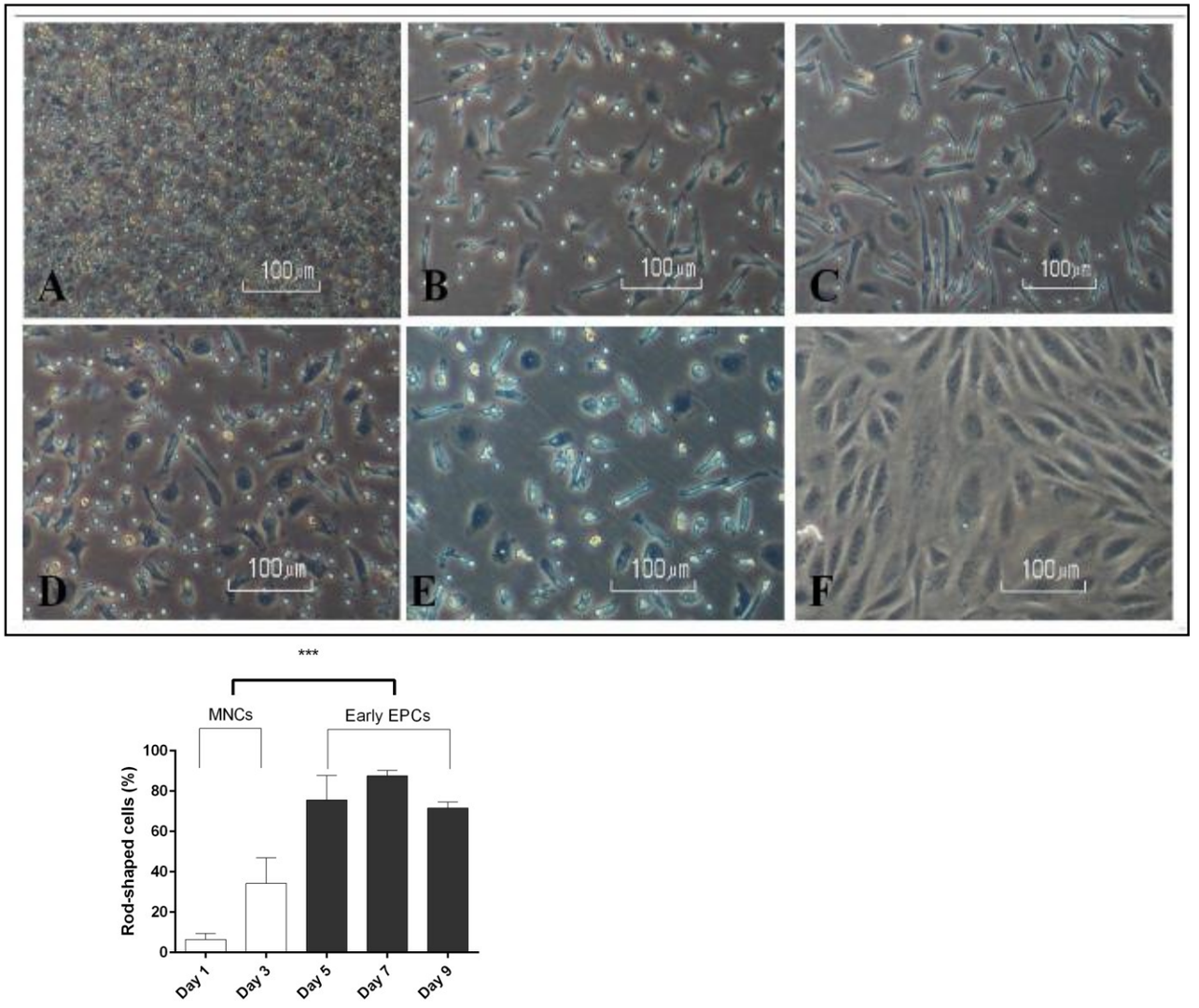

Figure 5: Morphology of leukapheresis-derived PBMCs during early and late EPC generation

(Top) (A) Mononuclear cells freshly isolated from leukapheresis possess rounded morphology for 24 hours. (B) By day 3, the emergence of non-proliferating rod-shaped cells begins and these cells continue to elongate while rounded cells fail to adhere and diminish. Throughout days 5 (C), 7 (D), and 9 (E), non-proliferating early EPCs persist with classic rod-morphology. By week 2 and 3 endothelial-like, colony forming late EPCs (F) emerge and gradually push off early EPCs from flask until confluence. Image produced using light microscopy (20X objective). (Bottom) Percentages of rod-shaped cells (based on asymmetry and >12 microns in size) during 9 days of MNC and early EPC culture. Data presented as mean ± SEM, n=3.***$p<0.001$

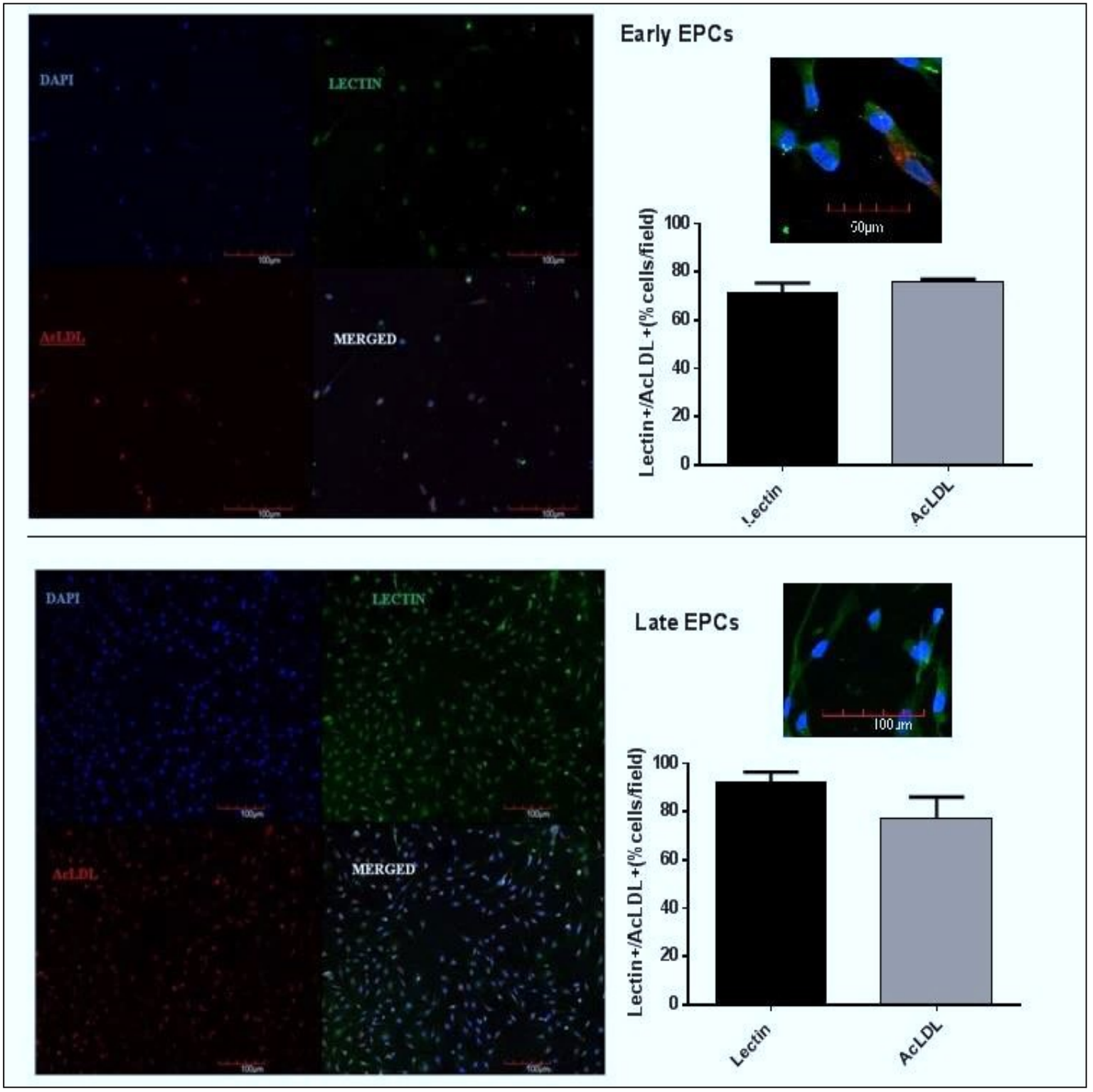

Figure 6: Immunofluorescence – Classical EPC Characterization

Representative images of EPC characterization performed on early (top) and late (bottom) EPCs. All cells were identified by staining with 4', 6-diamidino-2-phenylindole (DAPI) nuclear stain, FITC-conjugated Ulex europaeus lectin 1 (Lectin), 1, 1'-dioctadecyl-3, 3,3',3'-tetramethyl indocarbocyanine perchlorate-labeled acetylated low-density lipoprotein (AcLDL). Cells imaged at 100x magnification. Data represent mean ± SEM.

c) Assessment of early and late EPC markers using flow cytometry

To assess whether early and late EPCs expressed typical early and late EPC markers, flow cytometry was used. Flow cytometric analysis showed high expression of endothelial marker CD31 in early and late EPCs, as well as leukocyte marker CD45 in early EPCs (Figure 7). VEGFR2 expression was variable in early EPC samples as has previously been observed in our lab. To illustrate this further, four more representative flow cytometric histogram plots are included in (Appendix A). We also noted low expression of VEGFR2 in HUVECs using the same technique (Appendix B).

d) Candidate microRNA array

In our candidate microRNA array, we assessed the expression of 13 biologically relevant microRNAs to early and late EPCs. Candidate microRNA profiling revealed a consistent pattern of microRNA expression across the 8 participants during culture of MNCs to derive early and late outgrowth EPCs. There was little change in microRNA levels during the first 3 days of culture. However, by day 5 there was a noticeable increase in miR-34a, -132 and -146a; with a decrease in miR-92a, -126 and 130a (Figure 8). These changes in microRNA expression corresponded with the emergence of early EPCs based on morphology and overall cell markers as described above. The apparent change in morphology (including the emergence of rod-shaped cells among rounded cells) is indicative of motility in early EPCs which is mostly absent before day 5. Day 5 was consistently the earliest time point where early EPCs were the predominant cell population for each participant; and what appears to be a heterogeneous population at day 5 is in fact, the emergence of early EPCs displaying both motile and sessile properties. For later analyses we grouped cells from days 1-3 as MNCs and from days 5-

9 as early EPCs. With the emergence of late outgrowth EPCs after 2 weeks of culture there was the appearance of another distinct microRNA profile, with a notable marked increase in miR-126 and -130a. Additional microRNAs that were selectively increased in late outgrowth EPCs are shown in Figure 9. Moreover, the microRNA expression profile of late EPC was nearly identical to that of mature endothelial cells, HUVECs (Figure 10).

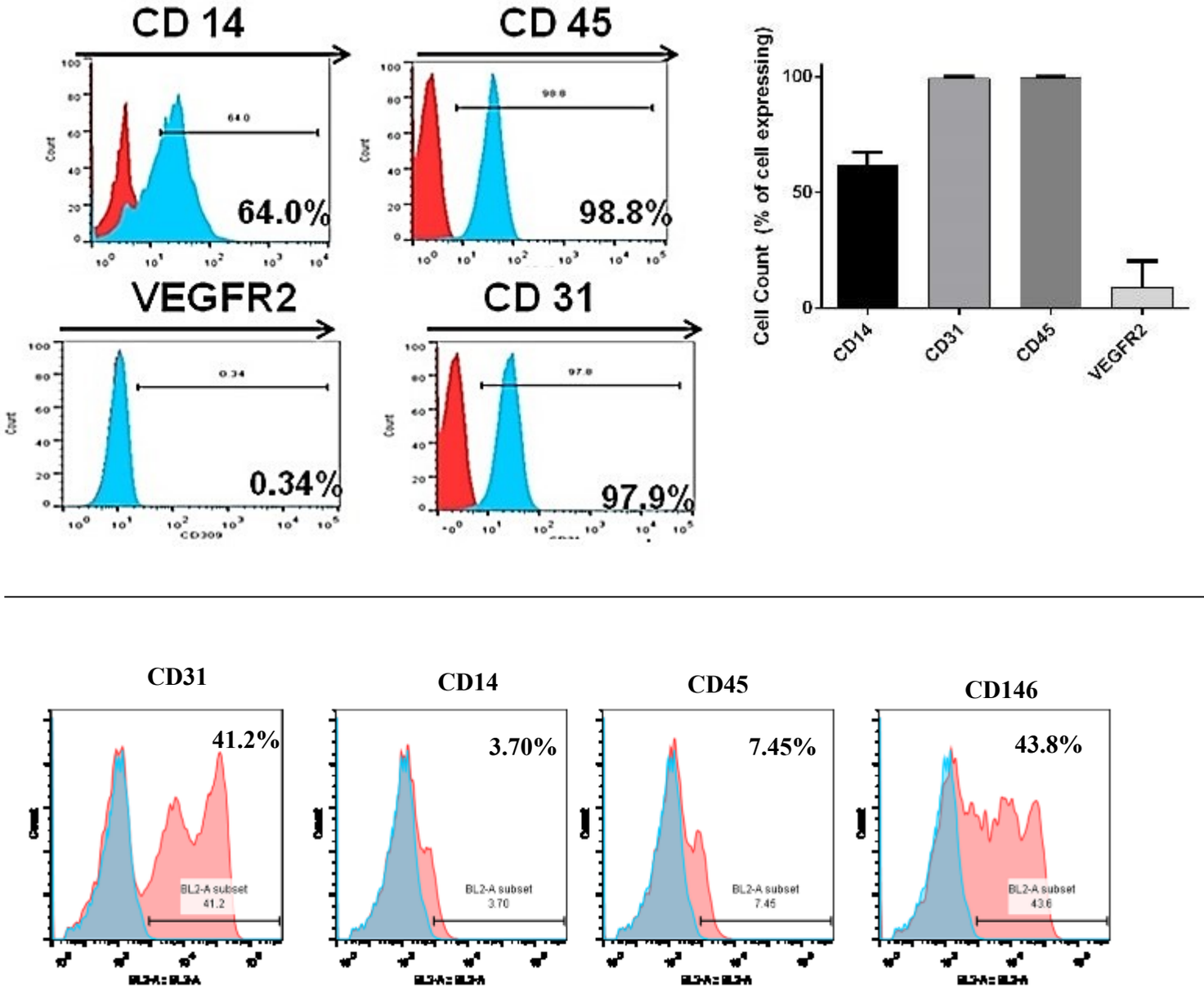

Figure 7: Characterization of early and late EPCs by flow cytometry

Representative histograms of early (top) and late EPC (bottom) characterization. Early EPCs where characterized on day 5 of culture and late EPCs where characterized at passage 3. We examined cells for CD14 and CD45 (which are classically expressed in early EPCs) in addition to VEGFR2 and CD31 (which are strong markers for endothelial cells). Low expression of VEGFR2 is seen with in vitro cultivation of EPCs. Data represent mean ± SEM, n=3.

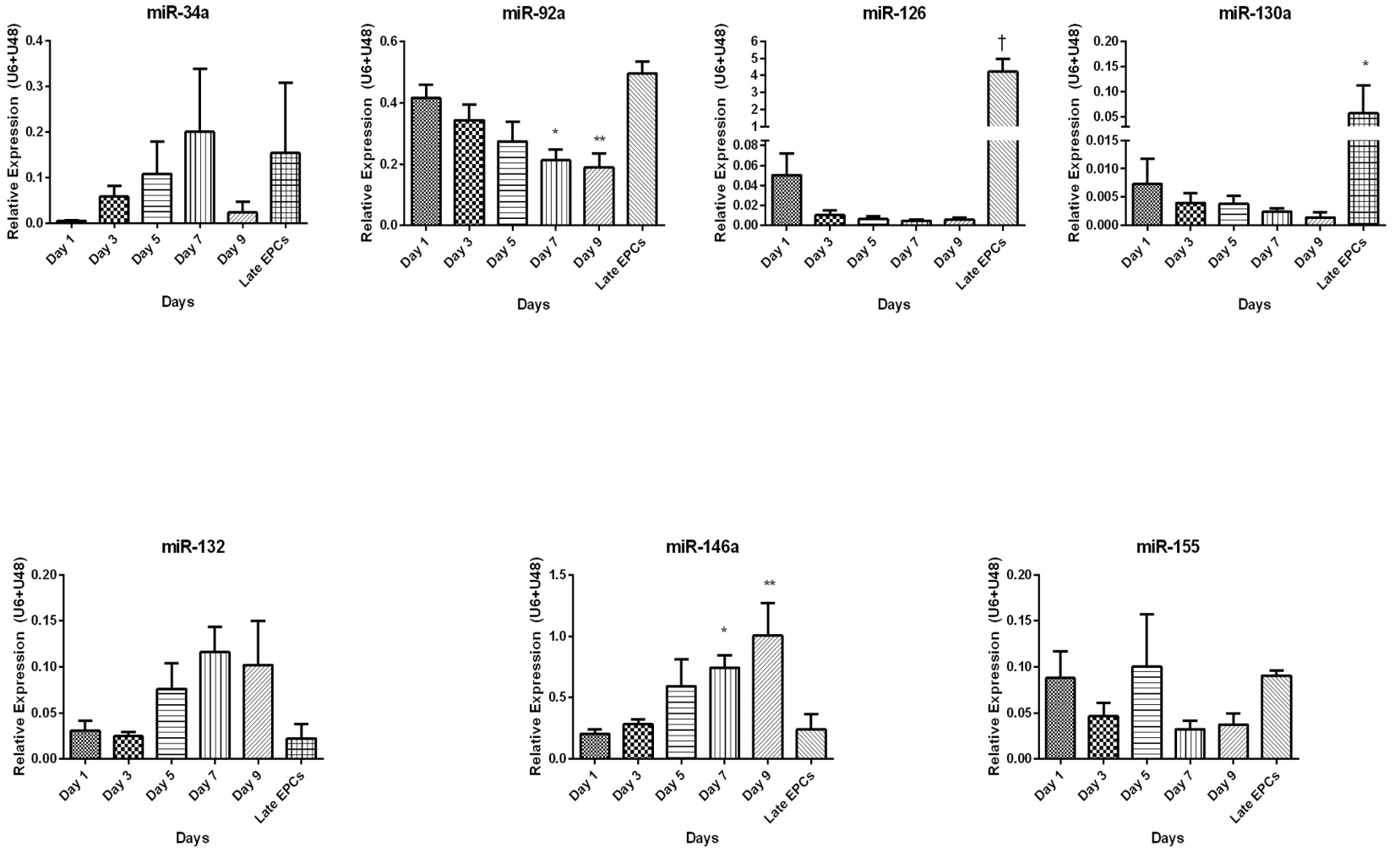

Figure 8: Candidate microRNA array panel 1

The selected microRNAs were chosen based on published literature (Table 1). During normal generation of early EPCs, cells were probed for microRNA expression of 13 candidate microRNAs on day 1, 3, 5, 7 and 9; and after generation of confluent late EPCs. At each time point, cells were lysed and RNA was extracted to monitor for changes in microRNA expression profiles as early EPCs emerged. Separate flasks were cultured to allow cell lyses every 48 hours. Unlysed flasks were maintained in culture for over two weeks until confluent late EPCs were generated. Late EPCs were cultured until passage 3. Progressive changes in microRNA expression profiles were compared between participants for congruence. Statistical comparisons were made to day 1 (ANOVA, followed by Dunnetts test). Data represent mean ± SEM; n = 5-8.*$p<0.05$, **$p<0.01$, †$p<0.0001$.

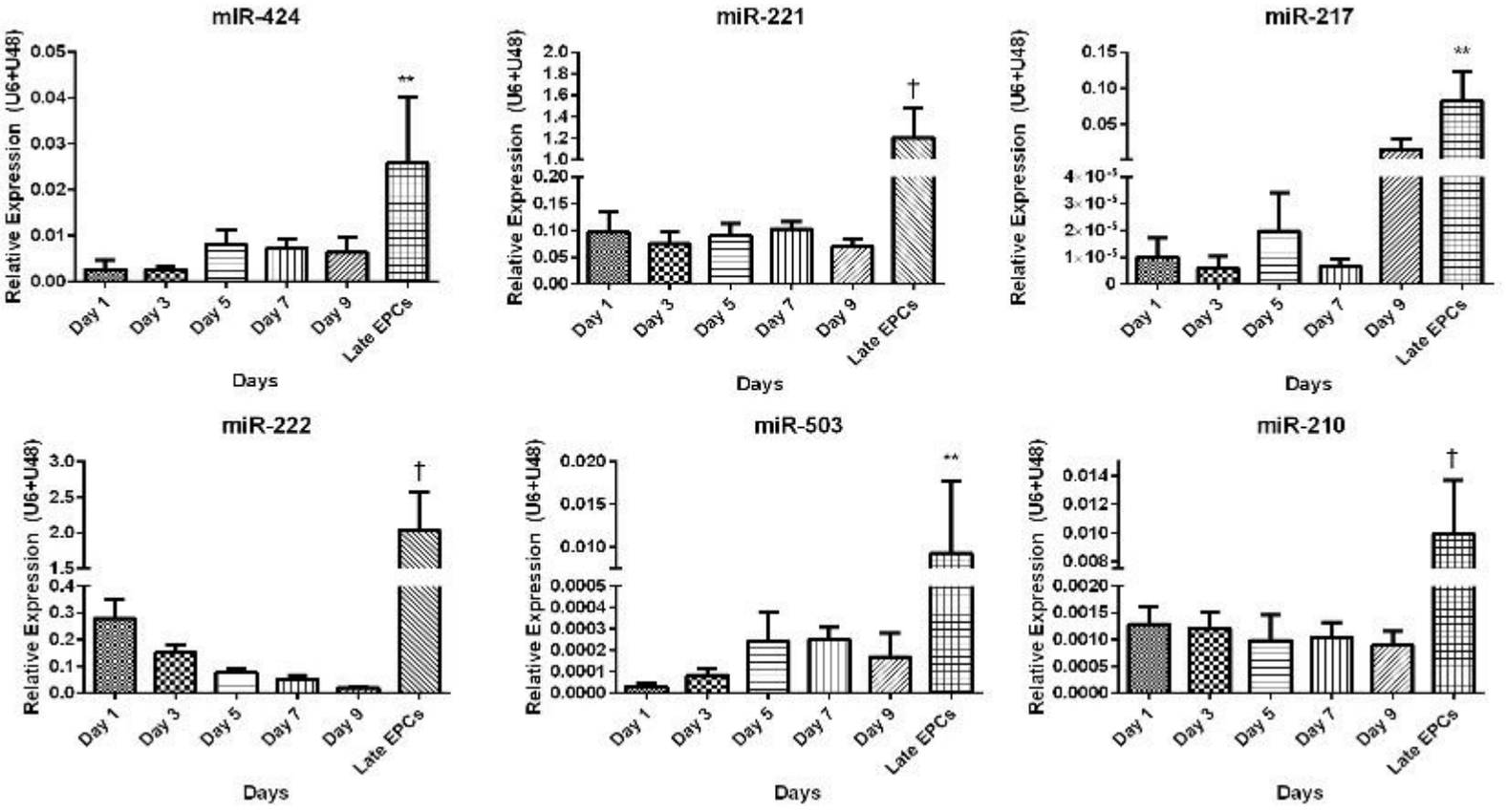

Figure 9: Candidate microRNA array panel 2

Panel 2 is a continuation of candidate microRNA array results. As previously noted, selected microRNAs were chosen based on published literature, then continually assessed during early EPC generation for 9 days. Late EPCs were lysed for RNA extraction at passage 3. Statistical comparisons were made to day 1 (ANOVA, followed by Dunnetts test). Data represent mean ± SEM; n = 5-8. *p<0.05, **p<0.01, †p<0.0001.

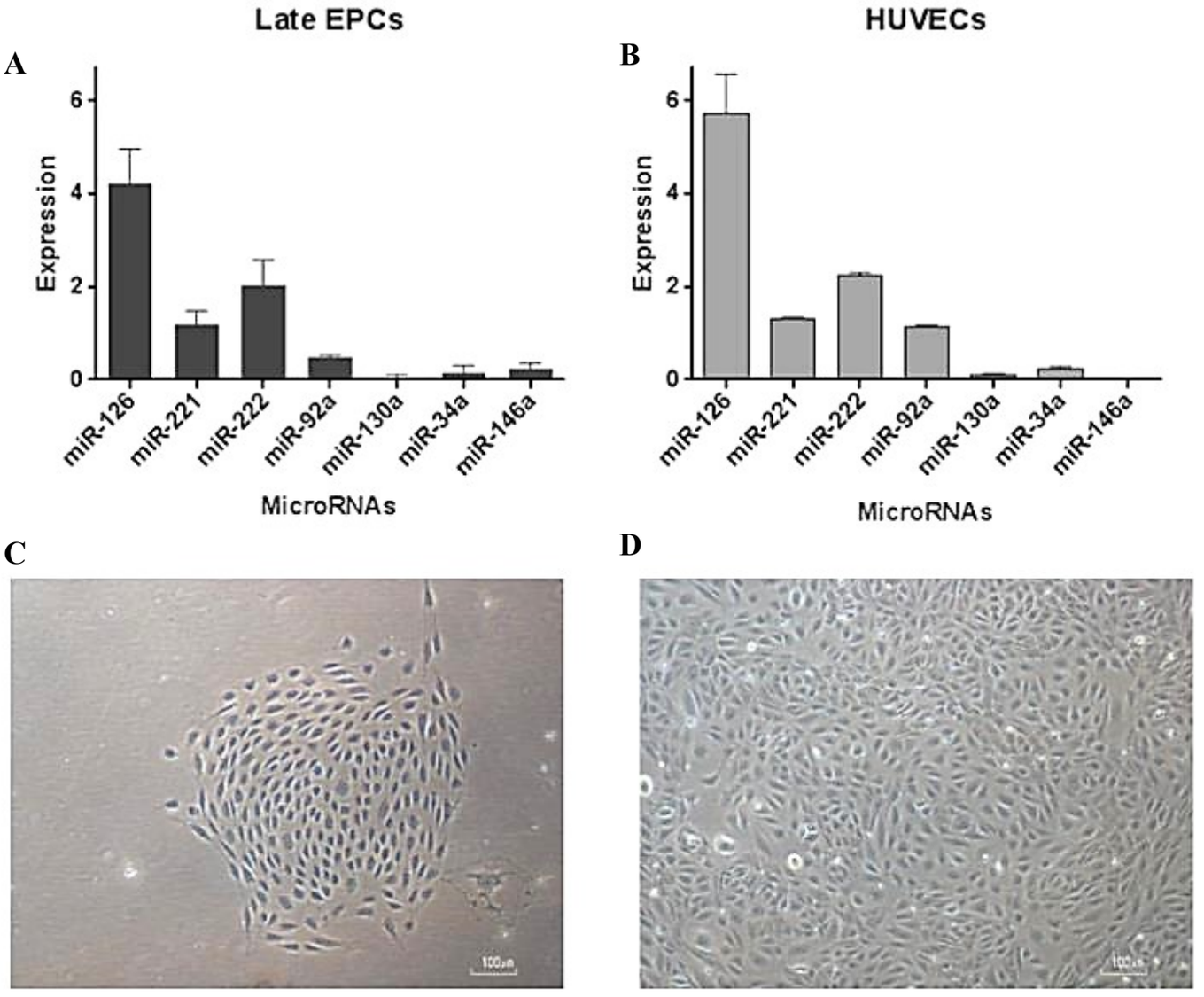

Figure 10: Late EPC vs HUVEC microRNA profiles

Seven of the highest expressed microRNAs from the candidate microRNA array were compared between late EPCs (A) and HUVECs (B) to assess congruence. MicroRNA expression was normalized to RNU48 and RNU6. Expression was calculated using the Livak ddCt method. Data represent mean ± SEM; n = 3-5. For comparison, representative images of late EPCs (C) and HUVECs are provided at 100x magnification (D).

3.1.4 Discussion

During the generation of early EPCs from MNCs, the classic elongated "rod-like" morphology of early EPCs first emerged after day 3 of *in vitro* cultivation (Figure 5). The typical morphology of early EPCs was most prevalent between days 5 to 9. During this period, early EPCs do not proliferate and beyond 9 days, they gradually decline in number due to apoptosis (152). We noted that throughout days 5 to 9 (inclusive), there is a distinct pattern of miRNA expression that is characteristic of early EPCs. Indeed, early EPCs are typically utilized in therapeutic application for their purported reparative potential during this period in culture (153). For statistical analysis, we grouped MNCs as cells cultured throughout days 1 to 3, early EPCs as days 5 to 9, and late EPCs at passage 3.

Our results indicated a consistent microRNA expression profile during the emergence of early and late EPCs. Additionally, late EPCs expressed a unique microRNA expression profile compared to MNCs and early EPCs. This suggests that either these cells represent an entirely different cell type or that they arise from early EPCs by a transdifferentiation process that involves a marked switch in the microRNA expression profile. As well, we compared the expression of seven of the thirteen highest expressed microRNAs in late EPCs with human umbilical vein endothelial cells (HUVECs). Our results showed that late EPCs possess a similar microRNA expression profile to HUVECs. With this finding, we postulated that microRNA expression profiles correlate with underlying physiological roles of their respective cells and therefore represent critical processes affecting phenotype.

One can only speculate about the mechanisms that underlie these shifts in microRNA profiles during progressive culture of MNCs. However, it is known that the emergence of early EPCs under these culture

conditions occurs by a process of attrition, since the more abundant cell types in the initial culture, i.e. lymphocytes, are progressively lost, resulting in an enrichment in the monocyte population (27). Moreover, the phenotype of these monocytes is altered by culture conditions, with the adoption of a modest endothelial phenotype, which likely is associated with some changes in microRNA expression. However, the dramatic shift in microRNA profile associated with the appearance of late outgrowth EPCs likely represents either the further differentiation of early EPCs, or the amplification of a very rare population of endothelial progenitor cells that were present in very low numbers in the original MNC sample. At this point we could not distinguish between these possibilities, but our later findings as presented in the Appended Chapter appear to support the latter hypothesis.

During the 5 to 9-day period of culture, early EPCs expressed the highest levels of miR-146a and miR-132 compared to MNCs and late EPCs. Interestingly, both microRNAs have been implicated in immunogenic responses in human monocytes and dendritic cells (DC) (154). Our lab previously showed that early EPCs share some features with mononuclear cell-derived DCs (70), and exhibit a profound anti-inflammatory response when stimulated with cytokines (e.g. release of high levels of IL-10). In a study focusing on human pathogenic response to Aspergillus fumigates, a mold that triggers severe inflammatory response in humans, Gupta et al. showed that miR-132 significantly modulated TLR inflammatory response (154). Similarly, miR-146a has been shown in numerous studies to control immune-response to various TLR4 ligands, including the endotoxin, LPS (105, 155). As such, we speculated that microRNAs could play an important role in the regulation of immunoregulatory properties of early EPCs, and the role of the top candidates, such as miR-146a, will be studied.

The similarity in microRNA expression profiles of HUVECs with late EPCs, together with their nearly identical morphology (Figure 10), suggests that late EPCs represent a highly differentiated endothelial cell

type, that still possesses high proliferation potential consistent with a true 'progenitor cell' phenotype and thus may have important therapeutic uses as well as providing a convenient source for cells that can be easily and efficiently reprogrammed (156). Interestingly, late EPCs had very high expression of the highly pro-angiogenic microRNA miR-126, which has been previously implicated in the regulation of angiogenic signaling and shown in numerous studies as being crucial for post-natal vascularization (66, 157, 158).

In contrast to the above-mentioned microRNAs, the levels of miR-92a gradually declined during the culture of early EPCs whereas its expression level recovered with the appearance of late outgrowth EPCs. MiR-92a has been shown to regulate the expression of integrin subunit α5 by a post-transcriptional mechanism. This integrin is known to influence the survival of cells on fibronectin and the upregulation of Bcl-2 expression, and thus its expression may be important in assessing viability of EPCs during the culture period (159, 160).

3.1.5 Chapter 3 Part 1 Summary

During the outgrowth of early and late EPCs, there was a consistent shift in microRNA expression profiles as cells differentiated in culture and this was consistently seen in multiple participants. This consistency in shift of microRNA expression profiles across all participants likely reflects recurring processes, which include (but is not limited to) enrichment of monocytes and their characteristic microRNA profiles, and the differentiation of surviving cell types (and with differentiation, transcription, fundamentally resulting in the production of microRNAs through excision). As a result, these processes likely led to early EPCs expressing higher miR-146a compared to MNCs and late EPCs. Interestingly, late EPCs expressed a much different microRNA expression profile when compared to early EPCs and MNCs, one that was highly congruent to HUVECs. Since early EPCs repair primarily through indirect mechanisms and late EPCs repair through direct mechanisms, we postulated that

miR-146a likely contributes to the indirect reparative action of early EPCs by suppressing inflammation during injury; while miR-126 may function through a more direct mechanism in late EPCs.

CHAPTER III – EXPRESSION PROFILING PART 2: Early vs Late EPCs, Global Arrays

3.2.1 Introduction

In the preceding section, we investigated only thirteen candidate microRNAs during the selection of early and late outgrowth EPCs, since performing an unbiased array at each time point would not have been feasible. Our approach allowed us to identify trends in microRNA expression profiles as early EPCs emerged from MNCs. Through this process, we identified day 5 as the optimal time point to perform our unbiased global gene and microRNA arrays since by this time point, all participants consistently had established cultures early EPCs with consistent miRNA profiles. These arrays provided us confirmation of our candidate microRNA findings and also novel insight into variations in gene expression across both cell types (which would then help in uncovering relevant mechanistic roles). To this end, we used six participant samples to compare early and late EPCs.

3.2.2 Hypothesis and Aim

Hypothesis: Early and late EPCs will express distinct microRNA expression profiles that reflect differences in biological activity and may provide new insights into the relationships between these cell types and the mechanisms underlying the origins of late EPCs from MNCs and early EPCs.

Aim: Directly compare global gene and microRNA expression between early and late EPCs.

3.2.3 Results

a) Analysis of collected RNAs prior to arrays

In order to confirm quality and consistency in RNA extraction technique, we measured purity and integrity in all of the collected samples (including those unused in the array). Four out of thirty-six samples had RIN values <7, indicating low integrity, (despite achieving high purity across all samples). However, the samples that did not meet the integrity criteria for the arrays were not in the day 5 early EPC sample groups and thus were not required or used for array (only samples highlighted in yellow in Figure 3A were used in the arrays). In addition, we ensured an equal number of male and female participant samples to be used for the array (Figure 3B).

b) MicroRNA array confirms candidate array findings

Our microRNA array revealed that early EPCs had high expression of both miR-146b-5p and miR-146b-3p (guide and passenger strands). In part one, we identified miR-146a as the highest expressed candidate microRNA in early EPCs. Using computational target prediction (TargetScan), we found that both strands of miR-146b and the parent strand of miR-146a share the same transcriptional control over gene targets, specifically, TRAF6 and IRAK1 (Figure 11). When we compared all the highest expressed microRNAs in terms of fold difference in expression in early and late EPCs from our global array, we noted that both guide and passenger strands of miR-146b were within the top 25 expressed microRNAs in early EPCs (Table 6). It should be noted that for our heatmap in Figure 13, we only presented the top 25 microRNAs in early EPCs based on absolute expression (not fold difference when compared to late EPCs); as such miR-146a/b is absent. The top of the heatmap contains the

cluster dendogram, which shows the degree of dissimilarity between participant samples shown through separation. In this heatmap, red (versus green) corresponds to high expression of the microRNA in question; and late EPCs are listed on the right side of the map. We noted that late EPCs exhibited a uniquely different list of robustly expressed microRNAs compared to early EPCs. In our candidate microRNA array, we noted that of the thirteen candidate microRNAs, miR-126 expression was the highest in late EPCs. In our global microRNA array, miR-126 was the sixth highest expressed microRNA in late EPCs overall (Table 6); and in our volcano plot of microRNAs miR-126 appeared in the top right quadrant, indicating highest expression in late EPCs as well as highest significance (Figure 12). For Table 6, we plotted the p-values of the microRNAs in their respective cell types and noted that miR-126 had a much lower p-value in late EPCs compared to mir-146a/b in early EPCs. For our heatmap (in Figure 13) we included only the 25 microRNAs with the lowest p-values (probability-values) in early and late EPCs.

TargetScanHuman
Prediction of microRNA targets
Release 6.2: June 2012

Human | miR-146ac/146b-5p

224 transcripts with conserved sites, with a total of **233** conserved sites and **88** poorly conserved sites.

Table sorted by total context score [Sort table by aggregate P_{CT}]

Genes with only poorly conserved sites are not shown [View top predicted targets, irrespective of site conservation]

The table shows at most one transcript per gene, selected for having the highest aggregate P_{CT} (or the one with the longest 3' UTR, in case of a tie).

Target gene	Representative transcript	Gene name	Conserved sites				Poorly conserved sites			
			total	8mer	7mer-m8	7mer-1A	total	8mer	7mer-m8	7mer-1A
TRAF6	NM_004620	TNF receptor-associated factor 6	**4**	3	0	1	**2**	0	1	1
IRAK1	NM_001025242	interleukin-1 receptor-associated kinase 1	**2**	2	0	0	**0**	0	0	0

Figure 11: MicroRNA 146a computational target prediction algorithm

Target prediction algorithms used in TargetScan identified TRAF6 and IRAK1 as possessing highly conserved target complementarity with miR- 146a. Numerous studies have confirmed that miR-146a modulates the TLR4 inflammatory signaling pathway mediated by TRAF6 and IRAK1. Image credit Targetscan.org

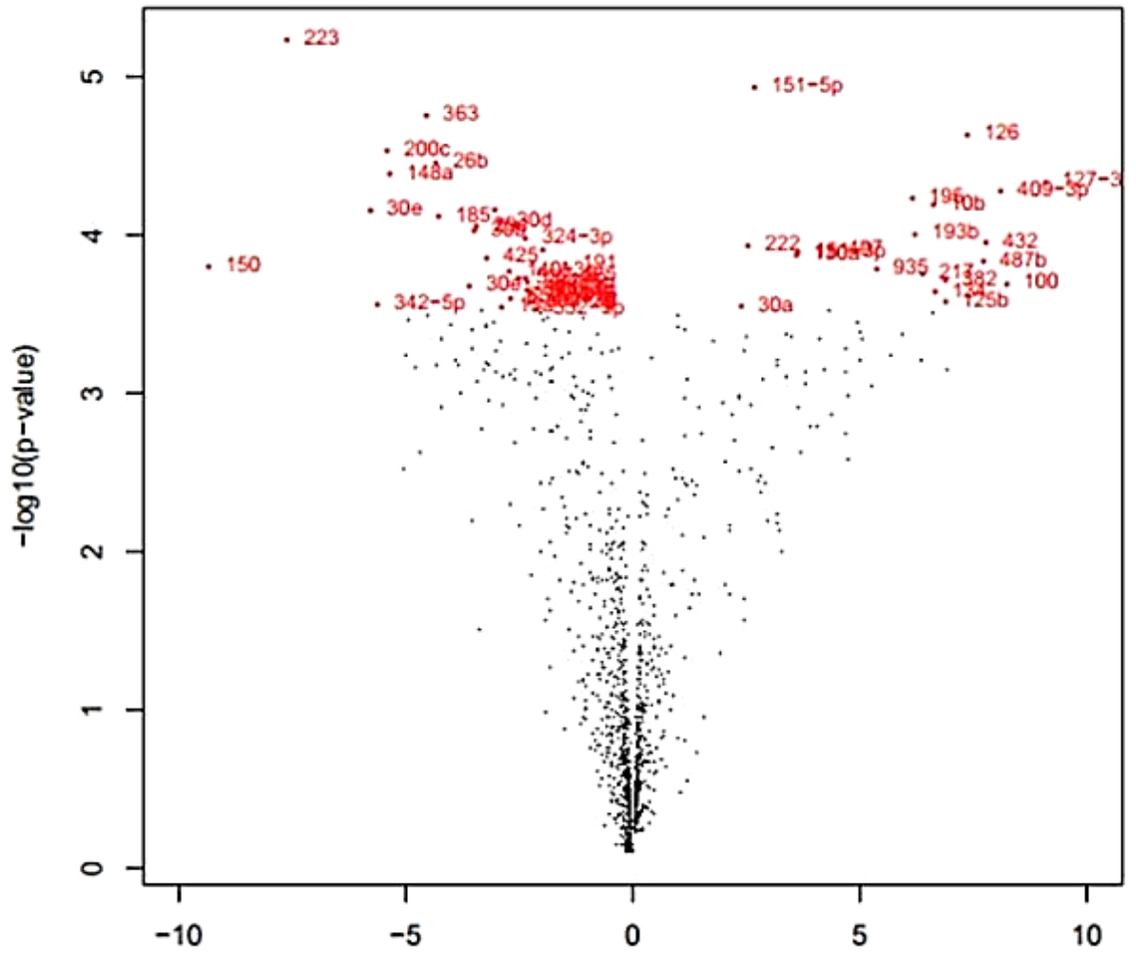

Figure 12: Volcano plot of top 50 microRNAs in early and late EPCs.

Global microRNA expression plot of early (left) and late (right) EPCs. Plot represents probability (y-axis) versus difference of group means or magnitude of the difference in expression (x-axis). The larger the difference of expression, the further on the x-axis the microRNA is plotted. Plots closer to the center are less differentially expressed between early and late EPC; while the top 50 microRNAs in early and late EPCs are highlighted in red.

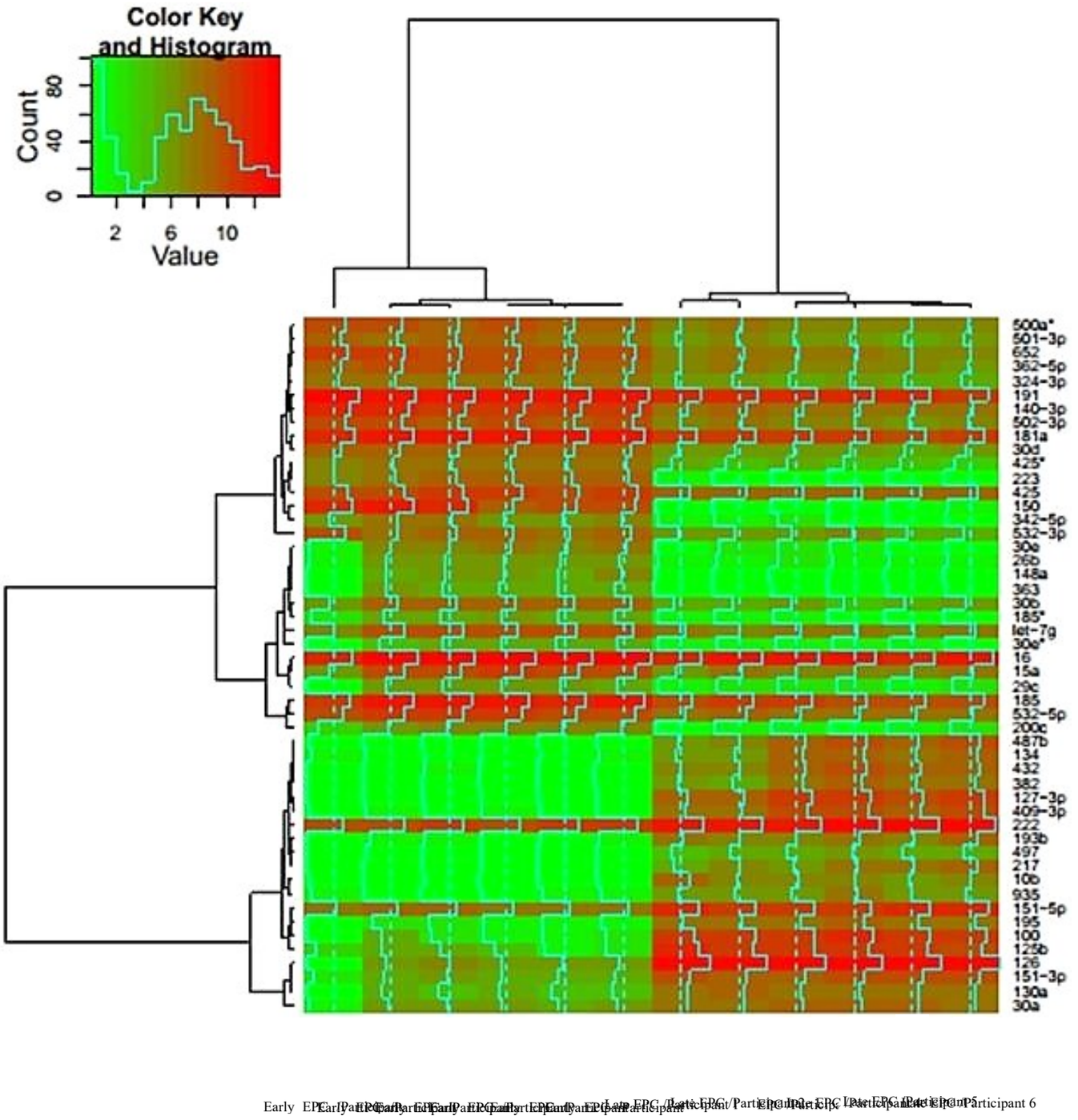

Figure 13: Heatmap and hierarchical cluster dendrogram of top 50 microRNAs in early vs late EPCs

Top expressed microRNAs between early and late EPCs at day 5 (left) and late EPCs (right) are presented. Colors reflect value of detection; green represents low expression, red represents high expression. Dendrogram separation represents degree of dissimilarity.

No.	MicroRNA Identity	Fold Increase in Early EPCs	P
1	hsa-miR-150	649.99	4.79E-05
2	hsa-miR-223	196.25	1.77E-06
3	hsa-miR-30e	54.87	2.13E-05
4	hsa-miR-342-5p	49.42	8.69E-05
5	hsa-miR-200c	42.56	8.87E-06
6	hsa-miR-148a	40.97	1.24E-05
7	hsa-miR-486-5p	33.62	0.00252
8	hsa-miR-378*	31.82	0.000232
9	hsa-miR-140-5p	30.70	0.000113
10	hsa-miR-4417	27.13	0.000291
11	hsa-miR-146b-5p	26.00	0.001745
12	hsa-miR-363	23.35	5.32E-06
13	hsa-miR-378e	22.65	0.000105
14	hsa-miR-26b	20.20	1.06E-05
15	hsa-miR-378g	19.80	0.00028
16	hsa-miR-185*	19.36	2.31E-05
17	hsa-miR-338-5p	18.78	0.000158
18	hsa-miR-378i	18.34	0.000708
19	hsa-miR-1303	16.27	0.000128
20	hsa-miR-378d	14.95	0.000259
21	hsa-miR-146b-3p	14.53	0.000284
22	hsa-miR-378f	13.68	0.0005
23	hsa-miR-30e*	12.13	6.74E-05
24	hsa-miR-212	11.72	0.005966
25	hsa-miR-30b*	11.50	0.000137

No.	MicroRNA Identity	Fold Increase in Late EPCs	P
1	hsa-miR-127-3p	547.33	1.42E-05
2	hsa-miR-100	302.39	6.38E-05
3	hsa-miR-409-3p	276.44	1.60E-05
4	hsa-miR-432	220.14	3.37E-05
5	hsa-miR-487b	211.72	4.43E-05
6	hsa-miR-126	165.87	7.09E-06
7	hsa-miR-214	120.54	0.000312
8	hsa-miR-125b	118.82	8.33E-05
9	hsa-miR-382	118.61	6.03E-05
10	hsa-miR-134	101.56	7.27E-05
11	hsa-miR-379	99.10	0.000101
12	hsa-miR-10b	98.66	1.95E-05
13	hsa-miR-217	83.66	5.32E-05
14	hsa-miR-99a	81.19	0.000255
15	hsa-miR-193b	74.53	3.01E-05
16	hsa-miR-195	71.51	1.77E-05
17	hsa-miR-431	61.79	0.000149
18	hsa-miR-139-5p	51.23	0.000231
19	hsa-miR-935	41.48	4.97E-05
20	hsa-miR-216a	37.96	0.000452
21	hsa-miR-584	32.86	0.000163
22	hsa-miR-370	32.69	0.000142
23	hsa-miR-376c	32.68	0.000266
24	hsa-miR-409-5p	31.22	0.000121
25	hsa-miR-487a	26.94	0.000525

Table 6: Top 25 expressed microRNAs in early and late EPCs

Result of top 25 microRNAs measured in global microRNA array between early (left) and late (right) EPCs. Table ranking is based on the comparative magnitudes of expression with highest fold increase ranked highest. The columns labeled “P” represent statistical probability of significance.

3.2.4 Discussion

We sought to confirm our limited candidate microRNA array results with our global microRNA and microarrays in order to find differences in relevant signalling pathways and gain insight into mechanisms for follow up studies. This allowed us to identify trends in changing microRNA expression profiles as early EPCs differentiate and to compare absolute differences in expression. The high expression of miR-150 in early EPCs agreed with existing literature (as mentioned in the introductory chapter). Early EPCs normally possess high expression of miR-150 (123). Upon injury, miR-150 expression is purportedly reduced in early EPCs while the expression of CXCR4 is increased, promoting recruitment to the site of injury through a process mediated by adenosine (123). Through luciferase reporter assays, Rolland-Turner et al. verified that miR-150 binds to the 3'UTR region of CXCR4.

In addition to miR-150, we also noted that the presence of both the guide and passenger strands of miR-146b were highly expressed in early EPCs. As mentioned earlier, miR-146b is within the same microRNA family as miR-146a, thus both miR-146a and miR-146b represent sequences that have evolved from a common ancestor. As such, both miR-146a and miR-146b have many of the same target sequences. The reason why both guide and passenger strands of miR-146b were detected in our global array (instead of only miR-146a) may reflect technical limitations in a chip-based array versus qRT-PCR (which was used in the candidate array). Nonetheless, both miR-146a and miR-146b have nearly identical targets. The most prominent targets were TRAF6 and IRAK1. Park et al. identified that both miR-146a and miR-146b play a crucial role in human dendritic cell apoptosis and cytokine production via TRAF6/IRAK1/NFKB pathway regulation (161). Since both dendritic cells and early

EPCs arise from a common monocytic cell populations, this finding suggestes an important immune-regulating role for miR-146 in early EPCs which has not yet been fully explored.

In late EPCs, the high expression of miR-126 (ranked as sixth highest expressed microRNA) confirmed our earlier findings, which had used a candidate microRNA array. In our previous candidate array, we selected miR-126 due to it being implicated in regulating the expression of proteins that modulate endothelial cell response to stimulation of the principle VEGF receptor, VEGFR2 (as noted in the introduction). Since late EPCs exhibited a strong mature endothelial-like gene expression profile, we suspected that miR-126 might be (at least partially) responsible for controlling the endothelial-like phenotype of late EPCs. This is supported by existing literature from numerous groups which have shown that there are severe defects in endothelial cells of mice with targeted deletion of miR-126, including diminished signalling by angiogenic growth factors that include VEGF and FGF (162); and that VEGF signalling is significantly augmented during aortic development upon overexpression of miR-126, thereby facilitating angiogenic sprouting (163). As such, we postulated that knockdown or manipulation of this microRNA in late EPCs could modulate the endothelial-like functions of late EPCs (thereby affecting angiogenesis). And these could then also be studied in early EPCs with over expression of miR-126.

Since MCAM is a strong marker for endothelial cells and a potential candidate marker for late EPC precursors in cord blood as mentioned, it represented a gene of high interest to us. The seventh highest expressed microRNA in late EPCs, miR-214, has been shown to promote MCAM expression through suppression of TFAP2C (164). Pena et al. have shown that miR-214 through targeting TFAP2C and ITGA3, suppresses inhibitory regulation of melanoma tumour cells, thereby promoting the expression of a number of cell adhesion molecules, which includes MCAM. Additionally, this group found that the manipulation of miR-214 resulted in modulation of metastatic potential (164). Given our previous experiences on MCAM as a candidate marker for late EPCs, we postulated that this cell adhesion molecule likely serves an important role in late EPCs, which could

possibly be exploited to uncover some of the previously unknown features of late EPCs. We chose not to pursue investigating miR-214 or other MCAM associated microRNAs so as to not deviate from our original hypotheses on miR-146a and miR-126.

In the end, our analysis of the global gene and microRNA arrays confirmed our initial observations regarding high expression of miR-146a/b and miR-126 in early and late EPCs (respectively) and provided new perspectives on the processes regulated by these microRNAs (Figure 14). Combined, these findings encouraged us to explore the role of miR-146a in early EPCs and also the role of miR-126 in enhancing the angiogenic potential of late EPCs.

3.2.5 Chapter 3 Part 2 Summary

Using a global microRNA array and microarray, we confirmed that the miR-146a family was prominent in early EPCs (by the presence of both guide and passenger strands of miR-146b) and that differences in the expression of the downstream genes affected by miR-146a should be further studied. Since miR-146b is within the same microRNA family as miR- 146a and that the top two predicted targets of miR-146a and miR-146b-5p are identical, we speculated an important role for TRAF6 and IRAK1 (especially considering a total of 3 and 2 evolutionary conserved 8mer sites as predicted by Targetscan). Since TRAF6 and IRAK1 are important in TLR4 signalling, we speculate that the immune-modulatory effects of miR-146a may contribute to the beneficial effects of early EPCs in models of vascular injury and ischemia for instance, by reducing expression of its targets IRAK1 and TRAF6. In late EPCs, we found that miR-126 was one of the most abundant microRNAs and this is consistent with an important role in promoting a pro-angiogenic phenotype in late EPCs (as seen typically in

mature endothelial cells). Finally, in the list of the top 25 microRNAs in late EPCs one microRNA (miR-214) was purportedly shown to upregulate expression of MCAM. In the following chapters we begin to explore the biological relevance of these findings on cell function and finally, on derivation of late EPCs.

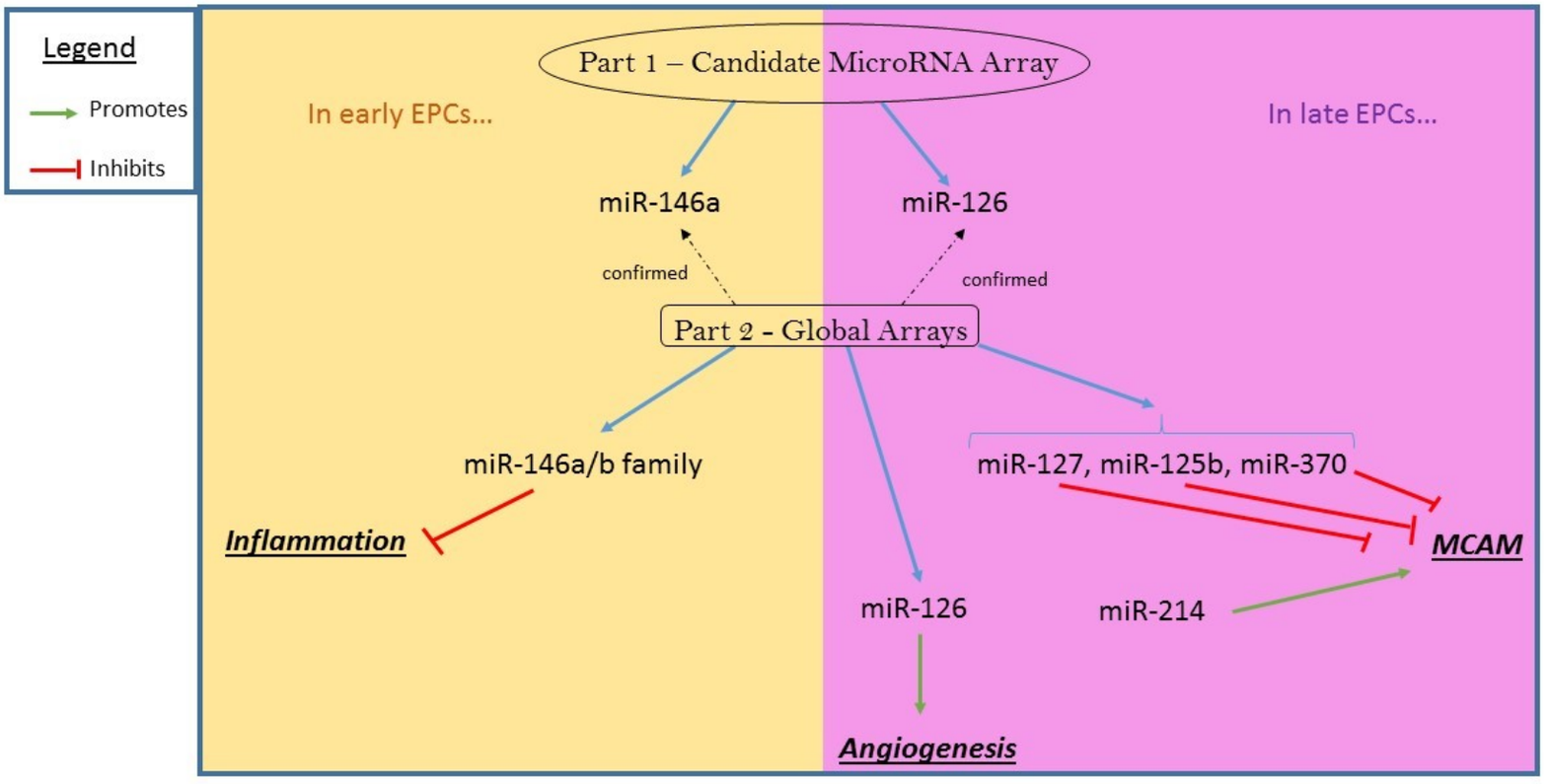

Figure 14: Schematic summary of Chapter 3 findings

In part 1, we used a candidate microRNA array to identify changes in microRNAs as a predominantly MNC population gradually gave rise to early EPCs and noted that miR-146a increased significantly as early EPCs became the predominant cell population. After the emergence of late EPCs, we noted a substantial and significant increase in miR-126. In part 2, our global microRNA and gene arrays corroborated with existing literature supporting MCAM as a gene of interest in late EPCs. Our combined array findings suggested that microRNAs mediate part of anti-inflammatory properties noted in early EPCs and the pro-angiogenic properties reported in late EPCs (via miR-146a and miR-126 respectively). Additionally, these findings also highlight an unknown feature in late EPCs through microRNA regulation of MCAM.

CHAPTER IV: MicroRNA 146a Modulates Immune Phenotype of Early EPCs

4.1 Introduction

In the preceding chapter we have shown that early EPCs possessed an entirely distinct microRNA expression profile compared to that of late outgrowth EPCs and mature endothelial cells like HUVECs. Specifically, we noted that as MNCs adopted an early EPC phenotype, miR-146a expression progressively increased, while miR-146a expression was substantially reduced in the late outgrowth EPCs emerging from these same cultures (Figure 8). This is illustrated in Figure 15, which presents expression of miR-146a relative to "housekeeping" microRNAs in MNCs, early EPCs and late EPCs (panel A) as well as the averaged fold change in miR-146a and miR-132 in early and late EPCs relative to MNCs (panel B). However, compared to miR-132, miR-146a had substantially greater basal expression in MNCs (Figure 8), suggesting a more meaningful fold increase in expression (for example, 0.004 to 0.016 versus 3.4 to 13.6 are both four fold increases).

Our lab has previously shown that the mechanism of action of early EPCs in preventing the establishment of pulmonary arterial hypertension in a rat model was at least in part mediated through an immune-regulatory mechanism (70). This finding prompted us to take a greater interest in the immunomodulatory ability of these cells. Moreover, there is growing evidence that miR-146a may play a key role in promoting an anti-inflammatory phenotype in monocytes and macrophages, which further encouraged us to explore its role in promoting an immunomodulatory phenotype that may be relevant for the therapeutic effects of early EPCs (105, 109, 111). Computational microRNA target prediction revealed that IRAK1/TRAF6 are highly conserved targets for miR-146a and play a crucial role in the regulation of TLR4/TRAF6/NFKB signaling (Figure 11). The results of our candidate and unbiased miRNA expression analysis showed that miR-146a/b family members were highly

enriched in early EPCs. Moreover, as shown in Figure 11 of the previous chapter, both family members share highly conserved sequences predicted to target the 3'UTR of TRAF6 and IRAK1, genes that are known to be important in the regulation of the response of MNCs to inflammatory stimuli. These findings suggest that miR-146a/b family may play an important role in regulating the immune modulatory activity of early EPCs. As shown in Figure 16, both TRAF6 and IRAK1 are involved in mediating the TLR4-stimulated inflammatory response that result in NFKB activation. Thus, since both targets of miR-146a/b are involved in the classic TLR4 inflammatory response pathway, we speculated that miR-146a would confer some inflammatory tolerance in early EPCs by silencing the expression of key intracellular components of this pathway. Indeed, it has previously been reported that in addition to activation of NFKB, TLR stimulation by cytokines can result in upregulation of miR-146a and the silencing of TRAF6/IRAK1 (Figure 17). Nahid et al. reported that TLR4-stimulated THP-1 monocytes exhibited higher expression of miR-146a, which resulted in an overall reduced inflammatory response (86). Therefore, miR-146a can mediate through a negative feedback mechanism that terminates the inflammatory response, reducing the NFKB activity and potential harmful effects of chronic TLR stimulation (165).

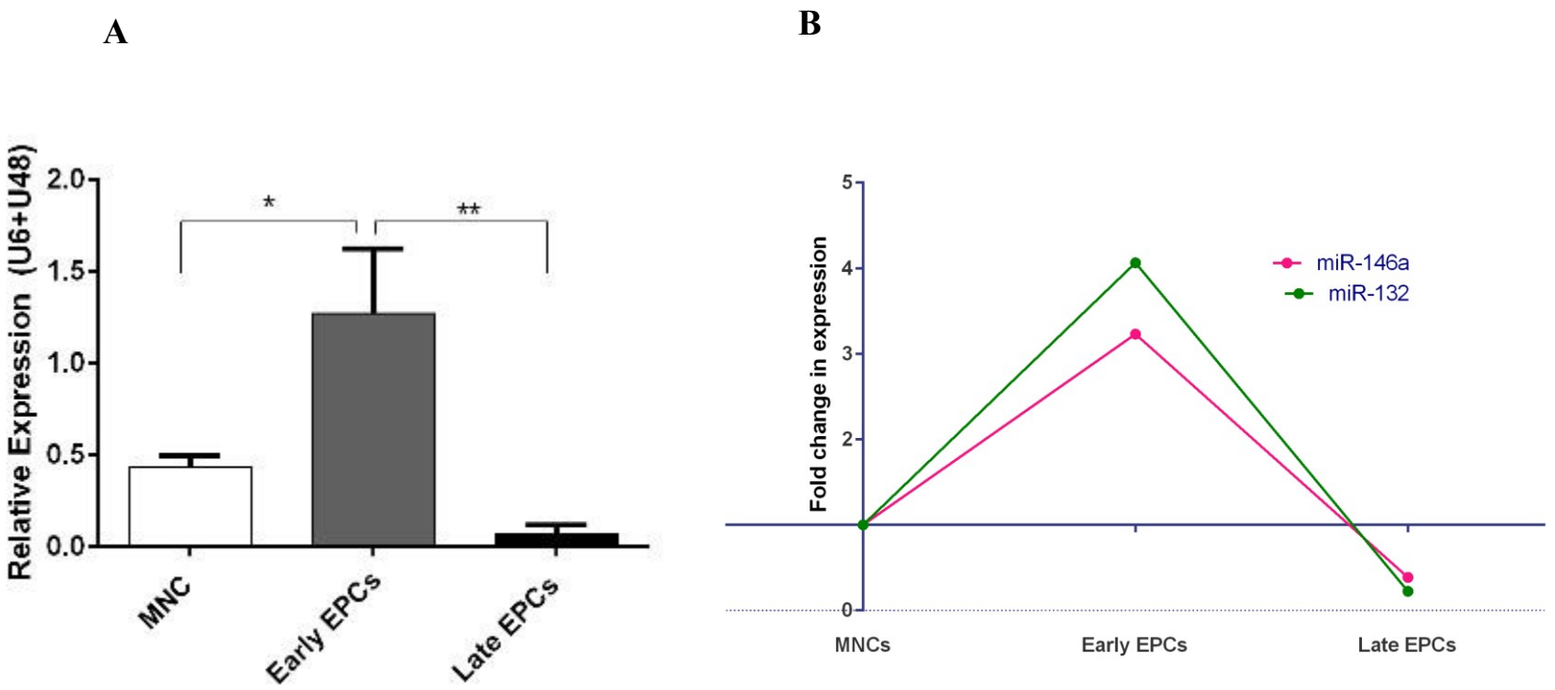

Figure 15: Expression of miR-146a in early EPCs

"MNC" represents a grouped population of cells cultured from days 1-3. "Early EPCs" represents grouped population of cells from days 5-9. Late EPC populations were grouped in "Late EPCs". (A) Early EPCs had significantly higher expression of miR-146a compared to MNCs. When compared to late EPCs, early EPCs had yet even greater expression. (B) To assess fold differences in expression, the expression values were averaged for the two highest expressed microRNAs in early EPCs (miR-146a and miR-132). Data represent mean ± SEM; n = 5-8. *$p<0.05$, ** $p<0.01$.

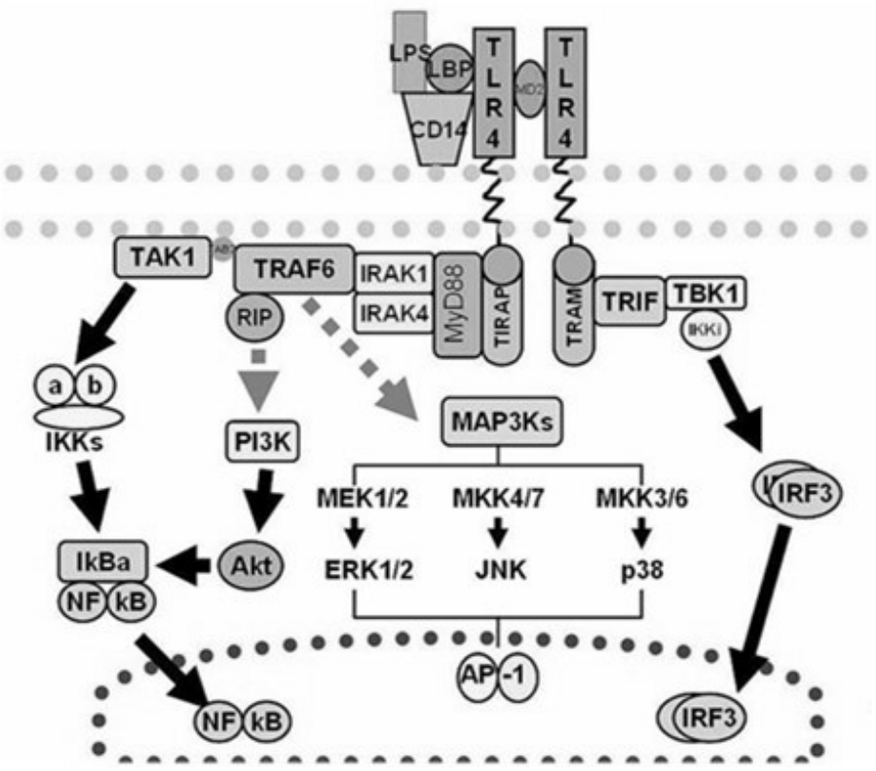

Figure 16: TLR4/TRAF6/NFKB pathway during inflammation

Classical stimulation of TLR4 receptors by inflammatory ligands results in the downstream activation of NFKB, causing an overall increased cytosolic p50 and ultimately, translocation of the p65 unit into the cell nucleus. Interaction of TRAF6 and IRAK1 with the TLR4 receptor complex is essential for the activation of PI3K and subsequently NFKB, a central regulator in inflammatory cell activation. Thus, the predicted effect of miR-146a would be to silence the expression of these two components of the TLR4 signaling cascade, likely blunting the inflammatory response of the cell to TLR4 ligands such as LPS. This, coupled with our previous finding that miR-146a is expressed very highly in early EPCs, would suggest that these cells are already primed to exhibit a blunted immune response to this stimulus. Image is open access.

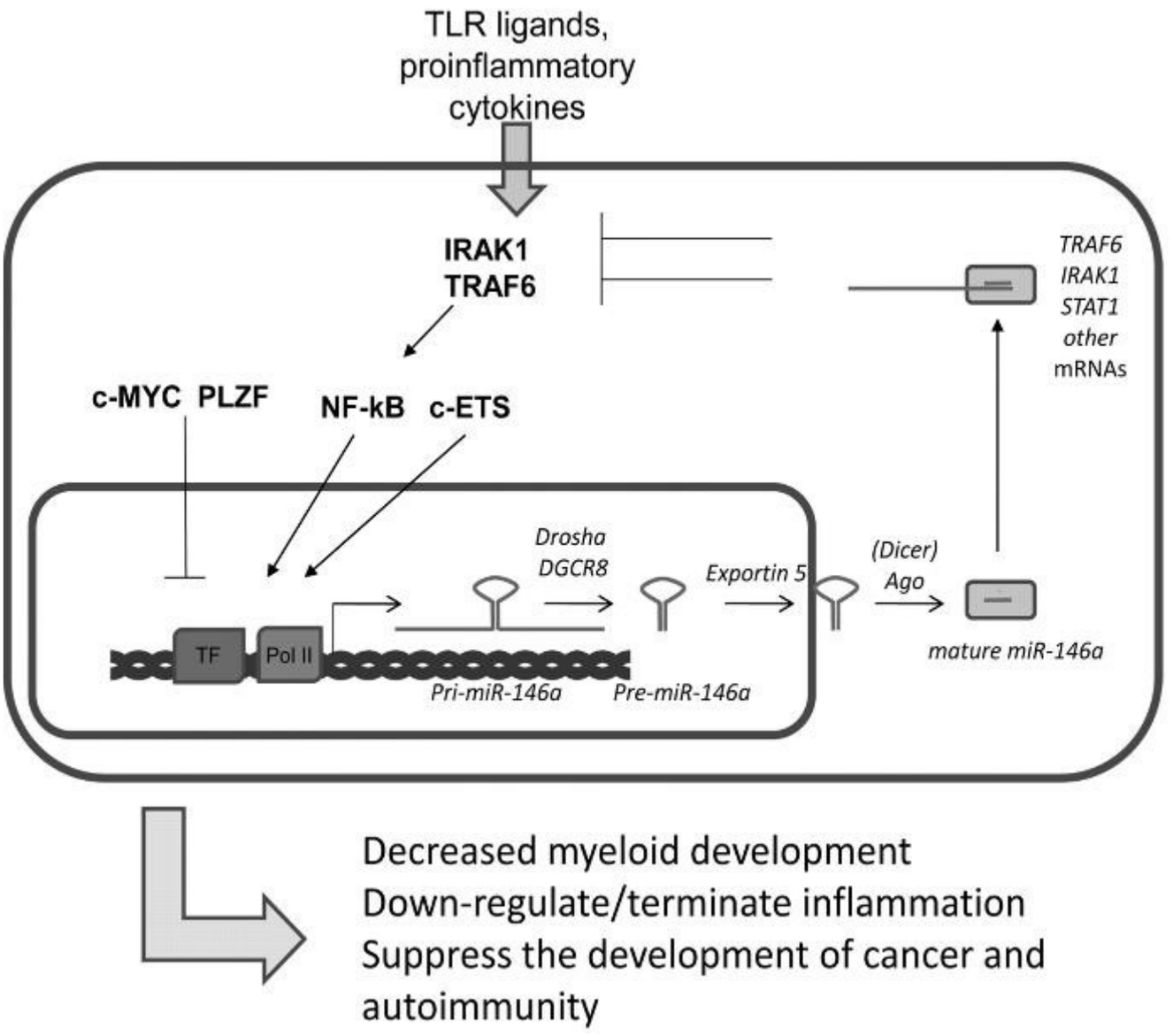

Figure 17: Negative feedback loop of miR-146a on TLR4/TRAF6/NFKB signaling

Inflammatory cytokines stimulate TLR4 receptor, initiating an inflammatory response via MyD88/IRAK1/TRAF6 and downstream cytosolic signaling resulting in the translocation of NFKB. This process starts a negative feedback causing miR-146a inhibition of the inflammatory cascade through sequestering of IRAK1/TRAF6. Obtained with permission from O'Connell et al (2011).

4.2 Hypothesis and Aims

Hypothesis: MiR-146a represents a key regulator of the immune modulatory activity of early EPCs by terminating the pro-inflammatory response to sustained cytokine stimulation and reducing NFKB activation.

Aim 1: To evaluate the effect of miR-146a in modulating early EPC response to TLR4 stimulation.

Aim 2: To determine the effects of miR-146a manipulation on pro/anti-inflammatory cytokine release by early EPCs.

4.3 Results

a) Expression of miR-146a increases during early EPC outgrowth

We first assessed whether mononuclear cells grown heterogeneously gave rise to early EPCs with different miR-146a expression compared to early EPCs grown from a homogeneous CD14 MACs-sorted population. At the first day of plating, the $CD14^-$ (non-monocyte) population had significantly higher expression of miR-146a compared to the $CD14^+$ (monocytes), $p<0.01$ (Figure 18). 9 days of *in vitro* cultivation of mononuclear cells resulted in marked enrichment of the $CD14^+$ monocytes with an increase in miR-146a (especially after 5 days in culture). This finding is consistent with a marked increase in miR-146a in culture modified, as opposed to circulating, monocytes.

b) Treatment of early EPCs with LPS augments miR-146a expression

Early EPCs treated with the TLR ligand LPS exhibited a rapid change in phenotype after 24 hours (Figure 20A). With LPS treatment, early EPCs lost their rod-shaped morphology and regressed towards a rounded cell type (Figure 20A). Using qRT-PCR we detected that LPS-treated early EPCs exhibited significantly higher expression of miR-146a ($p<0.0002$) compared to the untreated group (Figure 19). As control, we treated early EPCs with IL-4, a non-TLR4 ligand that induces M2 macrophage phenotype by binding the IL4 receptor and signals in a manner distinct from TLR4. IL-4 treated early EPCs exhibited less pronounced change in phenotype and no change in miR-146a expression. This finding confirms that as in monocytes, miR-146a is increased in response to TLR stimulation in early EPCs, and thus could potentially mediate a negative feedback mechanism modulating the long response of these cells to pro-inflammatory cytokines. Therefore, we next sought to manipulate miR-146a levels in order to confirm its role in immune regulation of early EPCs.

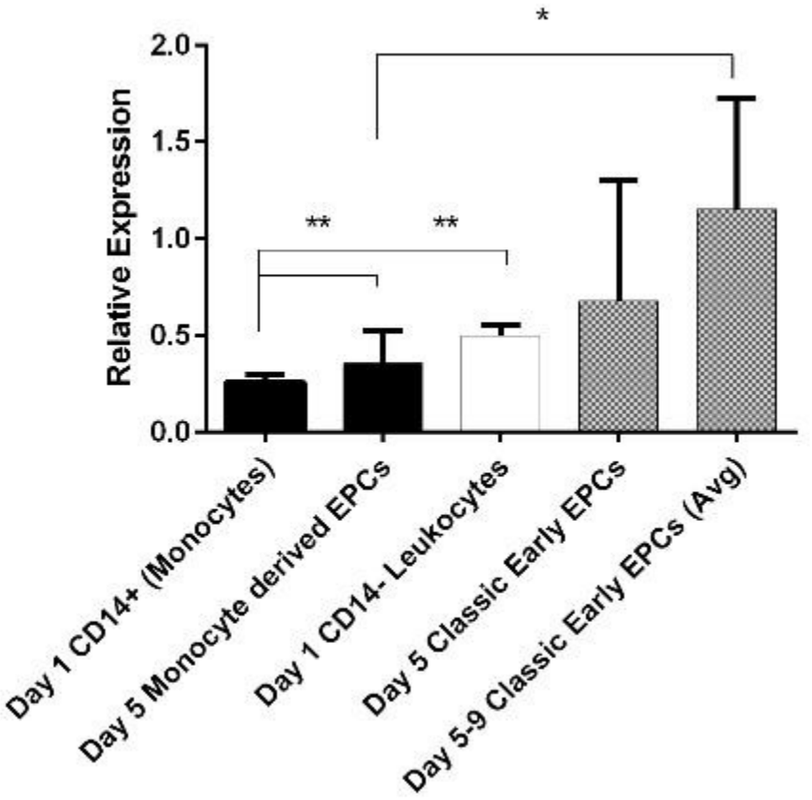

Figure 18: Progressive increase in miR-146a occurs with maturity of early EPCs

Day 5 ($CD14^+$) monocyte-derived EPCs expressed higher miR-146a than day 1 ($CD14^+$) monocytes. Day 1 leukocytes depleted of $CD14^+$ cells expressed higher miR-146a than day 1 monocytes. "Classic" refers to cells grown from heterogeneous MNC population as usual. Data represent mean ± SEM; n = 3-7. *$p<0.05$, ** $p<0.01$.

A

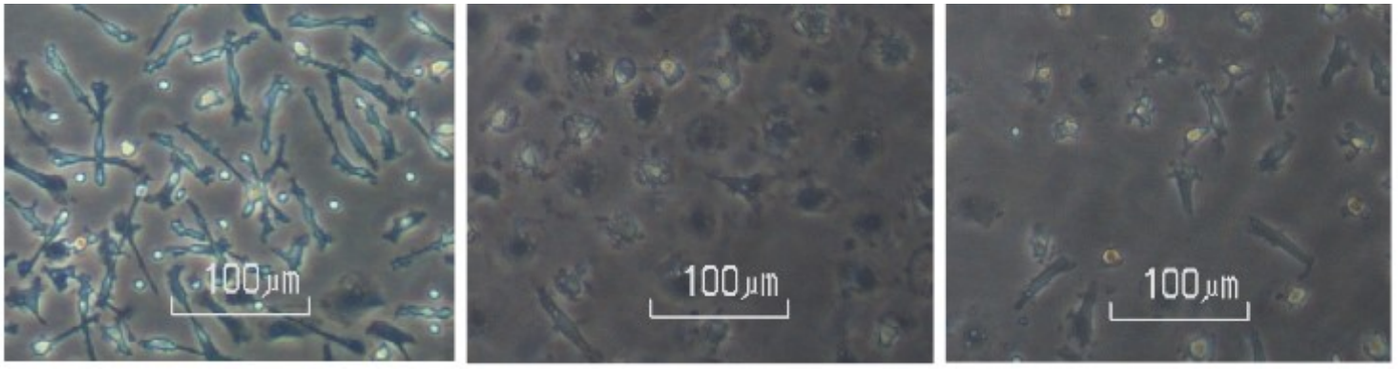

B

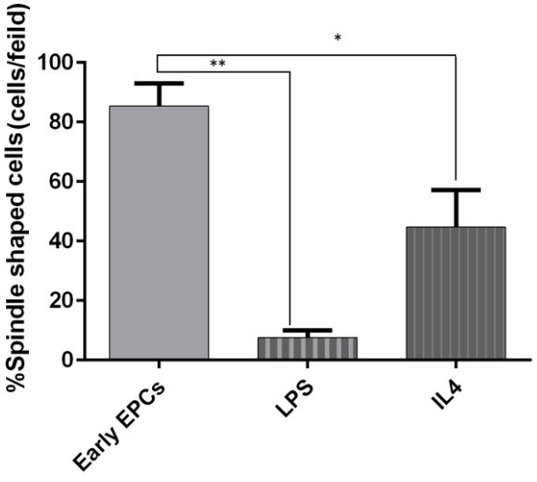

Figure 20: Endotoxin-induced loss of rod morphology within 24 hours

Upon treatment with LPS, early EPCs underwent rapid loss of classical morphology. (A) From left to right, normal, LPS-, IL4-stimulated early EPCs at 300x magnification. (B) Significant loss of rod morphology in early EPCs treated with LPS. Data represent mean ± SEM; n = 3. *p<0.05 **p<0.01.

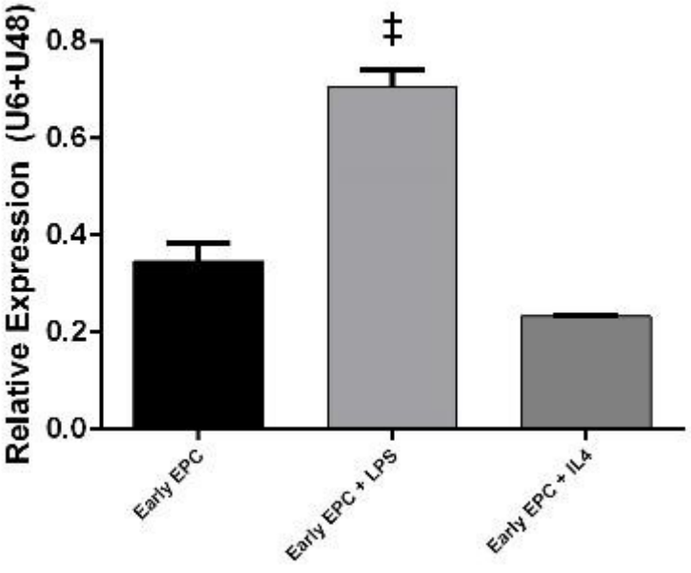

Figure 19: Stimulation of early EPCs with LPS induces increased miR-146a

Early EPCs grown under normal conditions were stimulated with LPS or IL4 (at day 5) for 24 hours. Data represent mean ± SEM; n = 3. ‡p<0.0002.

c) Assessing distribution and transfection efficacy using FAM-labelled oligonucleotides

In order to further explore how manipulation of miR-146a affects early EPCs, we first confirmed distribution and uptake of microRNA inhibitors using immunofluorescence and flow cytometry, respectively. Day 5 early EPCs transfected with fluorescently-labeled miR-146a inhibitors were visualized using fluorescence microscopy. Fluorescence imaging confirmed presence of labeled oligonucleotides within the cytoplasm. Following

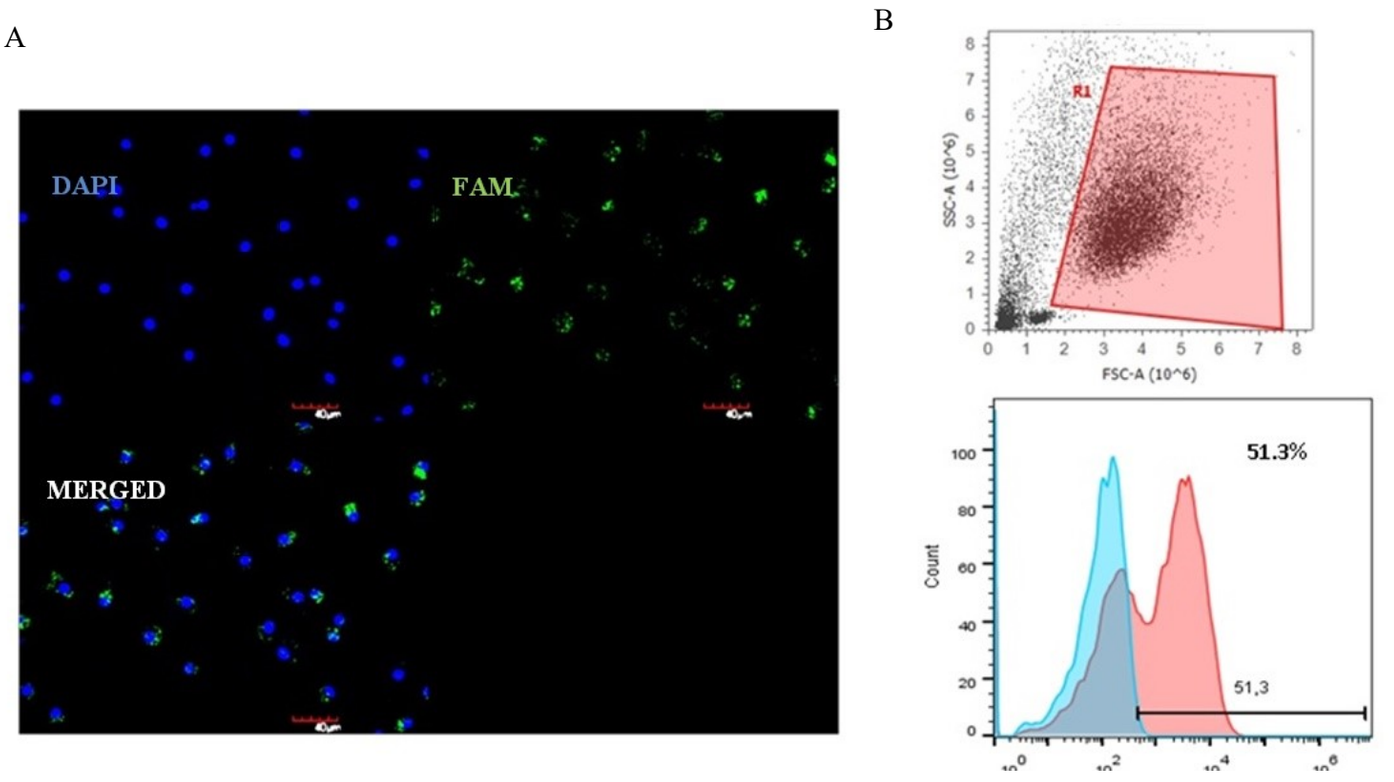

Figure 21: Detection of FAM-labelled microRNA inhibitors in early EPCs

(A) Early EPCs were transfect with fluorescently-tagged (FAM-labelled) miR-146a inhibitors using Lipofectamine 2000™ on day 5 of culture. Cells were fixed and imaged for fluorescence to detect distribution. FAM-labelled uptake was also measured using flow cytometry (B). Representative images at 100x magnification were produced 24hours post-transfection. Scale bar represents 40μm.

transfection, flow cytometric analysis showed that at least half of the cells had uptaken microRNA inhibitors (Figure 21B).

d) Sequence confirmation of miR-146a and target MRE using luciferase reporter construct

To confirm that our microRNA mimic sequence for miR-146a appropriately targets the 3'UTR of TRAF6 (and thus has validity) we performed a luciferase reporter assay. Using the algorithm predicted TargetScan sequence alignments in Figure 22 (and the complete human gene sequence for TRAF6 found in Appendix C) we designed a TRAF6 luciferase construct with LightSwitch 3'UTR GoClone reporters. Using this 3'UTR reporter system, successful miRNA targeting should result in reduced luciferase signal detection. Co-transfection of miR-146a mimic with TRAF6 reporter construct resulted in greater than 52% reduction in luciferase signal compared scramble-miR control $p<0.01$ (Figure 22B), thus confirming that TRAF6 is a target for miR-146a.

e) Knockdown of miR-146a in early EPCs increased NFKBp50 expression

To assess the impact of manipulation of miR-146a on the immune activation state of early EPCs, we measured NFKBp50 expression. Basal expression of NFKBp50 was minimal in early EPCs under usual culture conditions (Figure 23A). Transfection of early EPCs with scramble-miR resulted in no change in NFKBp50. With LPS treatment, a noticeable increase in NFKBp50 expression was detected (Figure 23A). Knockdown of miR-146a in early EPCs using microRNA inhibitors induced a significant increase in NFKBp50 expression compared to scramble-miR control, which was comparable to LPS. Quantitative RT-PCR indicated that knockdown in concert with LPS induced even greater increase in NFKBp50 mRNA (Figure 23B).

A

Position 59-65 of TRAF6 3' UTR
hsa-miR-146a

```
5'    ...GCCUUUCCUUGCCCUGUUCUCAA...
                          ||||||
3'       UUGGGUACCUUAAGUCAAGAGU
```

Position 473-480 of TRAF6 3' UTR
hsa-miR-146a

```
5'  ...UGCUCUAGAAAGUUGAGUUCUCA...
                        |||||||
3'      UUGGGUACCUUAAGUCAAGAGU
```

Position 538-545 of TRAF6 3' UTR
hsa-miR-146a

```
5'   ...UCCUUGGAAAACUUAAGUUCUCA...
           |||||       |||||||
3'    UUGGGUACCUUAAG---UCAAGAGU
```

Position 1272-1279 of TRAF6 3' UTR
hsa-miR-146a

```
5' ...AAUAUCGUGGAAUCUAGUUCUCA...
             ||||||   |||||||
3'     UUGGGUACCUUAAGUCAAGAGU
```

B

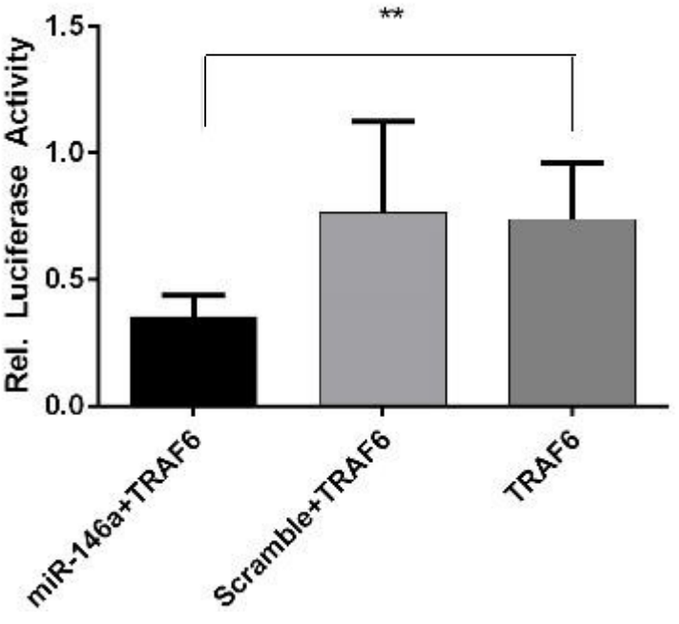

Figure 22: TRAF6 luciferase reporter silenced via miR-146a mimic

(A) The putative 3' UTR targets of miR-146a were initially predicted by TargetScan algorithm. (B) In HEK293T cells, co-transfection of miR-146a and TRAF6 reporter construct resulted in reduced luciferase detection (non-targeting miRNA was used for control). Data relative to TRAF6 construct alone; and represent mean ± SEM; n = 6-7. **p<0.01.

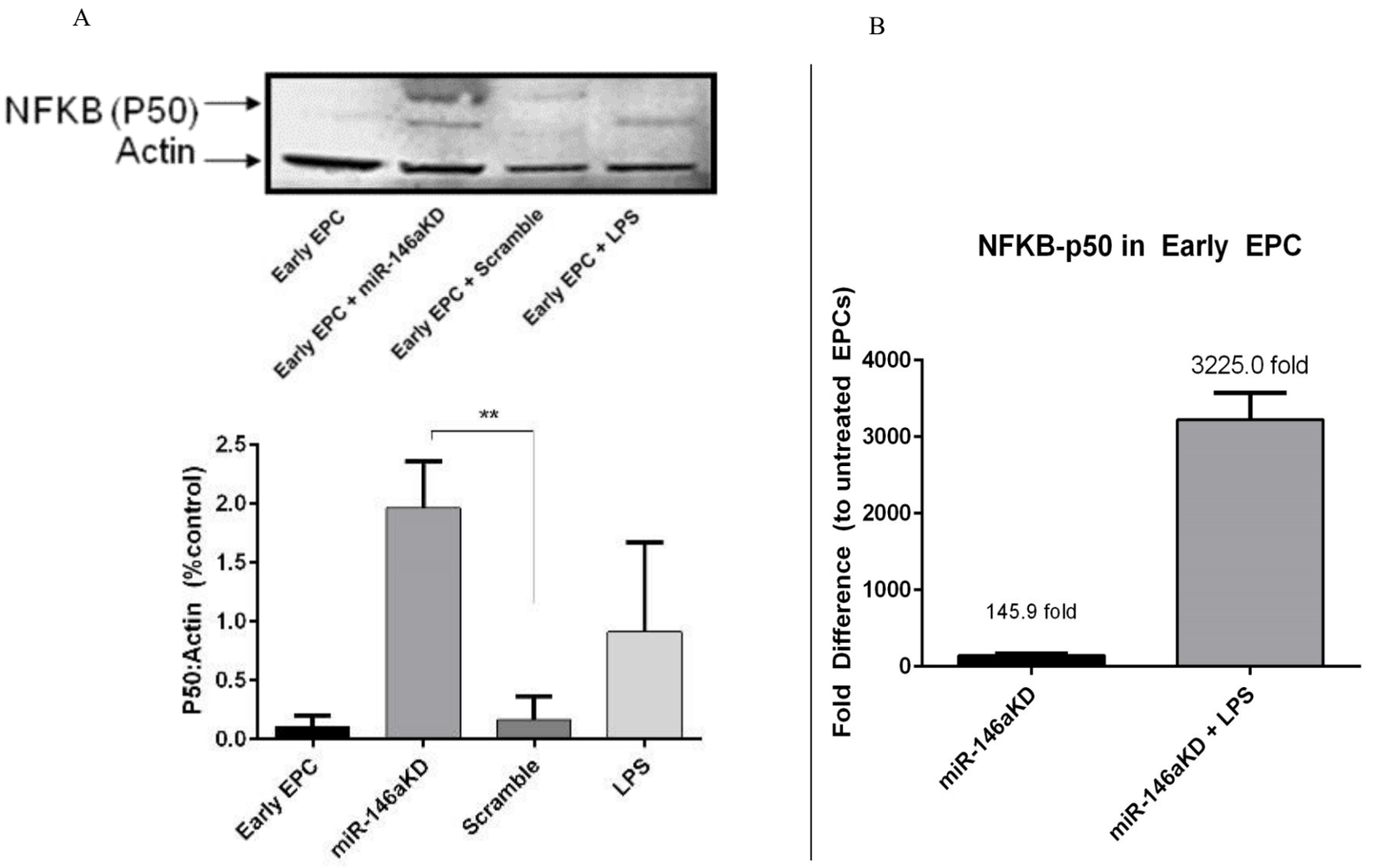

Figure 23: Knockdown of miR-146a induces increased p50 in early EPCs

(A) Representative Western blot and quantification by densitometry show significantly increased expression of NFKBp50 in early EPCs with miR-146a knockdown (using beta actin as control). (B) Fold differences in NFKBp50 expression in early EPCs (upon LPS treatment and miR-146a manipulation) by qRT-PCR. The values shown above the bars in (B) represents fold differences when the data in each group is averaged and compared to untreated early EPCs. Data represent mean ± SEM; n = 3. ** $p<0.01$.

f) Knockdown of miR-146a in early EPCs increases BrdU, but not total early EPC count

To assess whether changes in miR-146a levels alter EPC proliferation we conducted a BrdU assay. BrdU measures the presence of cells undergoing DNA synthesis. This was measured to assess whether EPCs where undergoing proliferation when NFKB expression had increased. Early EPCs were grown to day 5, transfected with miR-146a inhibitors and then assayed for BrdU after 24 hours. The cells that had been transfected with miR-146aKD (which had increased NFKB) also showed increased BrdU using ELISA (Figure 24). Despite this evidence of increased proliferation, no noticeable change in cell number was detected using hemocytometric cell counting (data not shown). We speculated that increase in measured BrdU reflected an increase in S-phase activity of early EPCs.

g) MiR-146a manipulation causes no change in cell adhesion or apoptosis

Cell adhesion to fibronectin was measured on captured images using ImageJ. Using the technique outlined in section (m) of the material and methods chapter, we sought to measure changes in the number of adherent cells. Early EPCs were grown to day 5, transfected overnight as previously described and imaged to assess cell adhesion prior to ELISA. No significant changes with treatments were detected with miR-146a knockdown (Figure 25A). We also looked at apoptosis because both miR-146a and miR-126 (which was focused on in the next chapter) are known to affect apoptosis and CCASP3 is one method to assess apoptosis. To measure changes in apoptosis, ELISA was performed for cleaved caspase3 activity. Likewise, no significant differences were detected in

apoptosis between miR-146a knockdown or over expression compared to control (Figure 25B). These findings were consistent in showing no increases in cell number despite increased S-phase activity.

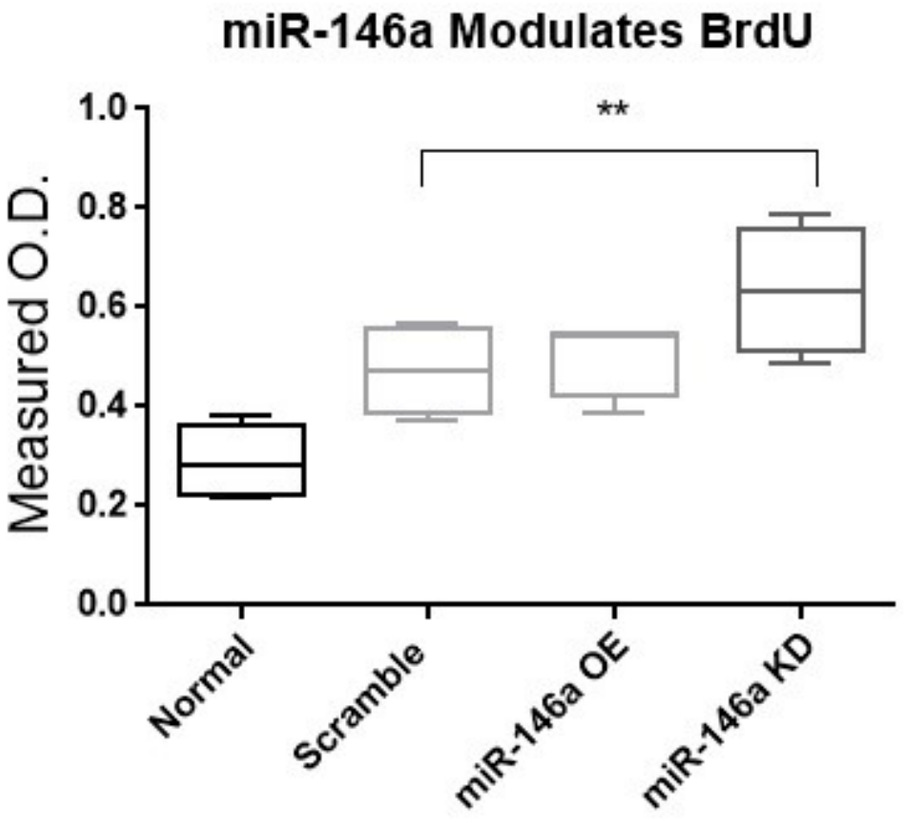

Figure 24: Knockdown of miR-146a augments detected BrdU in early EPCs

Early EPCs treated with microRNA mimic (OE) or inhibitor (KD) or scramble-miR was assessed for proliferation. Data represent median ± interquartile range; n = 3-4. ** $p<0.01$.

A

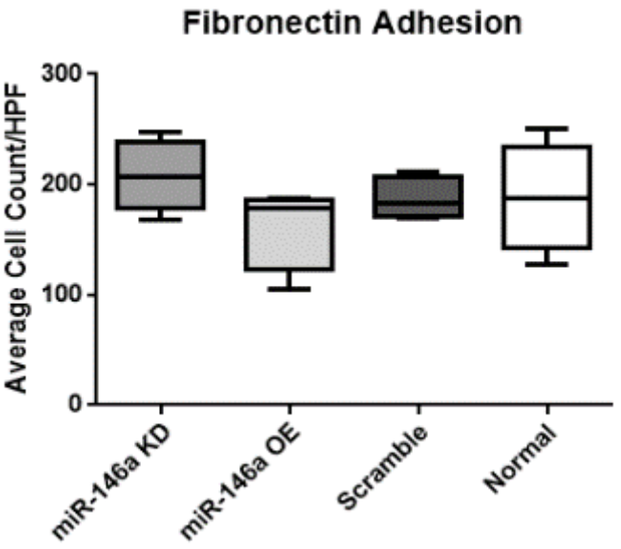

B

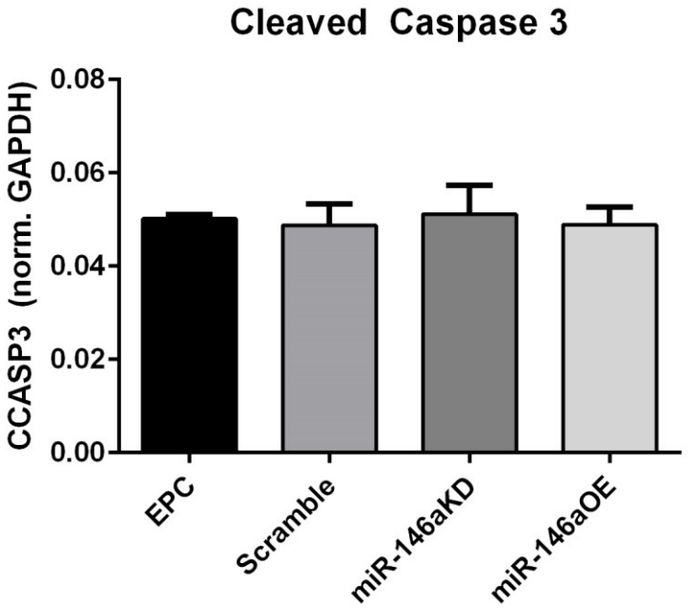

Figure 25: Manipulation of miR-146a in early EPCs does not affect adhesion or cell death

(A) Over expression and knockdown of miR-146a had no significant effect on EPC adhesion to fibronectin. (B) Cleaved caspase 3 activity assay was conducted for early EPCs and miR-146a manipulated early EPCs. HPF refers to high-powered field. Normal refers to early EPCs grown per normal protocol. EPC refers to typical or normally cultured early EPCs. CCASP3 data was normalized to GAPDH for each respective group. Fibronectin adhesion data (top) represents median and CCASP3 is mean ± SEM, n=3.

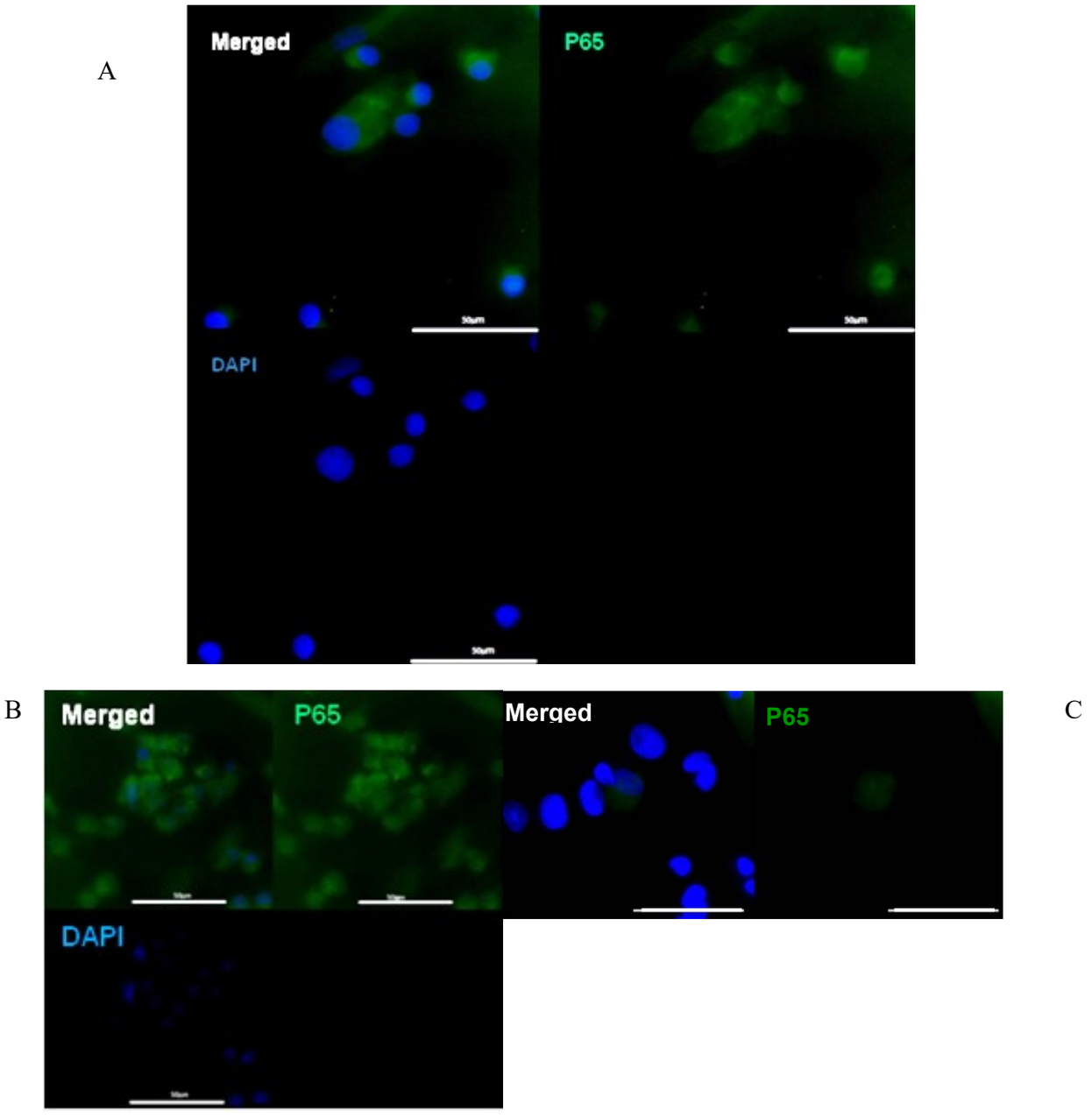

Figure 26: Knockdown of miR-146a induces translocation of p65 to early EPC nucleus

Representative immunofluorescent images showing increased p65 expression within the nucleus of early EPCs with mir-146a knockdown (A) and LPS treatment (B). Scramble treatment (C) showed no nuclear p65 expression, with comparatively less cytoplasmic presence. N=3, scale bar represents 50μm.

h) Knockdown of miR-146a in early EPCs induces nuclear translocation of NFKBp65

To confirm canonical NFKB activation, we tested whether nuclear translocation of NFKBp65 occurred. Using immunofluorescence we confirmed that knockdown of miR-146a in day 5 early EPCs resulted in noticeable translocation of NFKBp65 into the cell nucleus (Figure 26A). Since LPS affects the entire TLR4 inflammatory pathway, we expected higher fluorescence in B; whereas in A we only partially targeted the pathway, and hence observed reduced fluorescence (as expected). Comparatively, we noted the same response in early EPCs treated with TLR4 ligand, LPS (Figure 26B). No change was noted with scramble-miR transfection of early EPCs (Figure 26C).

i) MiR-146a promotes anti-inflammatory cytokine response in early EPCs

A major mode of repair by early EPCs in injury is via cytokine release, so we assessed the effect of miR-146a manipulation on cytokine expression in early EPCs. As we had expected, LPS treatment of early EPCs increased both inflammatory cytokines IL-1 and IL-8. Additionally, we noted an increase in anti-inflammatory cytokine 1L-1 receptor antagonist (IL-1RA), which likely participates in blunting the inflammatory response. Knockdown of miR-146a had no effect on the release of the IL-1RA (Figure 27) under basal conditions; however, after pro-inflammatory stimulation with LPS, knockdown of miR-146a significantly reduced the release of this anti-inflammatory cytokine. In contrast, miR-146a knockdown potentiated the release of the pro-inflammatory cytokines, IL-1b and IL-8, after LPS treatment. These results are consistent with miR-146a modulating the response of early EPCs to LPS stimulation by shifting the release profile from pro- to anti-inflammatory cytokines.

Thus far, compared with LPS treatment alone, knockdown of miR-146a in concert with LPS treatment reduced IL-1RA and augmented IL-1b and IL-8 significantly ($p<0.01$, 0.001 and 0.01, respectively). No changes were detected with scramble-miR treatment. No significant changes were detected in the remaining 24 human cytokines assayed.

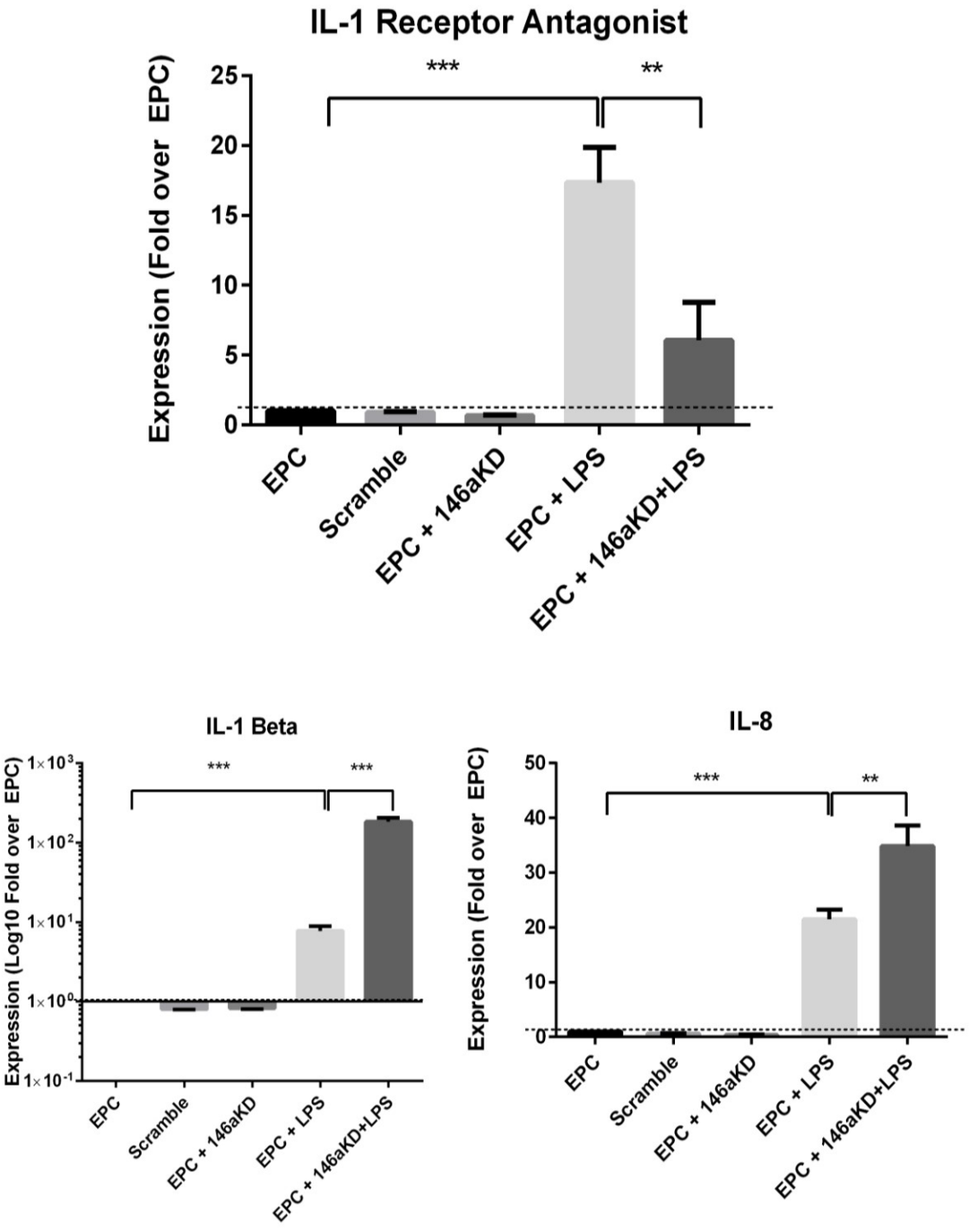

Figure 27: Knockdown of miR-146a exacerbates inflammatory cytokines in endotoxin-stimulated early EPCs

Early human EPCs were grown to day 5 and treated with LPS following knockdown of miR-146a. Anti-inflammatory (IL-1ra) and pro-inflammatory (IL-1b and IL-8) cytokines were quantified using ELISA. Data represent mean ± SEM; n=3. *** $p<0.001$, ** $p<0.01$.

4.4 Discussion

The high specificity of miR-146a for TRAF6 and IRAK1 as shown in Figure 11, representing 3 and 2 conserved 8mer sites (respectively) signifies conserved target branch length; the higher the #mer (corresponding to the number in complementarity in seed sequence), the stronger the regulation by the microRNA in question, with 8 being the highest (and rarest). Additionally, the top targets are ranked based on existing literature, which corroborates the predicted complementarity. This clearly suggested a role for miR-146a in the modulation of the TRAF6/IRAK-dependent activation of early EPCs in response to TLR stimulation by LPS (Figure 16). Since the same microRNA targets two interacting proteins in the same pathway, it may further enhance its inhibitory effects. In this case, miR-146a likely plays an important role in modulating inflammatory NFKB signalling within early EPCs. To this end, our results support the notion that increased miR-146a mediates negative feedback regulation of NFKB expression in early EPCs after TLR4 stimulation. The higher level of miR-146a in early EPCs is consistent with numerous reports that support an immune modulatory role for early EPCs (70, 166, 167). To confirm that miR-146a modulated the response of early EPCs to pro-inflammatory stimuli, we compared miR-146a expression in early EPCs treated with TLR4 ligand LPS; and to cells treated with IL4, which acts through a separate receptor and signalling pathway. Stimulation of early EPCs with LPS resulted in robust increase in miR-146a expression compared to untreated early EPCs ($p<0.0002$, Figure 19B). However, IL4 had no significant effect on miR-146a. This immune-modulating feature of miR-146a that blunts inflammatory stimulation was previously reported by Nahid et al. (105). We postulated that the progressive increase in miR-146a in early EPCs acts as a negative feedback brake on inflammation for early EPCs, thereby terminating their activation in response to sustained exposure to pro-inflammatory cytokines such as LPS, and restoring the balance of pro- and anti-inflammatory responses.

Since NFKB is a downstream mediator of LPS response, we compared its expression in untreated early EPCs, early EPCs with LPS treatment and in early EPCs with miR-146aKD. We speculated that a knockdown of miR-146a in early EPCs would remove an inhibitory brake on the TLR4/TRAF6/NFKB pathway and therefore increase NFKB expression/activation in response to TLR stimulation. Indeed, miR-146aKD resulted in a more robust increase in NFKB expression than that of LPS alone (Figure 23B; $p<0.001$). As well, knockdown of miR-146a, resulted in a much greater increase in NFKBp50 (Figure 23B). These findings suggest that miR-146a plays a key role in fine-tuning the response of early EPCs to pro-inflammatory stimuli by providing a mechanism to terminate sustained activation via the TLR pathway, thus promoting a more anti-inflammatory phenotype. It is possible that the marked increase in miR-146a in early EPCs occurs in response to cell-cell interactions between monocytes and other lymphocytes during the initial period of cell culture. Eigsti et al. recently reported that co-culture of monocytes with non-monocytes during the generation of macrophages resulted in a progressive increase in miR-146a (168). This could be mediated by the release of inflammatory factors by non-monocytes and stimulation of the TLR4 pathway, and this has been speculated by others (167). Indeed, supplemental experiments showed that treating late EPCs with conditioned media taken from early EPCs resulted in a greater than fourfold increase in NFKB (Appendix I), supporting the evidence that the presence of non-monocytes contributes to the release of components within the media which contribute to stimulating the TLR4 inflammatory pathway.

Since NFKB activation is associated with increased inflammatory activity and cell proliferation, we sought to investigate the impact of miR-146aKD on early EPC proliferation using a BrdU proliferation assay. Knockdown of miR-146a in early EPCs resulted in a significant increase in BrdU incorporation ($p<0.001$), but this finding was not corroborated with increased cell counts as measured by hemocytometer (Figure 24). Additionally, no changes were detected in apoptosis as measured by cleaved caspase 3 activity or changes in cell adhesion (Figure 25). Therefore, we speculate the response measured by BrdU is indicative of EPCs that are

stalled in S-phase (but this needs to be experimentally validated). The significance of this is twofold, firstly it is known that cells in S-phase become hypersensitive to external changes in order to maintain genomic stability and minimize replication stress (169), as such miR-146a may serve to protect early EPCs from constant TLR4 stimulation and "hypersensitivity"; second, S-phase stagnation is closely linked with oncogenesis and thus miR-146a could be produced as a gatekeeper from erroneous DNA synthesis within forming early EPCs due to differentiation, and not from external stimulation (170). As early EPCs are normally non-proliferative, it is likely that despite increased NFKB activity they are unable to enter cell cycle.

Translocation of NFKB to the nucleus is necessary for its subsequent transcriptional regulation of target genes. Therefore, we performed NFKBp65 immunofluorescence staining to confirm nuclear presence of NFKB in response to LPS and miR-146a KD. For investigating NFKB activation, we performed an immunofluorescence assay for NFKBp65 since the p65 subunit gets translocated across the nucleus upon activation (Figure 26). Knockdown of miR-146a in early EPCs resulted in a noticeable increase in NFKBp65 in the nucleus of early EPCs (Figure 26). Since LPS stimulation results in a robust pro-inflammatory response involving both NFKBp50 and NFKBp65, we expected to detect much greater immunofluorescence when compared to just miR-146KD. Comparatively, miR-146aKD resulted in less immunofluorescence, which is expected because this knockdown would only shut off the basal inflammatory production of miR-146a, whereas LPS stimulation directly stimulates this process.

So far we showed that TLR stimulation of early EPCs with LPS exacerbated NFKB expression. Knockdown of miR-146a alone produced even greater expression of NFKB as detected by Western blot. Since it is known that via TLR stimulation, NFKB activation causes increased cytosolic levels of mature miR-146a in myeloid cells (92), our findings which showed an increase in miR-146a in early EPCs (with LPS stimulation), conforms with this

consensus. Indeed, nuclear presence of NFKBp65 in LPS-treated early EPCs confirmed canonical TLR4/NFKB activation. As such, our results so far have shown that increased miR-146a in early EPCs is likely mediated through NFKB activation, possibly through TLR4 activation.

Recently there has been considerable interest in alternative activation states of monocyte-derived macrophages. Graff et al. published a list of robustly expressed microRNAs in all macrophage polarization states, specifically the M1 and M2 states (155). Interestingly, this group reported mostly passenger-strand microRNAs as highly regulated in the polarized macrophage cell types. As discussed above, early EPCs are in fact a form of culture-modified mononuclear cells and thus it is not surprising that they would share some similarities with macrophages. Indeed, a comparison between early EPCs and macrophages reveals a clear overlap of top expressed microRNAs (155), in particular miR-146a as shown in Figure 8. Furthermore, Graff et al. showed enrichment of miR-146a upon differentiation of monocytes towards a macrophage lineage (155). This raises the question about whether early EPCs may share important similarities with M2 macrophages, which are well known to exert anti-inflammatory and pro-angiogenic effects.

Finally, to further assess the immune modulatory nature of early EPCs, we assessed pro/anti-inflammatory cytokines in early EPCs in response to TLR4 stimulation. In Figure 27, we conducted a human inflammatory cytokine array to 27 human pro/anti-inflammatory cytokines in early EPCs with miR-146aKD, LPS and LPS+miR-146aKD (with significance noted in only 3 of the cytokines, which are shown). We found that miR-146a reduced the expression of pro-inflammatory cytokines after LPS treatment, while increasing the release of the anti-inflammatory cytokine, IL1- receptor antagonist (or IL-1RA). No other significant differences were measured in the remaining 24 cytokines. Moreover, miR-146aKD shifted this balance now favouring the release of pro-inflammatory cytokines IL-1β and IL-8 in response to LPS treatment ($p<0.01$). Thus, miR-146a likely

represents an important mechanism that modulates the response of early EPCs to pro-inflammatory stimuli, promoting an immune modulatory and anti-inflammatory phenotype that may be a component of their therapeutic action.

4.5 Chapter Summary

Collectively, our results show miR-146a acts as a brake on of TLR4 inflammatory cascade in early EPCs. We speculate that a progressive increase in the expression of miR-146a expression during *in vitro* derivation and cultivation of early EPCs primes early EPCs for an inflammatory response to TLR4 activation. Inhibition of miR-146a in early EPCs was linked with increased NFKB levels despite no measurable increase in proliferation. In the presence of miR-146a, LPS stimulation of early EPCs favoured the expression of anti-inflammatory cytokines, such as IL-1RA, over the typical pro-inflammatory cytokines, such as IL-1b and IL-8. These findings support our postulate that miR-146a may be partially responsible for the noted immune modulating therapeutic effects of early EPCs; and confirm our hypothesis that miR-146a reduced pro-inflammatory response of early EPCs to TLR4 stimulation.

CHAPTER V: MicroRNA 126 Promotes Angiogenesis in Early and Late EPCs

5.1 Introduction

The difference in microRNA expression profiles between early and late EPCs suggests vastly different pathways and corresponding roles played by microRNAs in these cell types. The endothelial-like microRNA expression profile of late EPCs supports the possibility that late EPCs arise from a precursor cell type more similar to endothelial cells than early EPCs. Earlier, we showed that late EPCs had substantially higher expression of miR-126 than early EPCs, by greater than 100 fold (Figure 8 and Figure 28). However, the endothelial-like microRNA expression profile of late EPCs does not help distinguish between the two possible origins of these cells, i.e. whether late EPCs arise by differentiation of the early EPCs into a more mature endothelial cell phenotype, or from a precursor cell type that is predestined to give rise to highly endothelial-like late outgrowth EPCs. Nonetheless, the switch to high levels of miR-126 expression in cell transitioning to late outgrowth EPCs suggests ways in which these two possible mechanisms for the origin of these cells could be tested. Thus, miR-126 stood out as a potential microRNA marker for the late outgrowth EPC phenotype. For example, it is possible that miR-126 could drive the adoption of a highly endothelial phenotype and facilitate the differentiation of early EPCs into late EPCs. Alternatively, miR-126 could be expressed by a subset of early EPCs, or even circulating MNCs that are "programmed" to give rise to the late outgrowth cells. The present chapter will focus on the role of miR-126 in promoting an endothelial-like phenotype as well as pro-angiogenic properties of late EPCs.

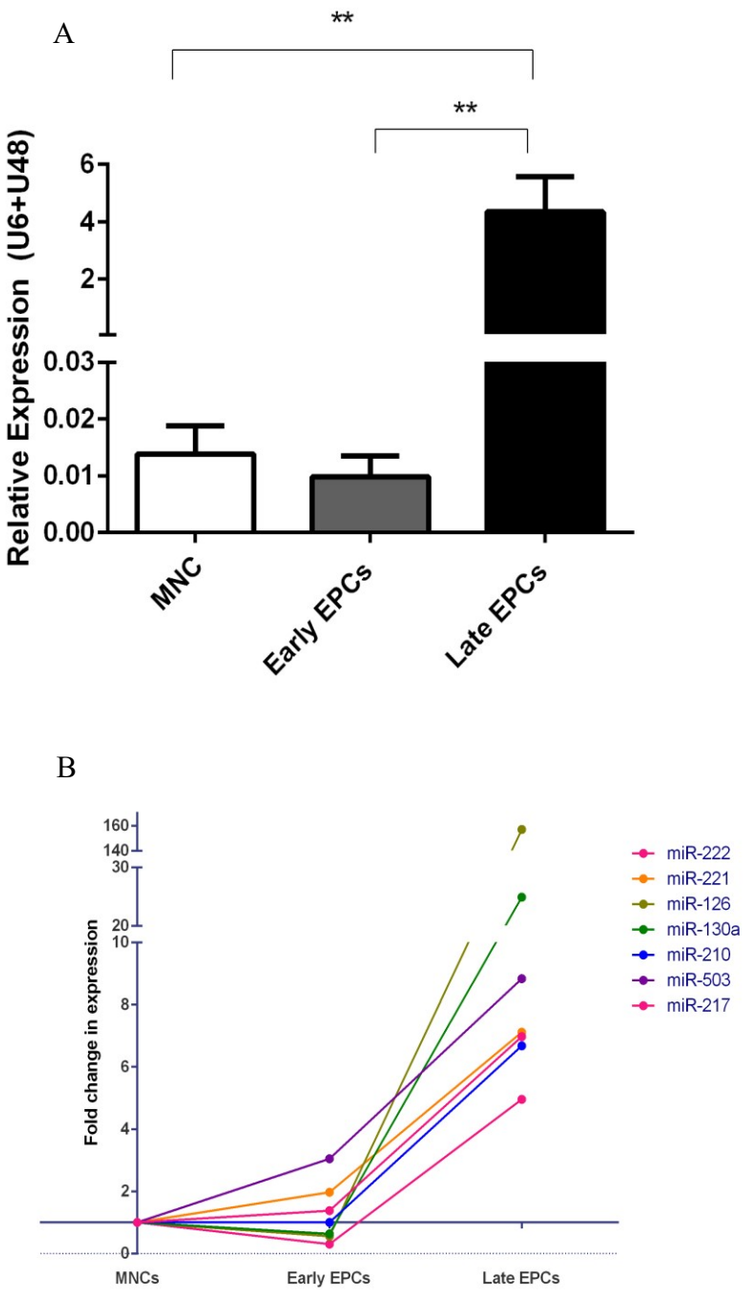

Figure 28: Late EPCs express higher miR-126 than early EPCs and MNCs by several orders of magnitude

During the derivation of early EPCs, the predominant existing cell populations within 1-3 days were MNCs; while early EPCs emerged during days 5-9. Once late EPCs emerged, they were grown to passage 3 at ~80% confluence. (A) The relative expression of miR-126 in MNCs and early EPCs was significantly lower than late EPCs as measured by qRT-PCR. (B) When compared to other microRNAs in the candidate array, miR-126 was the only microRNA with an increased expression in late EPCs by over 100 fold. Data represent mean ± SEM; n=5-8. ** $p<0.01$.

Several reports have shown that miR-126 confers improved endothelial properties in numerous *in vivo* models (66, 162). MicroRNA-126 controls angiogenic signalling and vascular integrity by targeting PIK3R2/p85-beta (phosphinolsitol-3 kinase regulatory subunit 2) and the sprouty regulated protein SPRED-1 (Figure 29) (66, 162, 171). Since late EPCs are thought to promote vascular repair by integrating into the endothelial layer of the tunica intima (28, 30), it is possible that this angiogenic property of late EPCs is related to their highly endothelial-cell like phenotype, and to the high levels of expression of miR-126. To date, several studies have linked miR-126 with regulating typical endothelial cell processes affecting proliferation (172), migration (66, 173) and even apoptosis (174). However, to date, it remains unclear whether over expression of miR-126 could augment the endothelial phenotype of early EPCs and whether this microRNA is essential for late EPC function and phenotype.

Melanoma cell adhesion molecule (MCAM) has long been investigated as a stem cell potency marker and thus has been of interest to our studies. During our global gene and microRNA array, we noted that the three highest expressed microRNAs in late EPCs (miR-125b, miR-370 and miR-127) all had algorithmically predicted seed sequences corresponding to MREs within the mRNA of the melanoma cell adhesion molecule, MCAM. Additionally, one of the highest expressed microRNAs, miR-214 had been reported to increase MCAM expression via suppression of TFAP2C, a homologue of melanoma tumour suppressor (164). These findings peaked our interest in MCAM as a late EPC marker, since it had been a candidate for us as an endothelial cell marker, as well as being a marker for mesenchymal stromal cells (175-177). Several groups have recently published that the presence of MCAM, in combination with the presence or absence of other determinants (178, 179), can identify a subpopulation of mononuclear cells that represent true late EPC precursors (i.e. pre-late-EPCs) from cord blood. MCAM has not been explored in adult progenitor cells as a marker for late EPCs precursors. But today, there is consensus that MCAM is a marker for late EPCs based on studies from cord blood, though it has yet to be established how this marker could be exploited to study the origin of adult late EPCs or identify adult late EPC

precursors (180). In the protocol that is included in the appendix, we present a methodology that we have devised to isolate late EPCs from $MCAM^+$ MNCs from adult peripheral blood. At the end of this chapter, we present our findings with $MCAM^+$ MNCs and the significance of miR-126 on the fate of late EPCs.

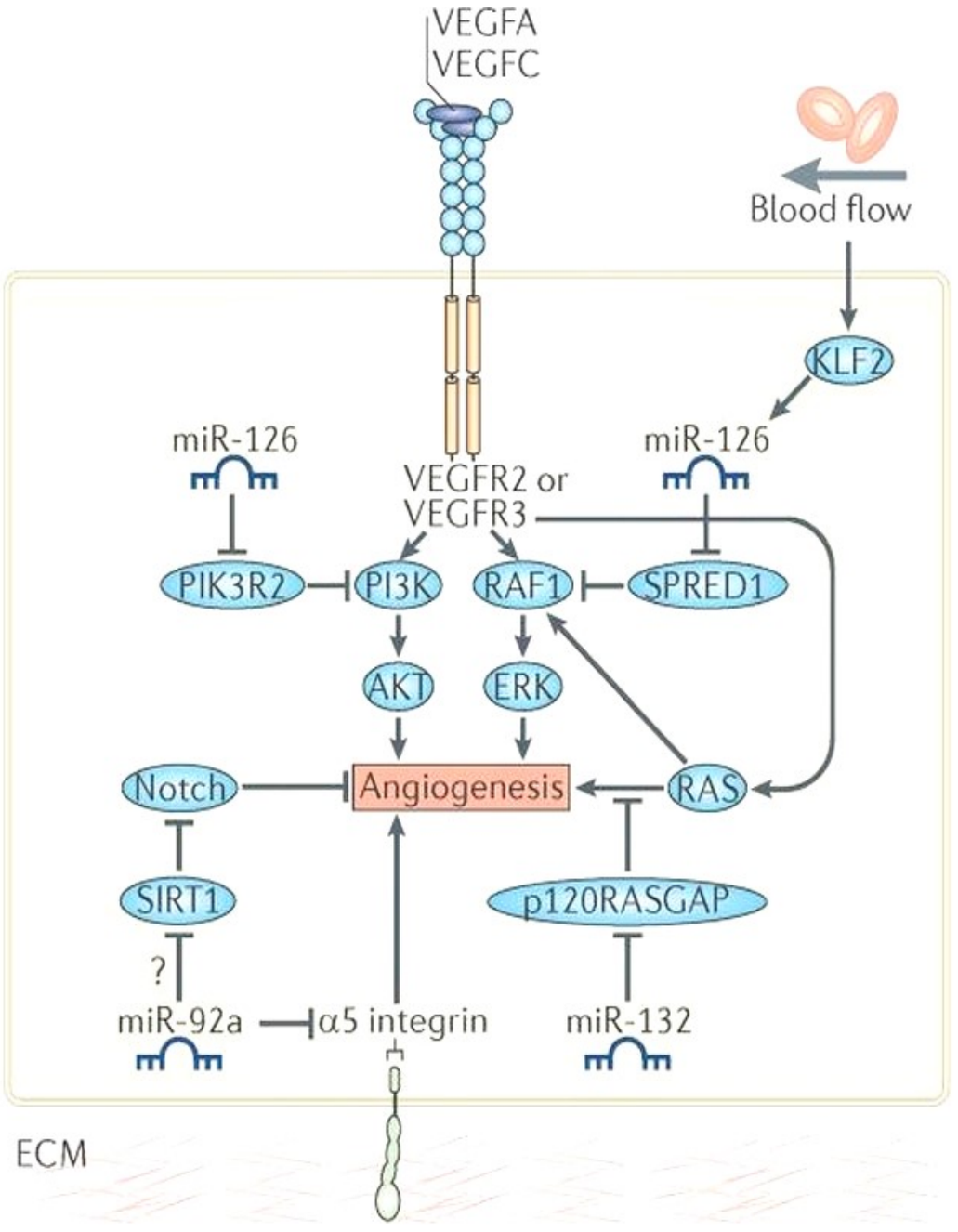

Figure 29: Post-transcriptional modification of angiogenic signalling pathways by miR-126

Mechanical stimulus of luminal blood flow leads to upregulation of Klf2, which causes increased miR-126. VEGF-induced angiogenesis pathway is promoted by expression of miR-126 through post-transcriptional repression of VEGF/AKT/ERK signaling inhibitors PIK3R2 and SPRED-1. MiR-132 also promotes angiogenesis by targeting p120RASGAP, an inhibitor of RAF1/RAS angiogenic pathway. Image obtained with permission from Herbert et al. (2011).

5.2 Hypothesis and Aim

Hypothesis: The high expression levels of miR-126 in late EPCs is indicative of endothelial differentiation and confers direct angiogenic activity. Moreover, to the extent that late EPCs may arise from early EPCs, over expression of miR-126 in early EPCs will promote endothelial differentiation and angiogenic potential.

Aim: To evaluate effects of miR-126 manipulation on the angiogenic phenotype of early and late EPCs.

5.3 Results

a) MicroRNA delivery, uptake and MRE complementation

To confirm complementarity of the predicted 3'UTR MREs with our mimics and inhibitors, we conducted a reporter assay. Using the 525-531 seed sequence of our target gene SPRED-1 (Figure 30), we designed a SPRED-1 luciferase reporter construct using LightSwitch 3'UTR GoClone reporters. Our transfection approach resulted in a greater than 33% increase in luciferase with a knockdown of miR-126 in HEK293T cells compared to scramble-miR controls $p<0.01$ (Figure 30).

To visualize distribution and uptake of miR-126 mimics into our early EPCs, we designed custom FAM-labelled miR-126 oligonucleotide mimics (Exiqon). Using immunofluorescence, we detected >50% fluorescence in miR-transfected early EPCs (Figure 31A).

Additionally, we confirmed increased miR-126 in early EPCs using qRT-PCR (Figure 31B). Our results

indicated a pronounced increase of miR-126 in early EPCs after transfection with miR-126 mimics.

b) Transfection of miR-126 mimic into early EPCs causes loss of rod morphology

In all of our conducted experiments involving transfection of early EPCs with miR-126, we noted dramatic changes in early EPC morphology, despite minimal changes in cell viability. Using the techniques discussed in the material and methods section (t), trypan blue vital staining and hemocytometric cell counting (Figure 32B), we confirmed that early EPCs progressively lose their elongated rod- shaped morphology following treatment but maintain viability. Loss of rod morphology occurred within the first three days after transfection.

A

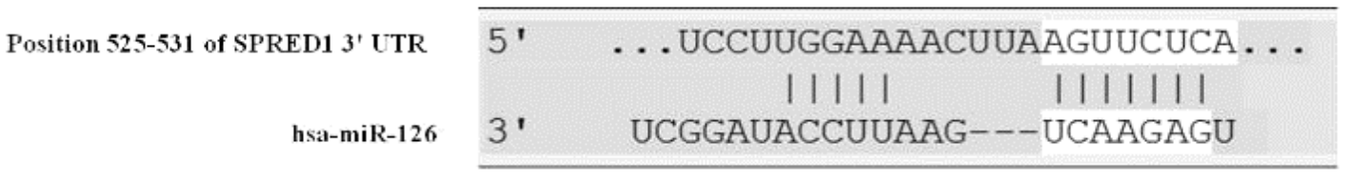

B

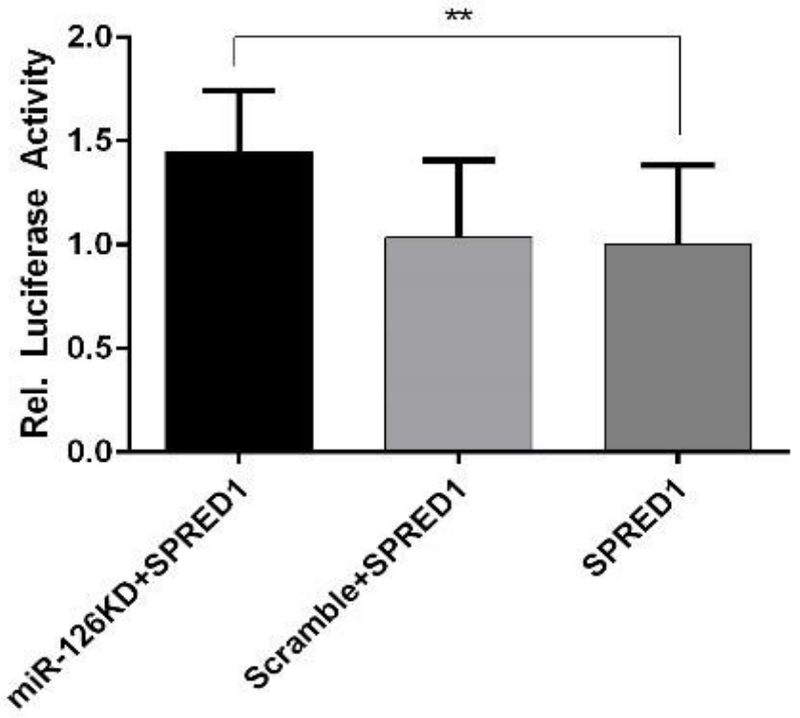

Figure 30: Knockdown of miR-126 increases SPRED-1 luciferase reporter signal detection

(A) miR-126 alignment with MRE on the 3'UTR of putative target, SPRED-1. (B) HEK293T cells were co-transfected with SPRED-1 reporter construct and miR-126 inhibitor at 24 hours post-seeding. 12 hours post-transfection cell plates were read using plate luminometer. The observed effect of miR-126KD in HEK293T cells is attributed to targeting of basal miR-126. Data represent mean ± SEM; n=7-10. ** $p<0.01$.

A

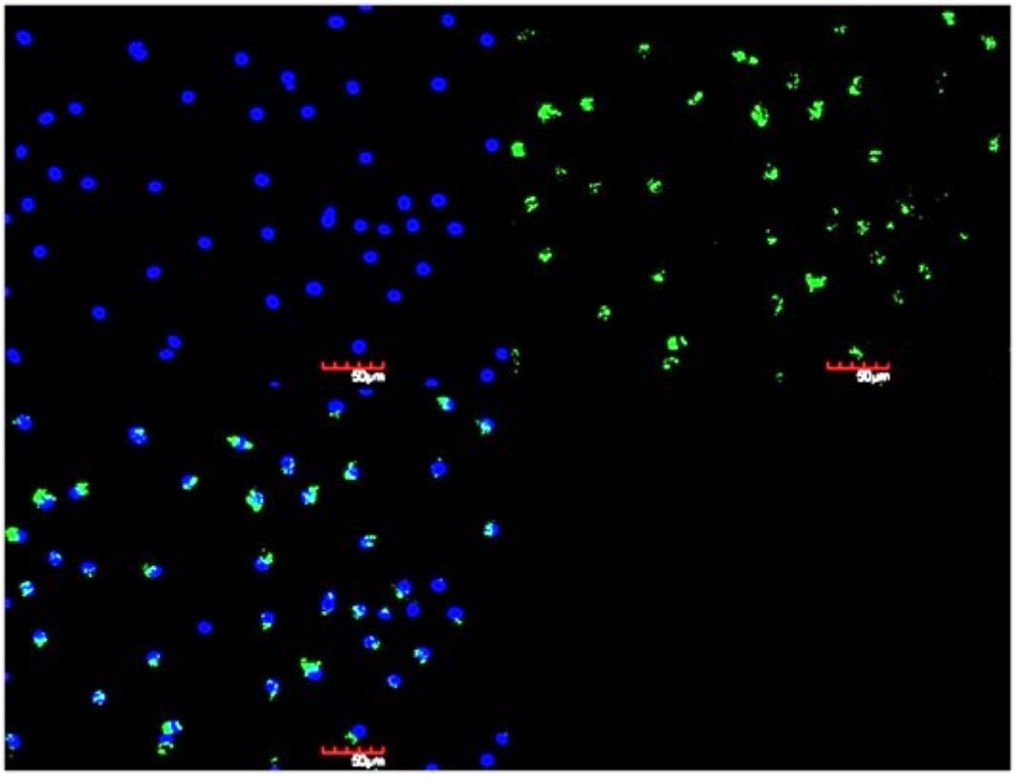

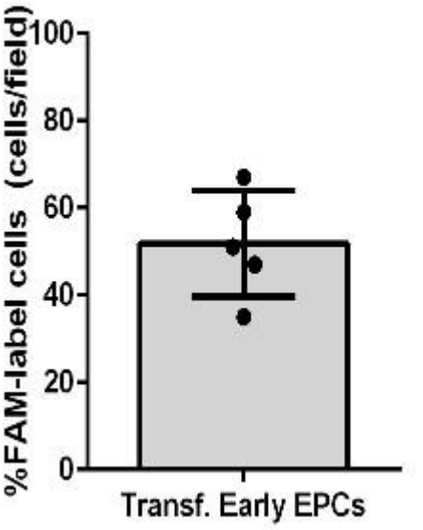

B

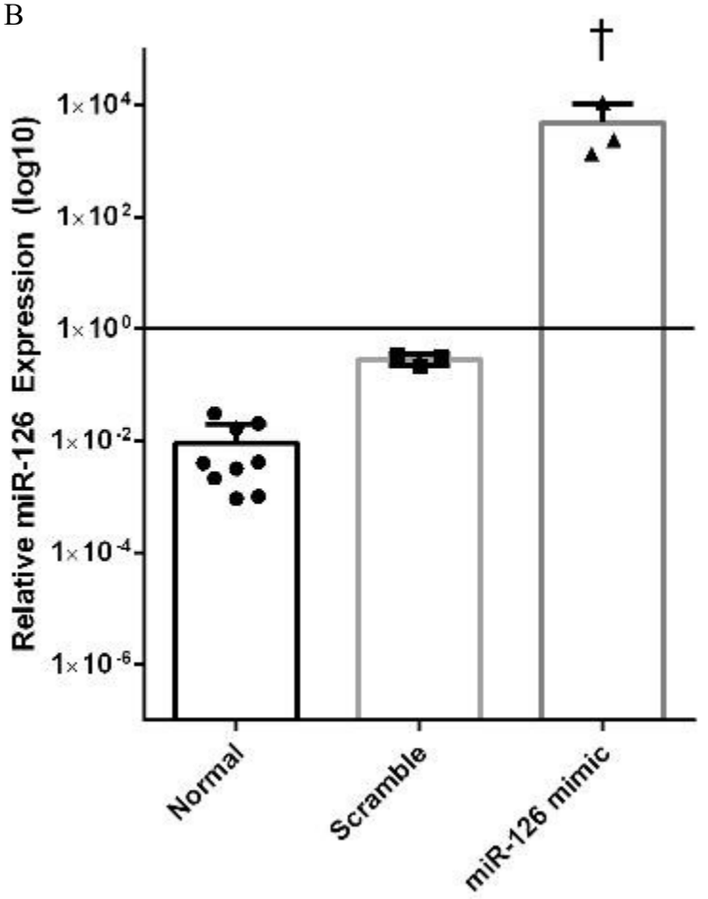

Figure 31: Confirmation of miR-126 mimic uptake using immunofluorescence and qRT-PCR

(A) An image of early EPCs at 100x magnification, transfected with FAM-labeled miR-126 mimic and corresponding histogram of quantified FAM-fluorescent cells. Data represent mean ± SEM. (B) Relative expression of miR-126 in miR-126 mimic, scramble and untransfected early EPCs by qRT-PCR (normalized to U6 and U48). Data represent mean ± SEM; n=3-9. † $p<0.0001$. Scale bar represents 50μm.

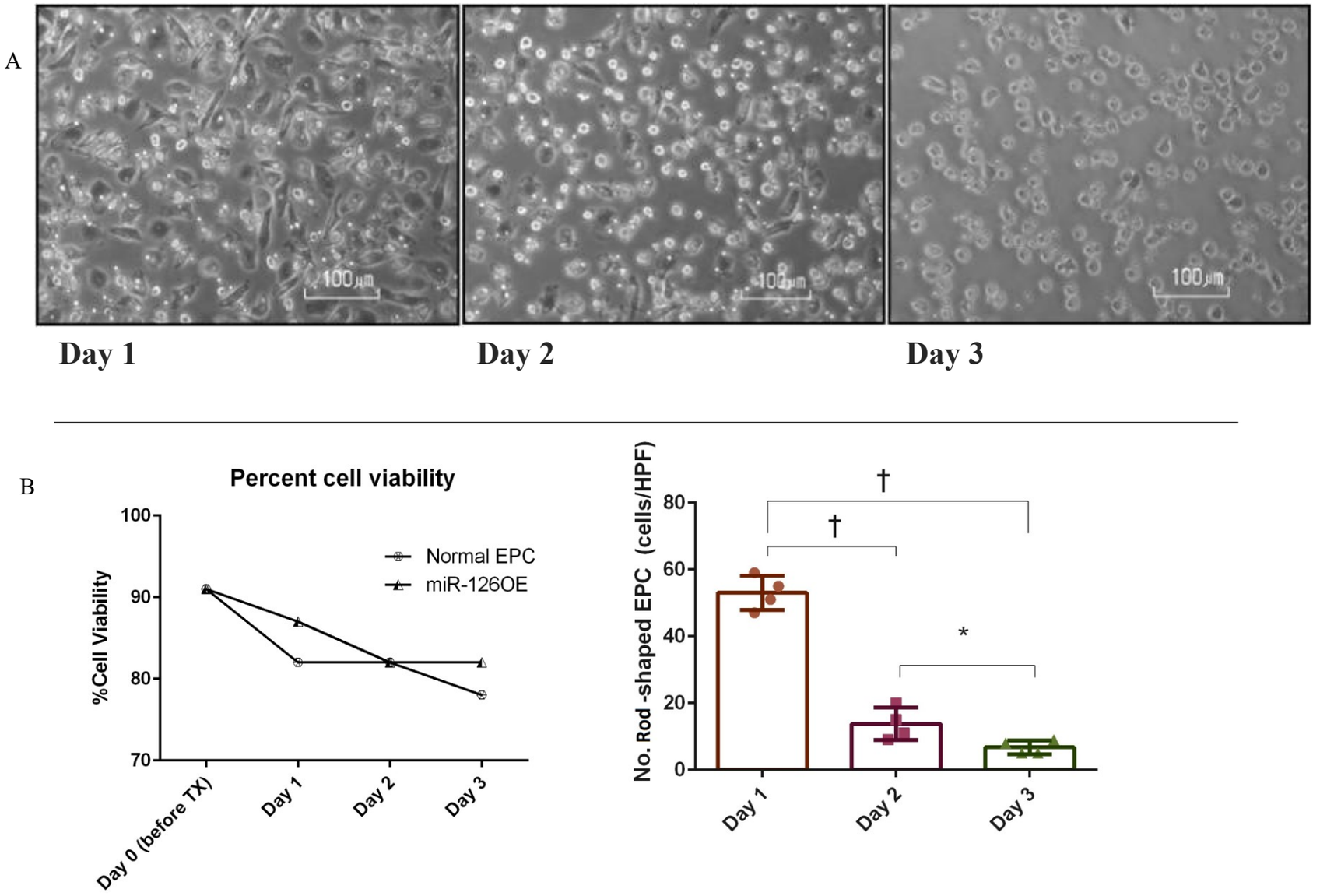

Figure 32: MicroRNA transfection of early EPCs with miR-126 results in loss of rod morphology

(A) Representative image of miR-126 over expression in early EPCs inducing loss of rod morphology (under 20x objective). (B) Graphical representation of change in cell viability with miR-126 transfection and loss of rod-morphology in early EPCs. Data represent mean ± SEM; n=3-9. † $p<0.0001$, * $p<0.05$.

c) MicroRNA-126 improves matrigel-network tube formation in early and late EPCs

Prior to conducting the indirect angiogenesis assay, early EPCs were transfected with miR-126 mimic or scramble control using the previously described transfection approach (refer to methods section), and then treated cells were co-cultured at 1:1 with HUVECs prior to plating on matrigel (Figure 33). We compared miR-126 treatment with untreated early EPCs, scramble-miR as negative control and HUVECs as positive controls. Due to the transient nature of *in vitro* angiogenesis, we analyzed network formation at 1.5 hours, 5 hours, 12 hours, 15 hours, and 24 hours and determined optimal assay time to be 12 hours as the differences between the groups were most apparent at this time point. We noted a modest but significant improvement in matrigel tube formation in co-cultured early EPCs treated with miR-126 mimic compared to scramble-miR control $p<0.05$ (Figure 33). Without HUVEC co-culture, no differences were detected with miR-126 treatment alone in early EPC network formation (data not shown). Since early EPCs function primarily through paracrine effects, a co-culture with a mature endothelial cell type like HUVECs was more appropriate. At the 12-hour mark, we noted a more-refined network formation in co-cultured early EPCs treated with miR-126 compared with non-transfected early EPCs grown with HUVECs alone (Figure 33). Upon analysis, we noted pronounced tube branch length and total number of branches in miR-126 mimic treated early EPCs compared to scramble-miR treated early EPCs ($p<0.05$, for both). Despite an increased trend towards greater number of nodes with miR-126 treatment, no statistical significance was detected.

In contrast to early EPCs, late EPCs were grown on matrigel without co-culture with HUVECs. Our results clearly showed that knockdown of miR-126 in late EPCs significantly diminished the number of nodes, branches and the branch lengths of the networks that formed on matrigel. These results suggested that the discrepancy in miR-126 expression across early and late EPCs likely contributes to the differences in therapeutic roles (in

promoting angiogenesis) between these two cell types. Indeed, when comparing number of nodes, branches and branch length, the effect of miR-126 knockdown in late EPCs (which normally have high miR-126 expression) was greater than the forced over expression of miR-126 in early EPCs (which normally have low miR-126 expression); and this suggests a bigger role for this microRNA in late EPCs than early EPCs.

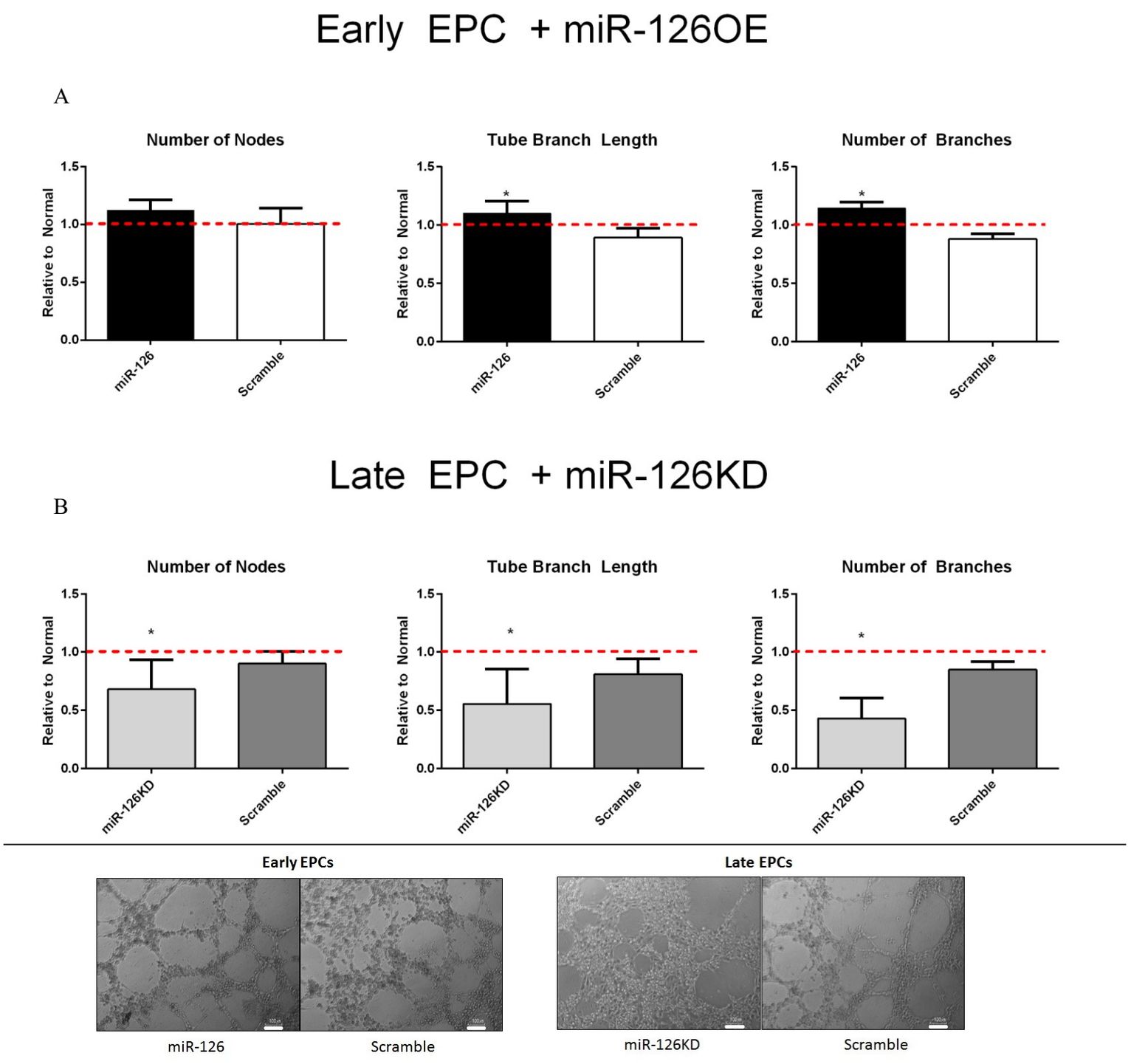

Figure 33: MicroRNA-126 augments network formation in early and late EPCs

(Top) Early EPCs treated with miR-126 mimic for 24 hours possessed augmented co-cultured matrigel network formation as measured by tube branch length and total number of branches as compared to scramble-miR transfected early EPCs. Dashed red line represents the normalizing control group of untreated EPCs co-cultured with HUVECs. (Middle) Late EPCs treated with miR-126KD displayed diminished branch lengths, number of branches and nodes as compared to scramble-miR transfected late EPCs. Dashed red line represents normalizing group of untreated late EPCs. (Bottom) Representative matrigel images at 12 hours. Scale bar is 100μm. Data represent mean ± SEM; n=3-9. * $p<0.05$.

d) Over expression of microRNA-126 in early EPCs improves chemotactic migration capacity

Since we were able to detect an improvement in matrigel network formation with over expression of miR-126 in early EPCs, we sought to measure whether using a modified Boyden chamber migration assay, we could also detect an improvement in chemotactic migration in early EPCs. Such an assay would be less effective on a highly proliferative cell type like late EPCs since proliferation would cause a confounding effect when counting migrated cells, so this experiment focused only on early EPCs. Compared to scramble-miR treated early EPCs, early EPCs treated with miR-126 mimic exhibited extensive improvement in chemotactic migration towards VEGF and SDF-1, $p<0.001$ (Figure 34). Transfection of early EPCs with scramble-miR resulted in a small decrease in migration capacity, but not significantly. This assay confirmed, in part, our postulate that miR-126 bestows improved chemotactic migration in early EPCs.

e) Manipulation of miR-126 in early and late EPCs does not affect apoptosis or proliferation

Using the same ELISA techniques for BrdU and CCASP3 as for our miR-146a studies, we noted no significant changes in proliferation or apoptosis with miR-126OE in early EPCs (Figure 35). Much like our findings with early EPCs, using our BrdU and CCASP3 assays, we were also not able to detect any significant changes with miR-126 knockdown on apoptosis or proliferation of late EPCs when compared to scramble-miR control (Figure 36).

f) Over expression of miR-126 does not affect eNOS

As discussed in the introductory chapter, the SDF-1/CXCR4 antagonist-receptor system is implicated in the homing of EPCs to injured sites and contribute to angiogenesis through eNOS (119). Since we noted improved angiogenesis and chemotactic migration in early EPCs with miR-126OE, we sought to measure any downstream augmentation in eNOS expression in early EPCs using western blot analysis. However, despite improved

chemotaxis and matrigel-tube formation, no significant change in eNOS expression with miR-126 over expression was detected (Figure 37).

g) High expression of miR-126 in MNCs is predictive of late EPC formation

Discussed in the appended chapter, during our experimentations in optimizing the yield of late EPCs from human adult peripheral blood MNCs, we discovered that if late EPCs colonies emerged, they only emerged from the $MCAM^+$ MNC population (Figure 38A). The $MCAM^+$ fraction of MNCs consistently made up only 1-5% of the total MNC cell population and this appeared to be independent of the donor's health status. Since this part of the project focused on cell isolation using MCAM and not the effects of microRNAs, it is more suitably discussed in the appendices. However, we noted that MCAM positive circulating monocytes from healthy donors expressed high levels of miR-126. Interestingly, monocytes from older patients with cardiac disease exhibited very low levels of miR-126, despite the fact that MCAM expression (as determined by selective sorting) was not different compared to healthy monocytes. These novel findings suggest for the first time that miR-126 is expressed in a distinct population of monocytes that are predetermined to give rise to highly endothelial-like late EPCs, and yielded late EPCs with higher proliferation and survived more cell passages (Figure 38B). Unfortunately, there is no robust method for isolating cell populations using microRNAs without lysing the cell populations. In our experiments, we lysed a portion of the starting $MCAM^+$ MNC population to assess miR-126 expression and then waited for the remaining cells to form late EPC colonies.

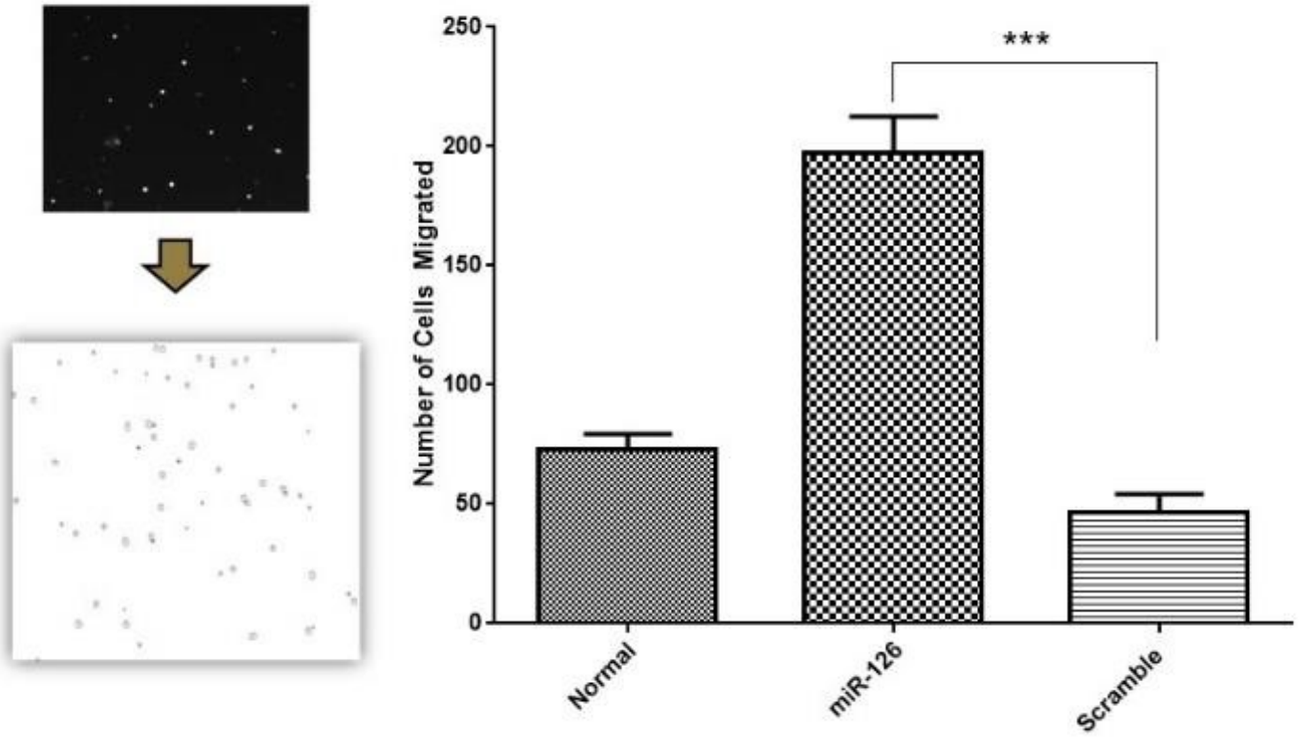

Figure 34: Chemotactic migration of early EPCs is increased following miR-126 delivery

Early EPCs transfected with miR-126 were tested for chemotactic migration capacity towards VEGF and SDF1 using a modified Boyden chamber migration assay. Following experimentation, cells were DAPI stained and quantification was performed on migrated cells under chamber using light microscopy (20X objective). The number of migrated cells were compared to normal EPCs. Data represent mean ± SEM; n=5-7. *** $p<0.001$.

A

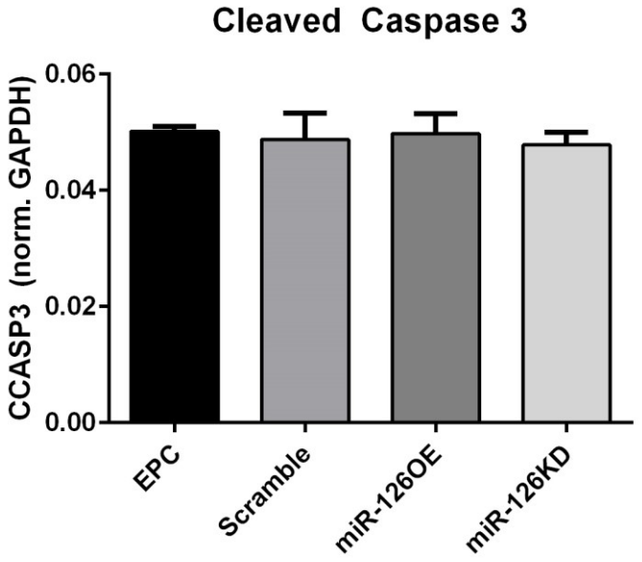

B

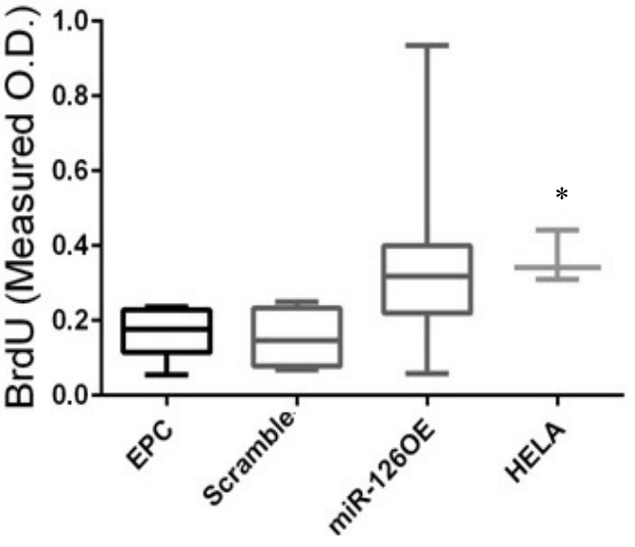

Figure 35: Modulation of miR-126 in early EPCs does not change proliferation or apoptosis

ELISA detection of CCASP3 (A) and BrdU (B) indicated no changes with manipulation of miR126 in early EPCs. CCASP data was normalized to GAPDH per group. *p<0.05. Data represents mean ± SEM; n=3-7.

A

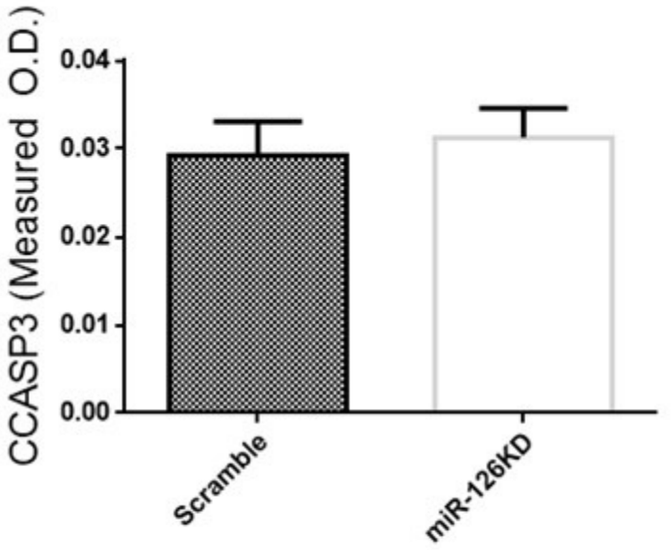

B

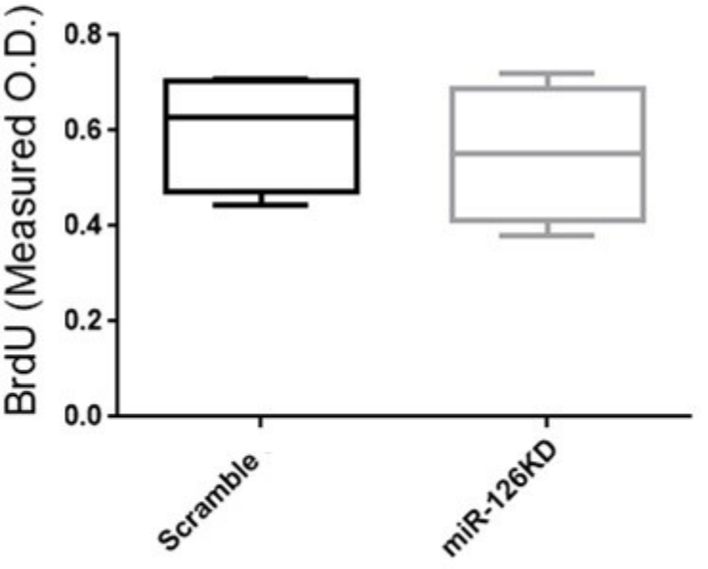

Figure 36: Knockdown of miR-126 in late EPCs does not affect apoptosis or proliferation

MiR-126 was knocked down in late EPCs and we measured CCASP3 and BrdU using ELISA. Apoptosis (A) and proliferation (B) was assessed 24 hours later. No significant changes were detected compared to scramble-miR transfection. Data represents mean ± SEM; n=3.

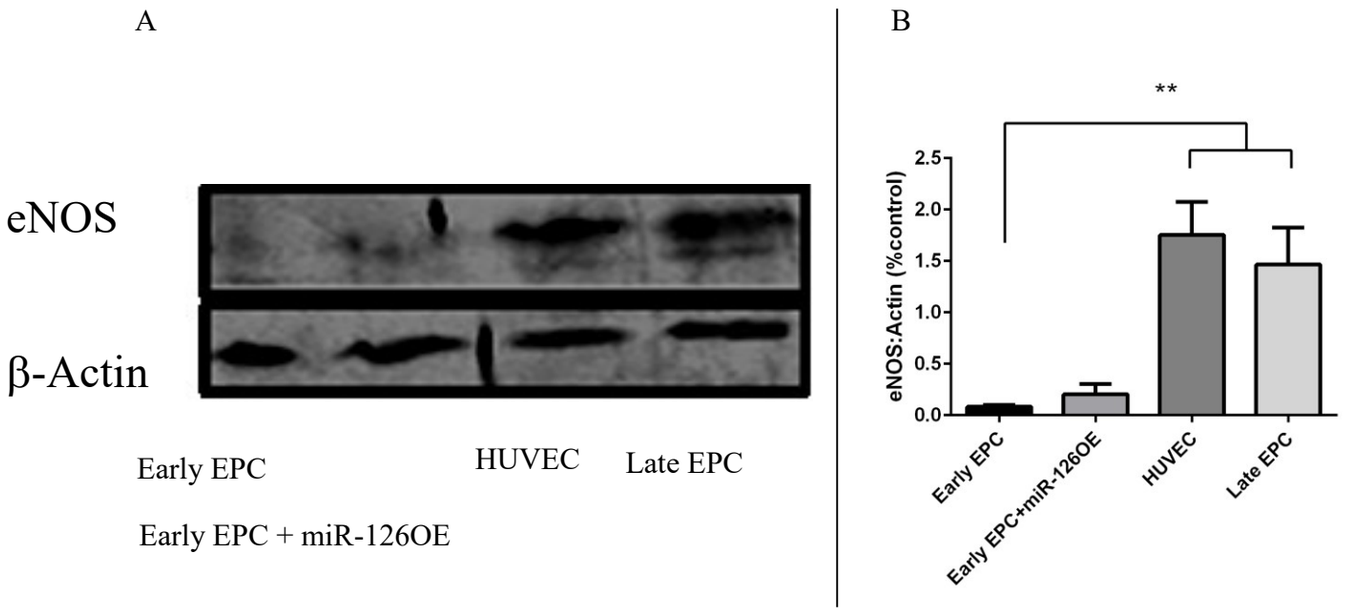

Figure 37: Over expression of miR-126 does not affect downstream eNOS in early EPCs

(A) Representative Western blot for eNOS expression in early EPCs with miR-126 over expression. (B) Densitometry. Over expression of miR-126 would promote the SDF-1/CXCR4 and VEGF/eNOS angiogenic pathways, and thus potentially promote vasodilation via eNOS. However, despite improved angiogenesis in early EPCs with miR-126 over expression, no significant change in eNOS was detected in early EPCs. Data represents mean ± SEM; n=4. ** $p<0.01$.

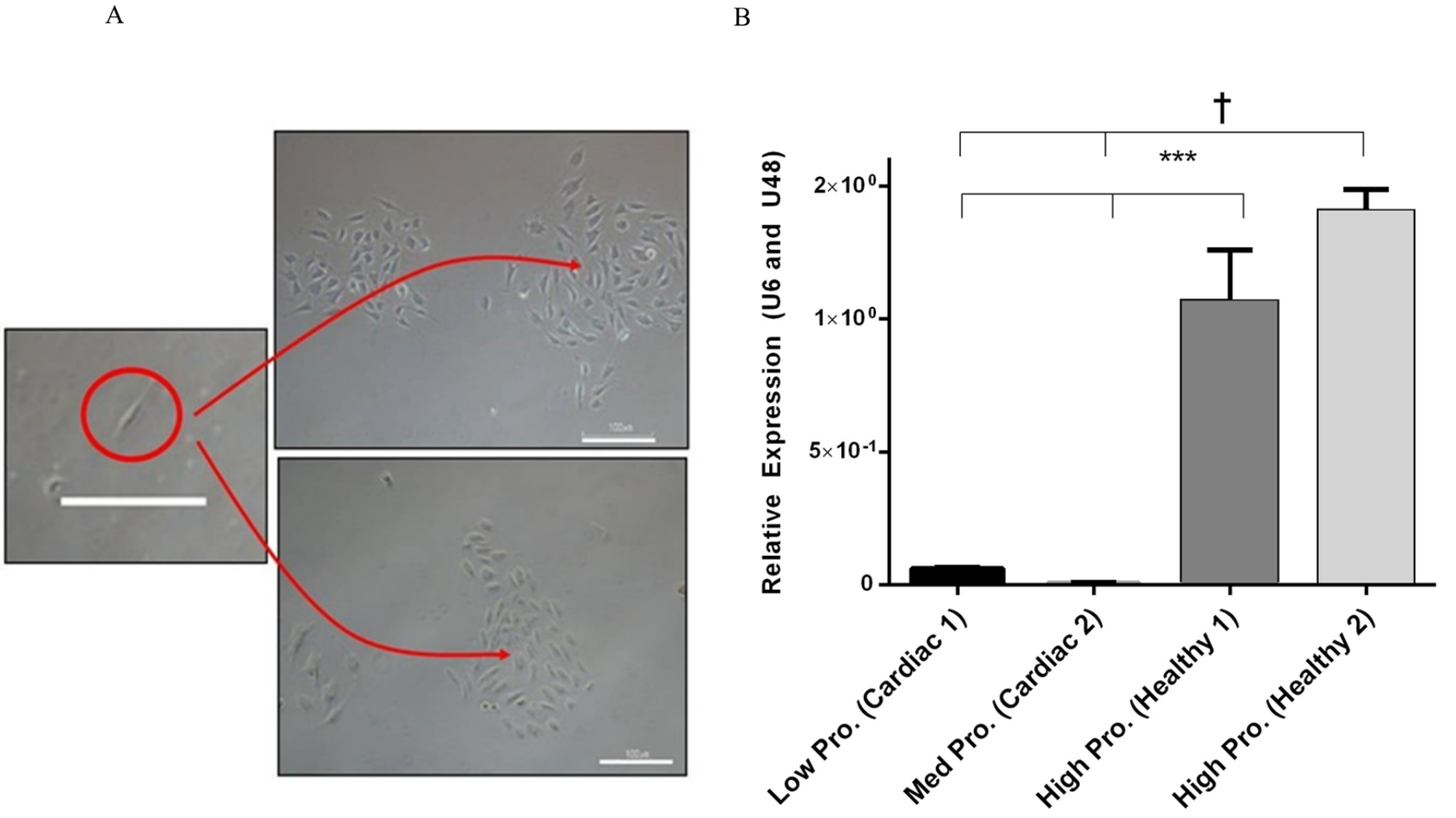

Figure 38: High expression of miR-126 in MNCs indicates yield of proliferating late EPCs colonies

Using the protocol we developed and appended to the appendices, we found a consistent method for generating late EPCs using only MCAM⁺ MNCs. Despite having a similar 1-5% total number of starting MCAM⁺ MNCs on day 0, compared to healthy controls cells from cardiac patients consistently yielded fewer overall late EPCs (with reduced proliferative capacity). MiR-126 expression correlated closely with proliferation and late EPC longevity. Each bar represents a single participant/patient repeated n=3 times. Groups analyzed using one way ANOVA followed by Tukey's post-hoc analysis. Data represent mean ± SEM; † $p<0.0001$, *** $p<0.001$.

5.4 Discussion

We used a luciferase-reporter assay to confirm our miR-126 oligonucleotide complementarity with predicted MREs. We next used FAM-labelling to detect distribution and uptake following transfection to ensure microRNA mimics were not degraded and were localized within cytoplasm of transfected cells (Figure 31A). Using qRT-PCR, we showed greater than a 100 fold increase in miR-126 in early EPCs following transfection with miR-mimic (Figure 31B). Upon transfection of early EPCs with miR-126, we noted significantly improved chemotactic migration to VEGF and SDF1 using a modified Boyden chamber assay (Figure 34). Transfection of early EPCs using miR-126 mimic consistently reduced rod-shaped morphology. Despite these changes, early EPCs remained between 15-25 microns in size. The noted change in early EPC morphology after transfection with miR-126 was not associated with any evidence of loss of viability (Figure 32B). This change in morphology likely corresponds with adaptation in cytoskeletal features, which was previously noted by Fish et al., who reported that miR-126 presence increases large actin filaments within the HUVEC cytoskeleton (66). However, we did not explore the effects on cytoskeleton in late EPCs with knockdown of miR-126.

Early and late EPCs express strikingly different levels of miR-126 so it is logical to associate high levels of miR-126 in late EPCs as contributing to the strong endothelial and angiogenic phenotype of late EPCs. So to test this, we performed two complementary experiments: In the first, we forced over expression of miR-126 in early EPCs to determine whether over expression alone was sufficient to induce endothelial differentiation (i.e.: emergence of late EPCs). Although there was some change in morphology and improvement in chemotactic migratory activity, there was no obvious transdifferentiation of early EPCs into endothelial-like cells. Additionally, forced over expression of miR-126 did not increase eNOS, which is an important hallmark of

endothelial cells (Figure 37). As well, during optimization of the matrigel assay, we noted that even after miR-126 transfection, early EPCs were not able to form capillary-like networks directly and in contrast to late EPCs, were only able to contribute to angiogenesis indirectly by enhancing the ability of HUVECs to form networks on Matrigel (Figure 33A). In endothelial cells, miR-126 has been shown to increase pro-angiogenic signalling mediated via VEGFR2 ligation (66). It is possible VEGFR2 signalling is also important for the paracrine angiogenic activity of early EPCs, or perhaps miR-126 can regulate other pathways that are involved in the release of angiogenic signals from these cells. Nonetheless, it is clear from these experiments that transfection of miR-126 into early EPCs alone may not be enough to fully commit early EPCs into late EPCs or a similar endothelial cell type. In the second experiment we tested whether high levels of miR-126 was necessary for angiogenesis in late EPCs, by miR-126KD (Figure 33B). As expected, inhibition of miR-126 had an impact on the ability of late EPCs to form capillary-like networks on Matrigel, which is consistent with its well-established role in modulating VEGF signalling. However, manipulation of miR-126 had no major effect on the overall endothelial phenotype, or on viability and proliferation (Figure 36). These findings suggest that while this microRNA may play a key role in angiogenic signalling, but by itself it does not specify endothelial phenotype in late EPCs. However, it is important to recognize that there are some important limitations in our studies. It is likely that we achieved only incomplete inhibition of miR-126. Moreover, we only performed experiments within 24 hours after manipulating the levels of this microRNA. It is quite possible that longer periods of miR-126 inhibition would be required to fully unmask its role in specifying the strong endothelial phenotype of late EPCs.

While experimenting with growing late EPCs from leukapheresis that was generated from adult peripheral blood, we continually investigated more efficient ways to grow late EPCs. We eventually optimized a more efficient protocol for generating late EPCs by sorting for $MCAM^{+}$ (CD146) MNCs, as we found that only this population, which consistently remained within 1-5% of the total MNC population (regardless of cardiovascular

health) yielded late EPCs (Figure 38). This protocol can be found appended in the appendices. When we analyzed miR-126 expression in $MCAM^+$ MNCs before the emergence of late EPCs, we consistently noted that less proliferative colonies emerged when these starting cell populations had significantly lower expression of miR-126 (Figure 38). Additionally, our findings showed that the cell populations, which had reduced initial miR-126 expression and limited proliferative potential, came from patients with cardiovascular pathology. This finding is consistent with our earlier results, which showed that miR-126 is an important feature in promoting a pro-angiogenic phenotype. It is likely that under normal conditions, circulating peripheral blood MNCs which have higher expression of miR-126 are the true precursors since MCAM selection alone only selects 1-5% of these adult peripheral blood MNCs and these do not always yield highly proliferative late EPCs, but those with high miR-126 do. In future experiments, it would be desirable to devise a method to over express miR-126 in $MCAM^+$ MNCs from cardiac patients to assess effects on subsequent late EPC colony formation. However, since $MCAM^+$ MNCs from adult peripheral blood are extremely few in number, this presents a technical limitation. Such an experiment would require a substantial amount of leukapheresis in order to isolate sufficient $MCAM^+$ MNCs which would survive transfection with miR-126.

5.5 Chapter Summary

Our findings showed that miR-126 is an important enabler of angiogenesis in both early and late EPCs. In early EPCs, miR-126 over expression augmented chemotaxis in a modified Boyden chamber migration assay. We also noted an increased number of branching and branch length in our matrigel network assay when miR-126 was over expressed in early EPCs. However, a knockdown of miR-126 in late EPCs resulted in a more robust effect

on angiogenesis as we noted a loss in branching, branch length and total number of nodes. It is likely that these findings reflect a more critical role for miR-126 in late EPCs than early EPCs. However, more research is needed in eliciting the precise impact of miR-126 on the VEGFR2/akt/eNOS angiogenesis pathway. Finally, using a protocol that our lab established, we discovered that $MCAM^{+}$ MNCs that were isolated from human adult peripheral blood consistently yield highly proliferative late EPCs only when they express a high relative expression of miR-126. This finding was consistent with our miR-126 manipulation studies which showed that miR-126 promotes a pro-angiogenic phenotype in late EPCs.

CHAPTER VI: PERSPECTIVE

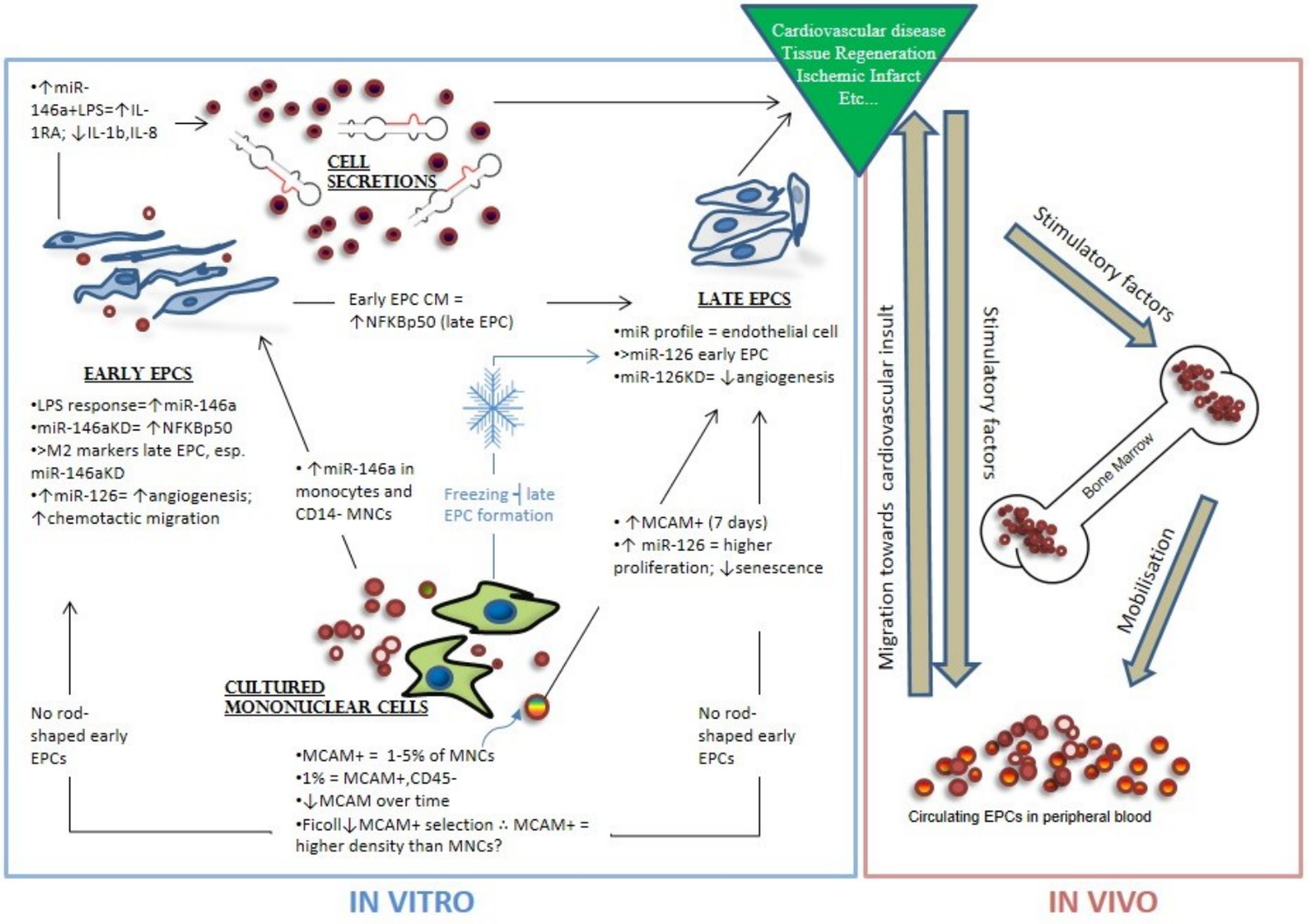

Figure 39: Summarized schematic representation of findings

As early EPCs emerge from MNCs, miR-146a expression increases and this confers added tolerance to negating NFKB response upon TLR stimulation in early EPCs. Conditioned media (CM) from early EPCs increased NFKB in late EPCs (unknown mechanism). Conversely, late EPCs only emerge from the $MCAM^+$ cell fraction of MNCs; and do not emerge from frozen tissue. Once late EPCs emerged, they had highly congruent microRNA expression profile to mature endothelial cells, including robust expression of miR-126 (unlike early EPCs). Within early EPCs, miR-126OE conferred a change in morphology, improved matrigel network formation ability and improved chemotactic migration; but did not affect late EPC formation. M2 refers to M2 macrophages. In late EPCs, miR-126KD diminished matrigel network formation. When freshly isolated MNCs are prepared for plating, the total $MCAM^+$ cell population in this cell fraction consists of 1-5% regardless of the subject's cardiovascular condition. Compared to healthy participants, patients with cardiovascular conditions consistently had significantly lower miR-126 expression in their freshly isolated $MCAM^+$ MNC population, which then resulted in the yield of late EPCs with reduced proliferation and longevity.

6.1 Overall Discussion

The results from the candidate microRNA array and the global arrays truly convinced us that early EPCs and late EPCs represent entirely different cell types, increasing our interest into looking into how different the roles of microRNAs are within these two cell types. Though it had been reported that a mode of repair by early EPCs involves suppression of inflammation, our results further supported this through a novel mechanism mediated by miR-146a. We also noted that the sequential increase in miR-146a in early EPCs bore close resemblance to a similar process during macrophage differentiation. We showed that the presence of miR-146a in early EPCs confers an immune *primed* state that allows a 'shut off' of the TLR4/TRAF6/NFKB inflammatory pathway. This was a phenomenon recently reported by Eigsti et al. in monocytes during monocyte-to-macrophage differentiation (168). Since both macrophages and early EPCs share a common myeloid origin to monocytes, this finding was very telling. Closer examination showed that early EPCs possessed features akin to M2 (non-inflammatory) macrophages. The increased presence of miR-146a in early EPCs in our study was associated with an immune-related response. Eigsti et al. identified that the presence of non-monocytes in co-culture during culture of monocytes triggers TLR4 activation causing miR-146a to increase. We confirmed that the presence of non-monocytes certainly caused an increase in miR-146a, but a general increase in miR-146a appears to occur even in a monocyte-enriched population. The presence of miR-146a itself appears to support an early EPC anti-inflammatory phenotype through increased anti-inflammatory cytokine IL-1RA, and decreased pro-inflammatory cytokines IL-1β and IL-8 (under LPS-induced inflammatory conditions). In all, these findings support the miR-146a immune mediating benefits on early EPCs.

In contrast to early EPCs, the close similarity in microRNA expression profile in late EPCs with mature endothelial cells increases the suspicion of whether late EPCs could arise from a cell type closer to endothelial cells than MNCs or early EPCs or, at the very least, that microRNAs indeed have vastly different roles in early versus late EPCs. Since increased expression of miR-126 alone was enough to make early EPCs more angiogenic and its knockdown in late EPCs caused them to lose their angiogenic potential, it is possible that under pathological conditions, loss of miR-126 alone could indicate or cause future cardiovascular complications. Indeed there does exist literature to support this postulate as some studies have shown a link between miR-126 dysregulation and pathology (112, 117). Since it has already been established that under cardiovascular pathology, endothelial cells have reduced miR-126, it is possible that *in vivo* late EPC precursors, or pre-late EPCs or circulating late EPCs have reduced miR-126 and therefore reduced angiogenic capacity. Despite our presented findings with miR-126, we found that miR-126 manipulation alone was not enough to change proliferation in either early or late EPCs, suggesting that miR-126's effect on angiogenesis in late EPCs was likely not associated with proliferation. Nonetheless since miR-126 is a known pro-angiogenic microRNA, its abundance in late EPCs (and conversely lack of expression in early EPCs) does suggest that this microRNA could be attributed to some of the angiogenic properties seen in late EPCs, which may be lacking in early EPCs; or possibly, through another mechanism which promotes pro-angiogenic paracrine release (possibly explaining our observed effects with matrigel co-culture). Indeed, looking at pre-late EPCs using $MCAM^+$ MNCs between cardiac patients and healthy patients appears to support this (Figure 38).

The significance of MCAM on late EPCs presented us with another important factor relating to the origin of late EPCs. Based on our research (which is presented in the appended chapter), we are the first to establish that in adult leukocytes, only $MCAM^+$ MNCs (which represented only 1-5% of cells in human adult leukapheresis) give rise to colony forming cells that included late EPCs. Our results showed that MCAM positive cells in adult

blood represent a heterogeneous cell population, which included pre-CFU Hill cells and pre-late EPCs (Appendix O and Appendix S). The true significance of this is still under investigation but our results suggest that it is the $MCAM^+$ MNCs with high expression of miR-126 that yield late EPCs which have higher proliferation and longevity; and this suggests that either true pre-late EPCs are the $MCAM^+$ MNCs with robust miR-126 expression and that miR-126 expression decreases with cardiovascular pathology (impacting late EPCs reparative capacity). Alternatively, it may be possible that one subset of $MCAM^+$ MNCs which are not late EPCs (i.e.: cells of groups A, H or I in Appendix S), has robust expression of miR-126 which then decreases with cardiovascular injury. Future experiments could assess whether forced overexpression of miR-126 could push leukapheresis-derived $MCAM^+$ MNCs towards late EPCs.

6.2 Overall Conclusion

In conclusion, this thesis presents a new perspective on microRNAs in human adult progenitor cells. Though microRNAs are still a relatively new molecular phenomenon being studied in exploratory research and therapeutics, increasing evidence is mounting to suggest that these molecules represent important biomarkers of physiological status and could represent crucial prognostic indicators. The overall objective of this thesis was to investigate the role of microRNAs in the outgrowth and function of early and late EPCs. In pursuit of this objective, our studies shed light on the influence of microRNAs in the function of early and late EPCs, and also uncovered a novel and improved mode of generating late EPCs using a classical endothelial marker that may be regulated by microRNAs in late EPCs. An increased understanding of microRNAs could further help researchers uncover the exact processes and mechanisms relating to EPCs in cardiovascular repair, including the numerous roles played by the immune system in this process, thereby improving existing therapies and treatments.

6.3 Clinical Perspective

The data presented in this thesis provide new insight into existing roles of microRNAs in immune and cardiovascular functions. Our presented findings may provide new approaches to re-programming early EPCs with microRNAs to create more therapeutic applications directed toward cardiovascular regeneration. Typically, early EPCs have been studied more exhaustively than late EPCs since they are easier to generate and require less time to grow. Our findings with miR-146a could provide insight into culture conditions that could promote the production/expression of important microRNAs such as miR-146a, which confer therapeutic properties. As well, early EPCs could also be treated with miR-126 enhancements to promote angiogenic roles. Both of these ideas could be studied to provide new directions in future cell transplant studies. Finally, with new insight into identifying pre-late EPCs, new avenues open to researchers studying the uses and benefits of late EPCs for therapeutic applications. Our new protocol for the generation of late EPCs (which is appended to the end of this thesis) will undoubtedly provide new opportunities for researchers to bring late EPCs into clinical studies both in the form of cell transplants and potentially for regenerative medicine in the form of iPS-generated tissue, for example.

6.4 Future Directions

Our results highlight an important feature about microRNAs which helps in distinguishing not only how early and late EPCs may confer their therapeutic value, but also how truly different these seemingly similar cell

types are. Our candidate microRNA array study also helped in pinpointing specific changes in microRNA expression profiles, which reflect turnover of predominant cells while growing early EPCs and how similar this process is to that of macrophages.

Though there is general agreement over the influence of miR-146a in modulating the inflammatory response, there is still much work needed in exploring export of miR-146a from the cell. Future studies should further explore the potential role of miR-146a in extracellular vesicles, and its potential impact in cell transplantation. Additionally, the role of non-monocytes in stimulating TLR signalling and its potential implications on other pathways needs to be explored.

Our studies also highlighted the important role of miR-126 in conferring pro-angiogenic properties on EPCs. Though many studies have already highlighted the potent pro-angiogenic nature of miR-126, our study is the first to truly distinguish this microRNA as a vastly distinct characteristic of late EPCs, unique from early EPCs despite coming from the same donor and plated cell population. However, the full potential of this microRNA in promoting cell therapy is only just starting to be explored. Our study was the first to show that late EPCs emerge from a $MCAM^+$ MNC cell fraction of adult peripheral blood and that from those cells, only the ones with robust expression of miR-126 have longevity. Presently, there are controversies over miR-126 and its implications in cancer (181, 182), primarily as a promoter of blood vessel growth and angiogenesis in developing tissue (183). Given our findings that circulating $MCAM^+$ MNCs which co-express high levels of miR-126 are likely the true precursors of late EPCs, future experiments should also explore these cells in tumor progression (considering MCAM is a known marker for melanoma cells). Nonetheless, it is interesting to see this connection considering the ‘stem-ness’ of late EPCs and the stem cell nature of cancer cells.

Finally, the main focus in this thesis have been microRNAs. Given our findings and their implications, future studies could explore the potential of isolating or characterising cells based on microRNA expression levels. Given the potential implications that are beginning to be unraveled by these previously believed-to-be "junk" nucleic acids, growing evidence on the important transformative roles played by microRNAs is beginning to suggest that these small molecules may serve not only as important prognostic indicators but also as features to differentiate different cell types. As technology starts to catch up with science, we should expect to see more equipment geared towards measuring and tracking microRNAs in the near future.

CHAPTER VII: APPENDICES

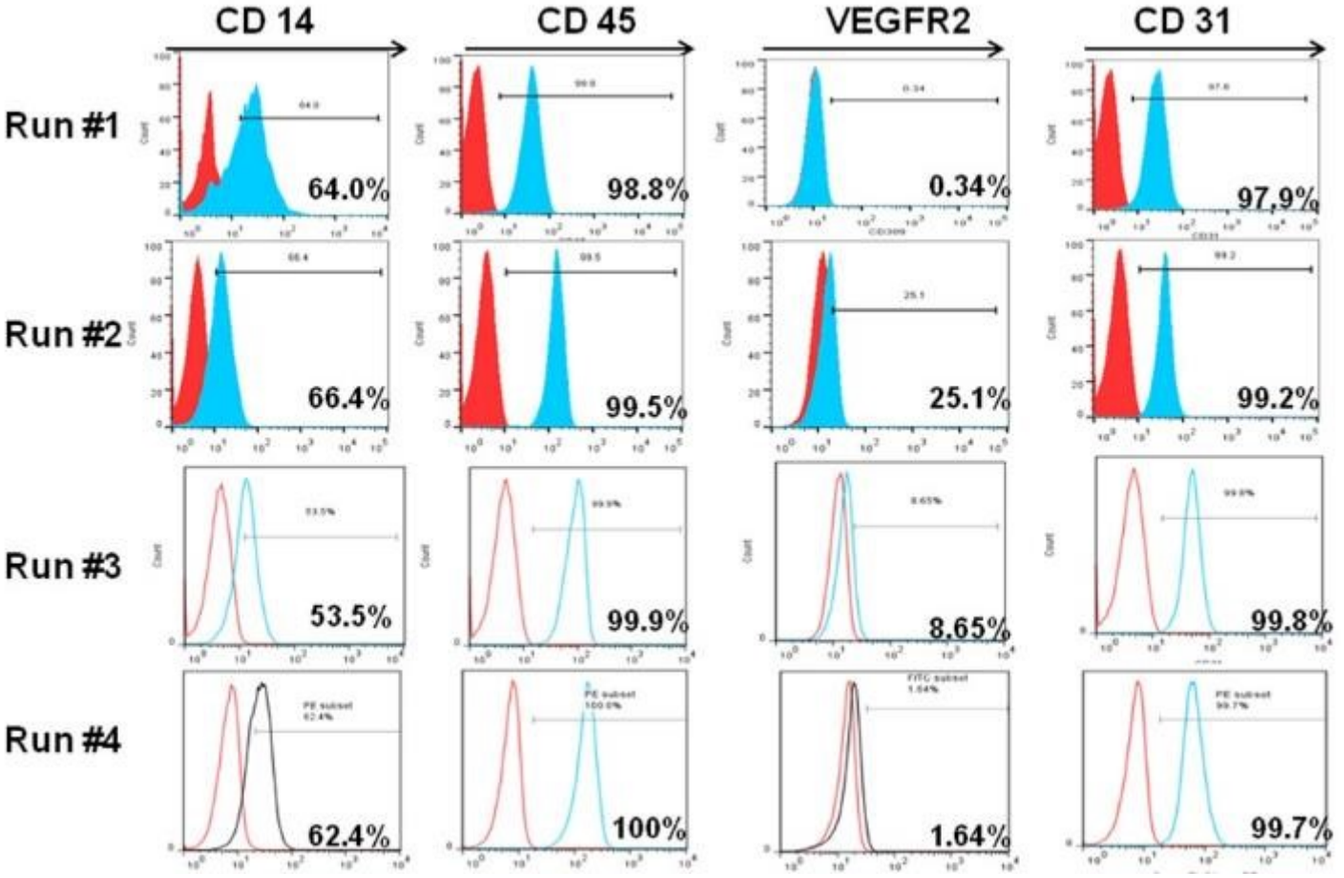

Appendix A: Characterization of early EPCs by flow cytometry

CD14, CD45 and CD31 in Early EPCs grown for 5 days. However, as mentioned previously, the expression of VEGFR2 remains an inconsistent marker for early EPCs.

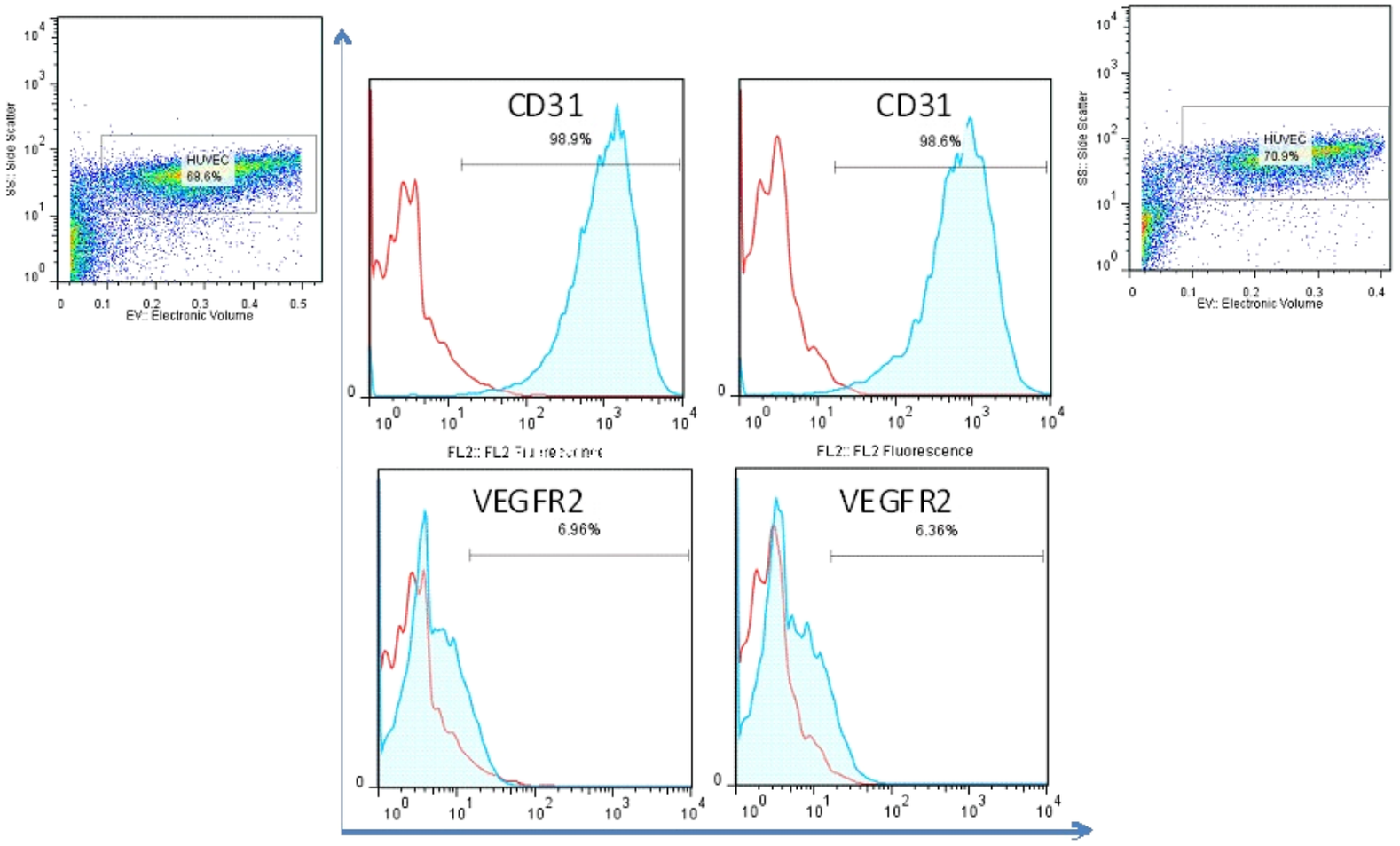

Appendix B: Characterization of HUVECs by flow cytometry

HUVECs characterized for CD31 expression and VEGFR2 prior to microRNA expression profiling for the candidate array revealed 6.35-6.96% VEGFR2 expression.

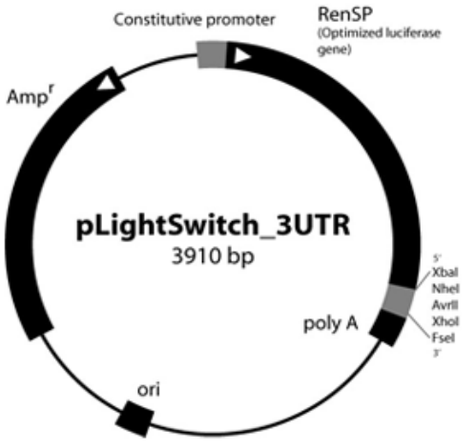

Appendix C: 3'UTR vector construct and gene sequences for luciferase assays

For microRNA mimic/inhibitor co-transfection with reporter construct, Dharmafect DUO was used. For single oligonucleotide transfections, Lipofectamine 2000 was used.

Gene	Human genome sequence used for 3'UTR vector design
TRAF6 (S813016)	TTTTCAGCCACGAAGTACTGATGCAGGGGTATAGCTTGCCCTCACTTGCTCAAAAACAAC TACCTGGAGAAAACAGTGCCTTTCCTTGCCCTGTTCTCAATAACATGCAAACAAACAAGC CACGGGAAATATGTAATATCTACTAGTGAGTGTTGTTAGAGAGGTCACTTACTATTTCTT CCTGTTACAAATGATCTGAGGCAGTTTTTTCCTGGGAATCCACACGTTCCATGCTTTTTC AGAAATGTTAGGCCTGAAGTGCCTGTGGCATGTTGCAGCAGCTATTTTGCCAGTTAGTAT ACCTCTTTGTTGTACTTTCTTGGGCTTTTGCTCTGGTGTATTTTATTGTCAGAAAGTCCA GACTCAAGAGTACTAAACTTTTAATAATAATGGATTTTCCTTAAAACTTCAGTCTTTTTG TAGTATTATATGTAATATATTAAAAGTGAAAATCACTACCGCCTTGTGCTAGTGCCCTCG AGAAGAGTTATTGCTCTAGAAAGTTGAGTTCTCATTTTTTTAACCTGTTATAGATTTCAG AGGATTTGAACCATAATCCTTGGAAAACTTAAGTTCTCATTCACCCCAGTTTTTCCTCCA GGTTGTTACTAAGGATATTCAGGGATGAGTTTAAACCCTAAATATAACCTTAATTATTTA GTGTAAACATGTCTGTTGAATAATACTTGTTTAAGTGTTCCTTCTGCCTTGCTTACTTAT TTCCTTGAGGTTACGAAGTAGCATCTTCCCCAGAGTTTATAATGCTGAGAACCACGTGGAT
SPRED-1 (S811430)	TATGTGCTGCTACGTCCCTTTGAGAATGTGCCATCGCTGTGGTGAGGCATGTGGTTGCTG TGGTGGGAAACATAAAGCTGCTGGATGAAATGGTCCAGTGCCAAAATGAGCTTAAAATCT TTGTTTCCAGGAATTAGCTAACTTGGATTTGTGGAAGCTTTTGGCAAGCAATATGGAATC TTGCCTGGTATCATTGAGCCCACACATGGAGGAAGCAGAACTCATCAGTTCTTGGCGTTT CACGCCATGCCTAACTTTTCCCTTGAGTGCATGGCATGTTTTGTTACAGGTTGTAGAGTA TTTGCAGAAGGAAACCATTTCTGGTTATTTGGCTATAAAAAGTCAGCATAAAATATGATC CAACTAAAAGGGATTAATTTTGGCATTTTTGTATATTTATGCATTAGGTGATGGGACTT TTAAAGGTTTGAATTTATTAGGACACGAACTAAAAATAAAAGTGCACTAGGGGACAGTTG ATTTCAATCTAAGAAAAGTTAACACTTGGGAATTACAAGAAGTAAAACAAGTGCAACTAA ATCATTTATTAGTTGTTTTTTGAAAGCAGTTTTATGTATAAATAACAAATGTTTATATTT AACTAAATGTAAGGTACGAATTATTACATATTAAACTTTTCTTCCCCTTCCTAGTTCTGA AGTAGATATATATATATATATCTACTGTCACATTCCATATATTTTGAATATTTAACTC ATCTAGTTAATAATGTTTTTATTCCATGCGAATGATTTGATATTTTCATCCTTATTTCTC TTTGGCTACAATTTATATTGAGTTATATCTGTACATTCTGGTAATCTAAAATCCTTAAAA ATACTCTAATAGCCTTGAGTGACCAACTTTTTTTTTAAAGCACAGATGTAATTGTCTAAT GTTCTGATGGGAACGTAACACTTATTTTTATATAAAAAGAGACTGAGTAAACAAACATTA TAGAAAAAAAGTGAAGTTTTTTAGTTGTTTTTTGTGGTATTCAACCAGCAAGTTGTTTTC TTTCAGAGTTTCCTCCTTCAAAAAGTTATATTGCATTTACAAATGTTTTACAAGGCAGAA AGTTTGACTGGATAGTTAGTGTAAAAGCTTCATGTTGAGATCTTCACGTATCATTCTGCT AAACCAGAATATGTTCAGCTGTGTTACTAATTTTTCAGCTTAATCCTCAGTGCTTATTAT TTACATAACAATAACTTTTTATCAGTTACATTTTATTTTTATTTAAACTGGCCAAAAGCA AAATTATTTTATGTTAAAATGTGTGCTAAACTATCCCAGGAAAGTATTTAATCCAACATT GTAAATGAAGTATCTTGTACATATAAATTTATTTCTTTTGCAGAGCATTATATTACTGGA TGTTTAATTTACAAAATAGTTGGGTAAATGTTCCAACAAACTTTAAAGTACCTTGAAGTC AAATTGTCTGTTTTTGTTTTGTTGTTGTTGTTGTTTTCTTAAGTGTTACATTAAAAC TCTAACCAAGGAAAGGGTTCTTTAAGAACATTCCCTTAGAGGGATAAAGTTGAGAAGTGT GCCTTTTTTTTAATGGCTTGAAGTTTCAGAGGTGATAAAAATTAAAATCACACTACTATT TGAAGCTCATTTTCTATGCAGGTTTTTAAACGTCATTTATGTATCATTCTTTTTATATAT CACACTTAAGCTTGTGTTAGCTTTTTTCTTTTGCCCCAGATCAAACTGAACAATGTATAT AACACTATCTGTCTGTAAAATACTTTTTTTAAGAAAGCATTTATATTTATATGACAGCTT GAACTGACAACATTGTGTATATAGATCATCTTGAAGTATTATTTCACATTGAAAAGAAGA AAATATATTGATAACTATAGATGTTATGAAGAAGAGGGTATTTCTAGTTTTGTACTAAAA ATCAATTGGATGAACTAAATCCAAAACATGACACTGTAGGCAGCAGTTTTAAGTCTTATT TTTACTGTTTATATATTTGAATGCTGCTACAACAGATGATCTTCATCCCTGAAGTTTTCA GCTAAACTTGGTTTCCTAGAATAGACTGTTAACTTTCAAAATTTTTATTGGTGAAATGGA AATACTGTTTTTCCTTGTGAATGAATTTTCATATTTGTAAGTGCTAAGTTTATAATTCAG GTTTGATCAAGGTGTGAATAACTGAAGAAAATAACTTGCTGGCTATATAGGAAAATGCTG TGGAAATGAACTGTGTATATACTTCTGGGAGGAACAAATTTAATCATTTCTTCTGTTAAG CACTAATCAGTATAGTGCAACTCCTGGTTCTGTACTGTATTTTATATGCAACATATATGC TTTAATATTTTAATGTTTGTGCATTAATATTTTCAATTTGTTTAACCACTTTGCTGCTAA GATTTTGCCGTCCCATTCCCATTTTTTCCTTTACAATTTTAAACAAGTTTCTTCATTAAA AACTATGGTGATGAAATGGTTTTTATTTTACCTTGGATCTTTATAGTTAACATACCCAGT TTCTTAATCAGTCTACAAGACTAACTGATGATATAATGTTCTCTGAATCCCTATATGGAA ATTTTCTTTTGAGTAAATGAGAATTCCTTTGTGAAAGCAAATGGGTAGTTTAAATCACTG ATTCTTAAACATGTGTATAGGCACCTTCAGGAACATTTTCTCATTCTCTGTACAGATTCG GCACTGCCAATTGGCTTTTCCTCTAAAACTTTTCTTTGTTTTTATCTGATATAAGCAGAT GGCTCAAGACAACTGC

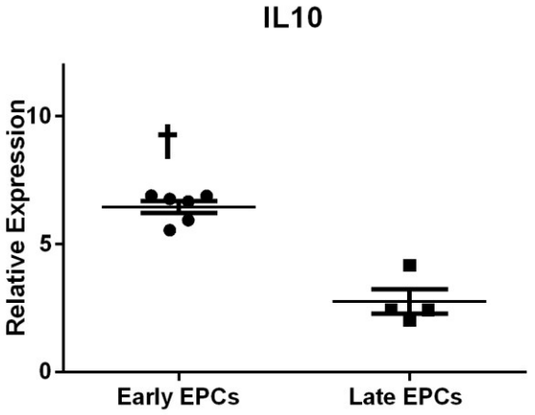

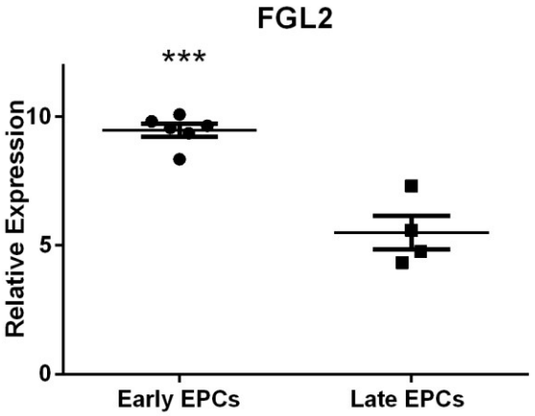

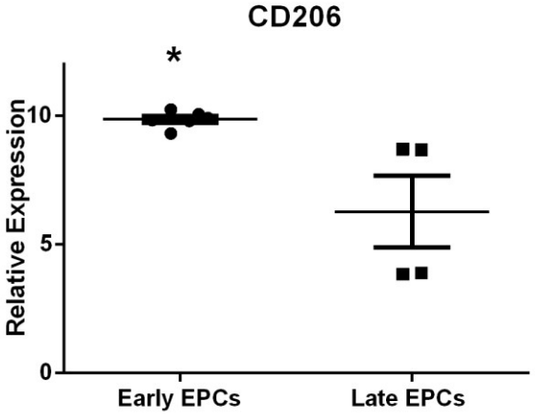

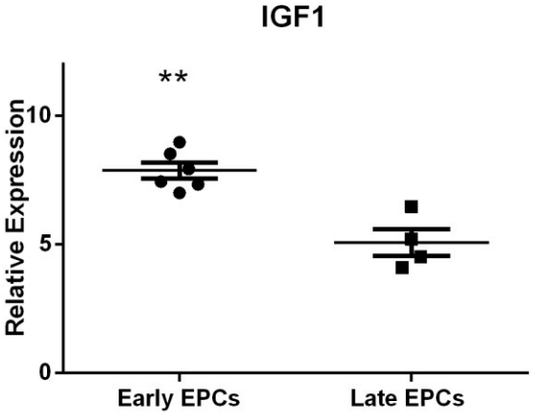

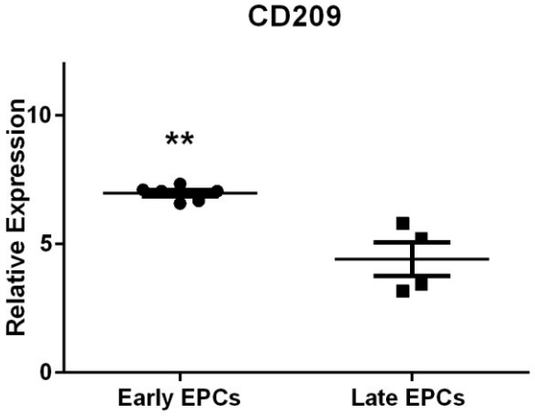

Appendix D: Early EPCs express higher anti-inflammatory markers than late EPCs.

The expression of 5 classic non-inflammatory (M2 macrophage) markers was compared between early and late EPCs. Early EPCs were studied at day 5, and late EPCs were studied at passage 3. Data represent mean ± SEM; n=4-6. †$p<0.0001$, ***$p<0.001$, ** represents $p<0.01$, * $p<0.05$.

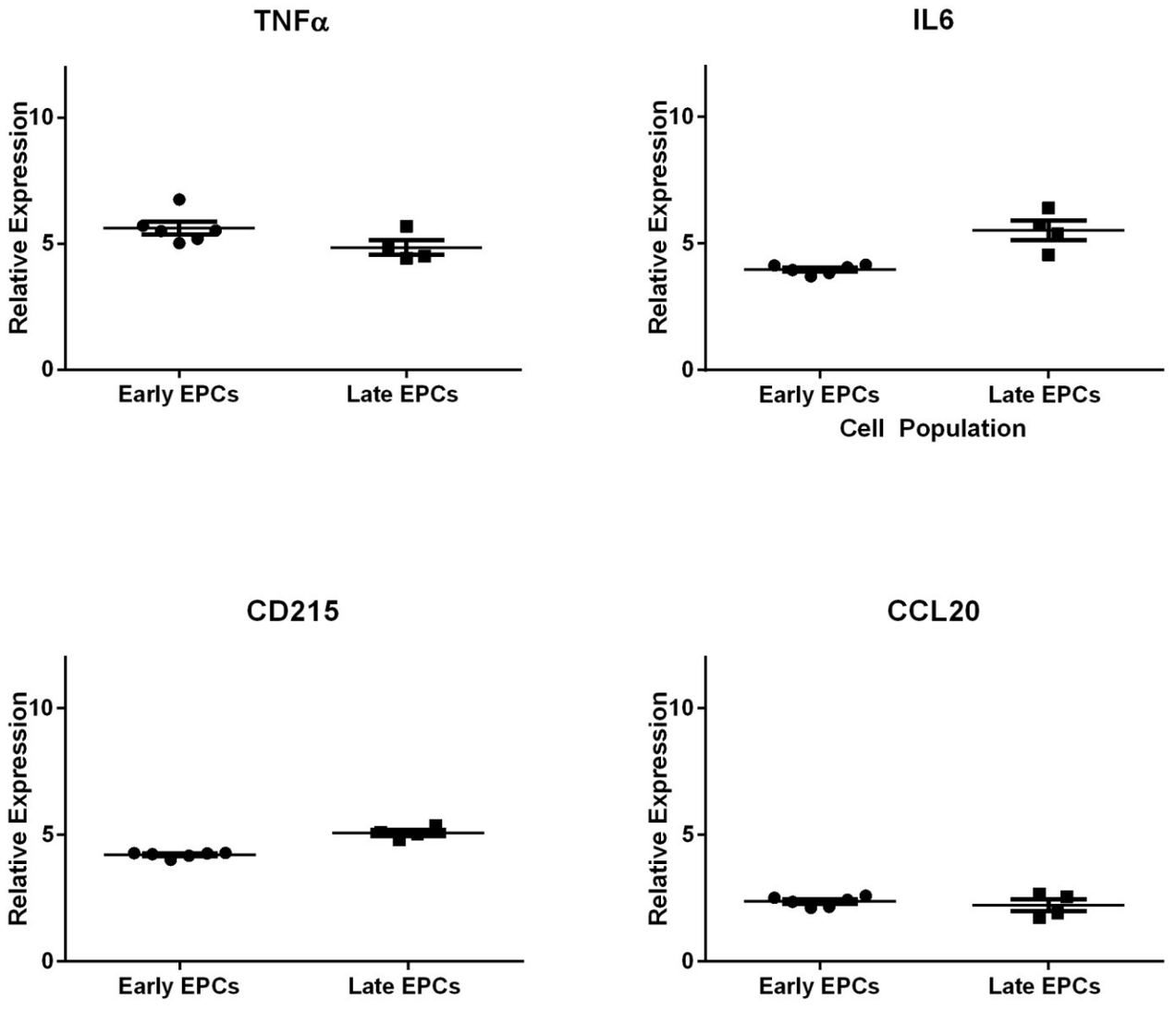

Appendix E: Expression of four classical inflammatory markers in early and late EPCs

Early EPCs were studied at day 5 and late EPCs were studied at passage 3. Data represent mean ± SEM, n=4-6.

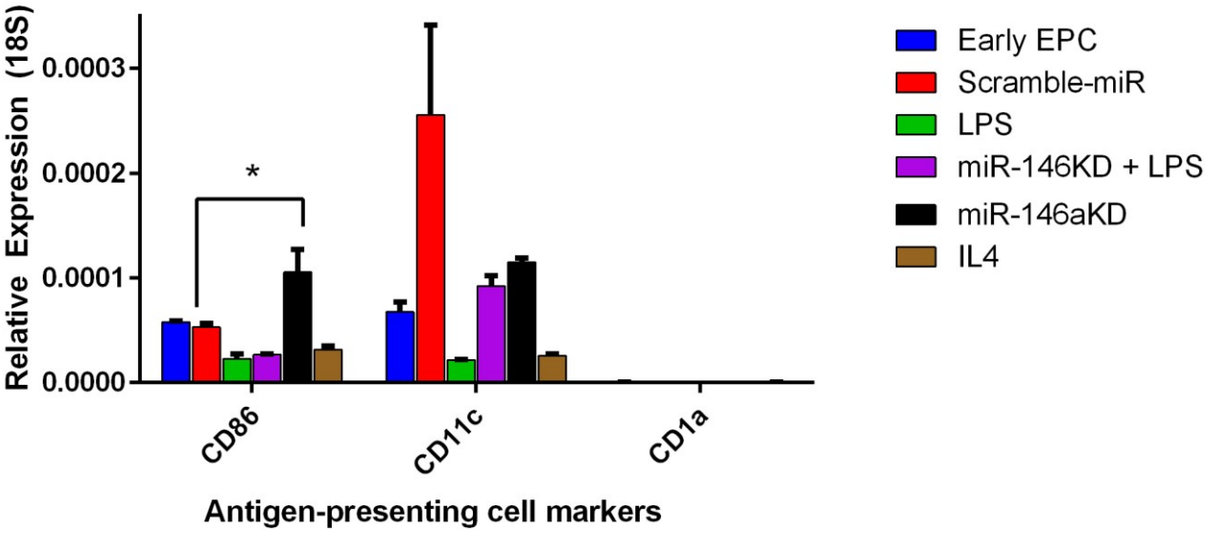

Appendix F: Modulating miR-146a confers changes in antigen-presenting markers in early EPCs

Using qRT-pCR, we compared changes in antigen-presenting cell markers with manipulation of miR-146a alone, and in concert with LPS treatment. We noted a decreased trend in CD86 expression with LPS treatment alone. However, this trend was not significant. We also noted a non-significant trend towards decreased CD86 expression with miR-146aKD in conjunction with LPS treatment. However, a significant increase in CD86 expression with miR-146aKD alone was measured. Comparatively, changes in CD11c were not assessed due to high variability detected with scramble-miR transfection alone. Detection of CD1a was minimal in comparison to other markers assessed, with no changes between treatment groups. The presence of miR-146a results in diminished CD86 expression with LPS as measured by qRT-PCR; no changes detected in CD11c or CD1a expression. Data represent mean ± SEM; n=3. † $p<0.0001$, * $p<0.05$.

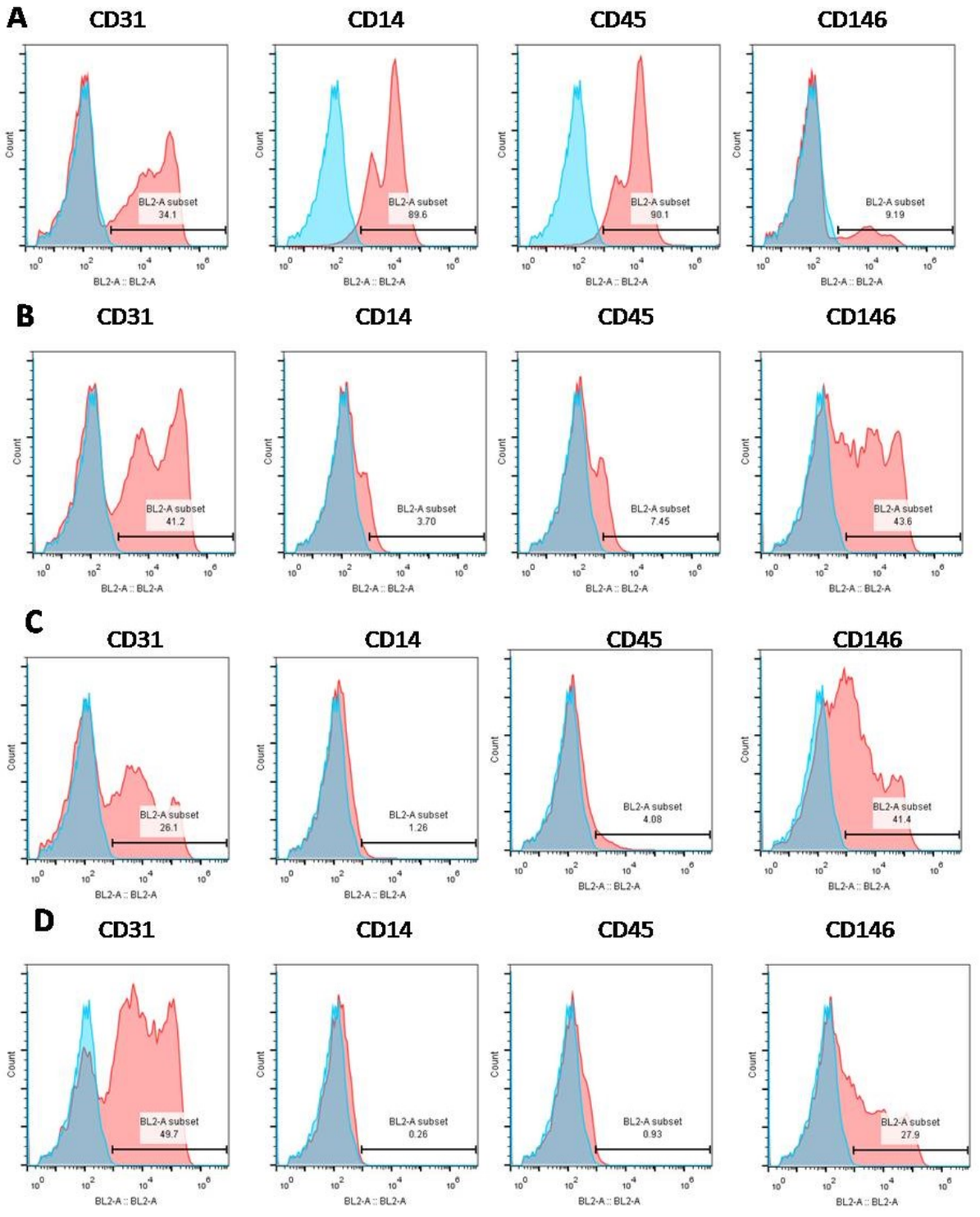

Appendix G: Expression of select markers in MCAM-generated ECFCs (1of 2)

Representative histograms from flow cytometric analysis on ECFCs generated from MCAM$^+$ precursor cell population.

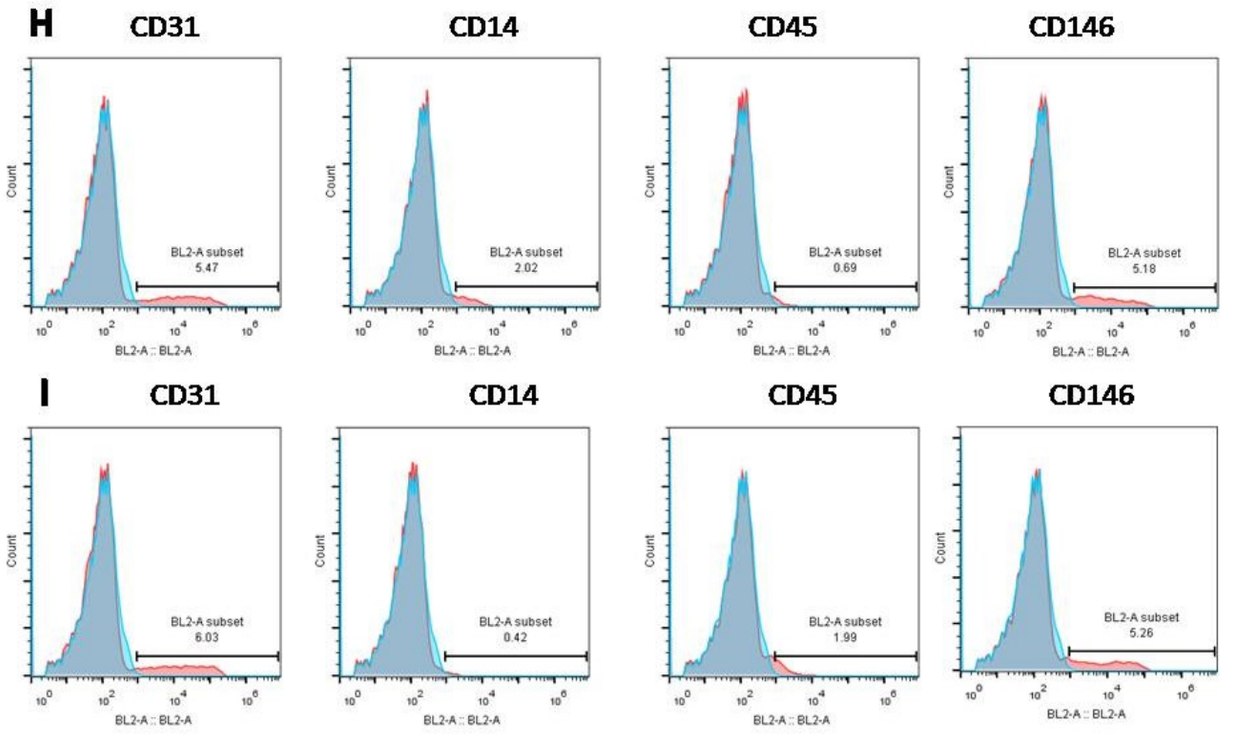

Appendix H: Expression of select markers in MCAM-generated ECFCs (2 of 2)

Continuation of histograms from flow cytometric analysis of MCAM-generated ECFCs. Note: Groups E, F, G were only used for quality control and subsequently omitted for analysis. Statistics for the ELCC group markers is presented in Appendix R.

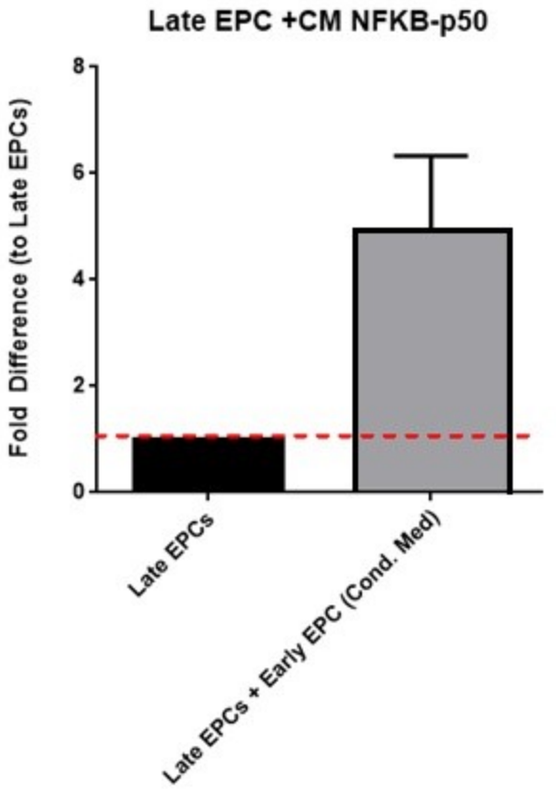

Appendix I: Conditioned media from early EPCs exacerbates NFKB-p50 in late EPCs

Media from normally cultured early EPCs was used on late EPCs in a 50% conditioned media (C.M.) per media change. Late EPCs grown for 3 days with early EPC media exhibited greater than 5 fold increase NFKB-p50. SEM, n=3

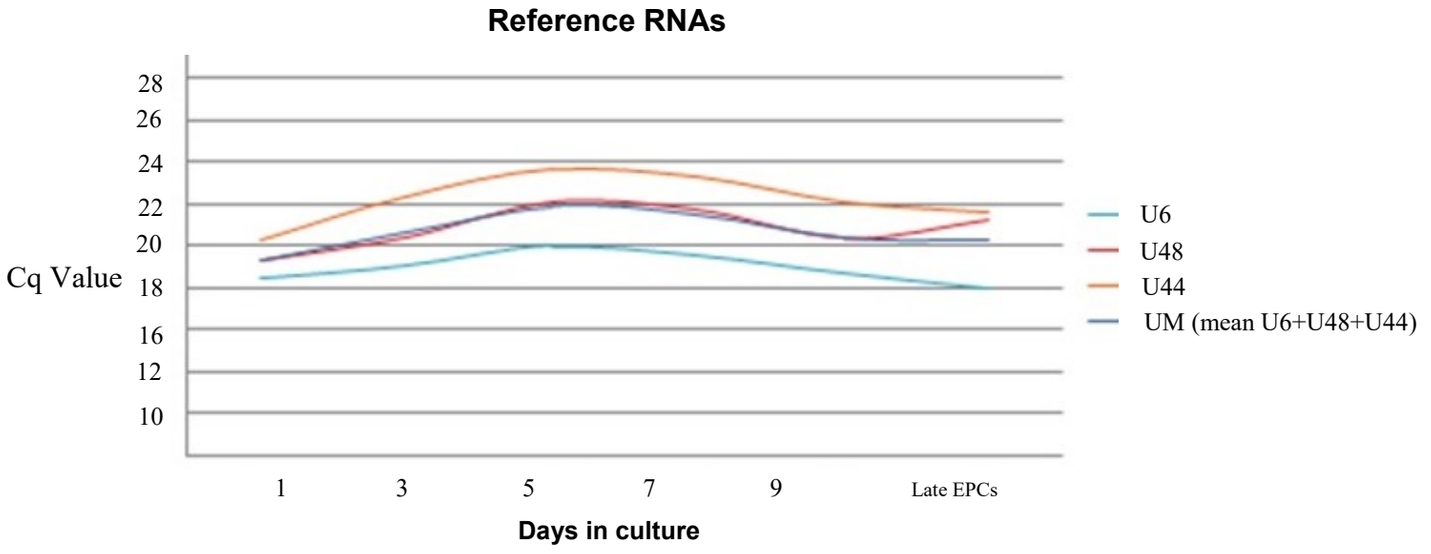

Appendix J: Stability of small-nucleolar microRNAs used for normalization

A plot of RNU6 (U6), RNU48 (U48) and RNU44 (U44) qRT-PCR Cq values during 10 day culture of early EPCs. The mean of RNU6 and RNU48 snRNAs were used for analysis.

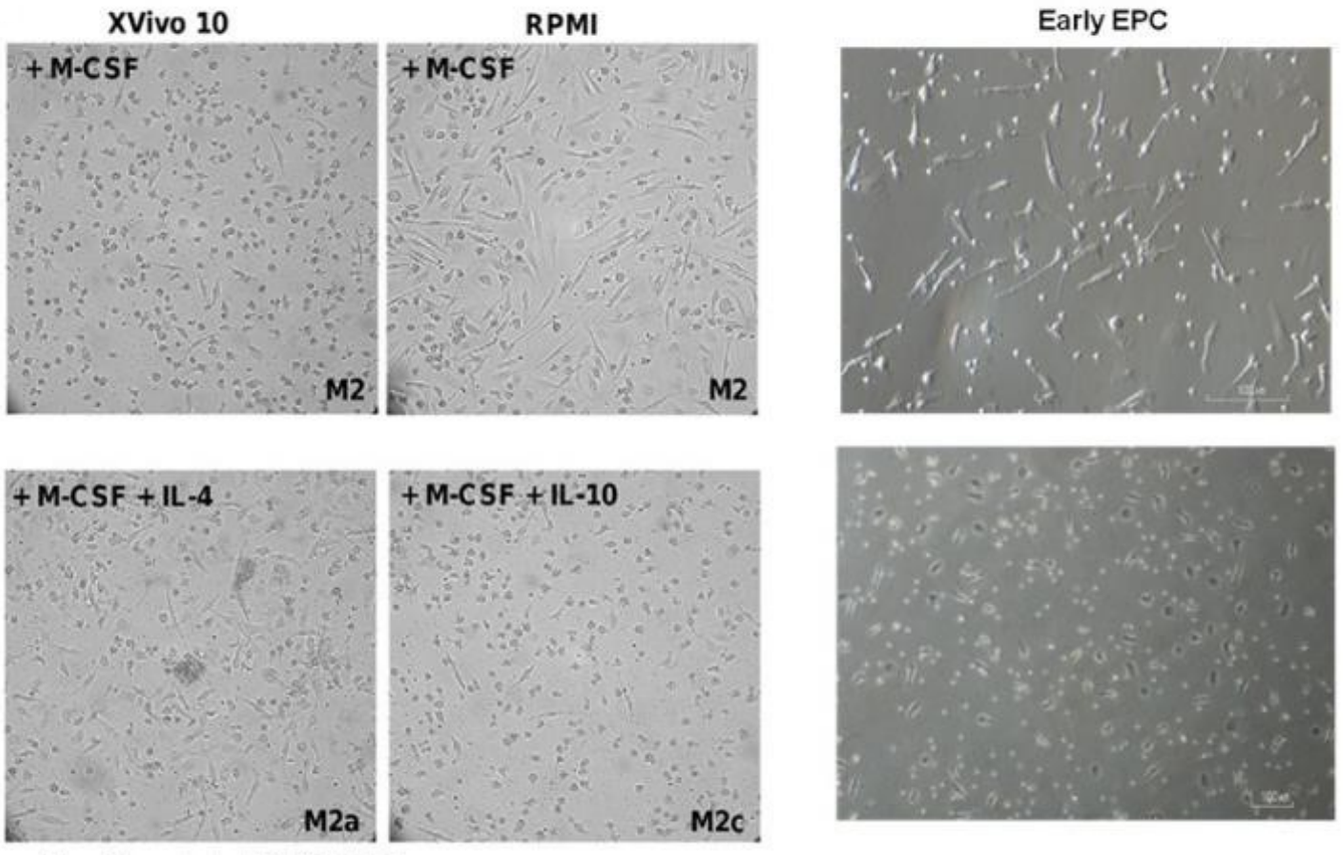

Appendix K: A Comparison of morphology between M2 polarized macrophages and early EPCs

Rod-shaped morphology of early EPCs (right column) bears similar character to M2 macrophages (left). Early EPCs shown under Hoffman modulation contrast (top-right) and phase contrast (bottom-right) to show granularity. Image adapted with permission from Rey-Giraud et al. (2012)

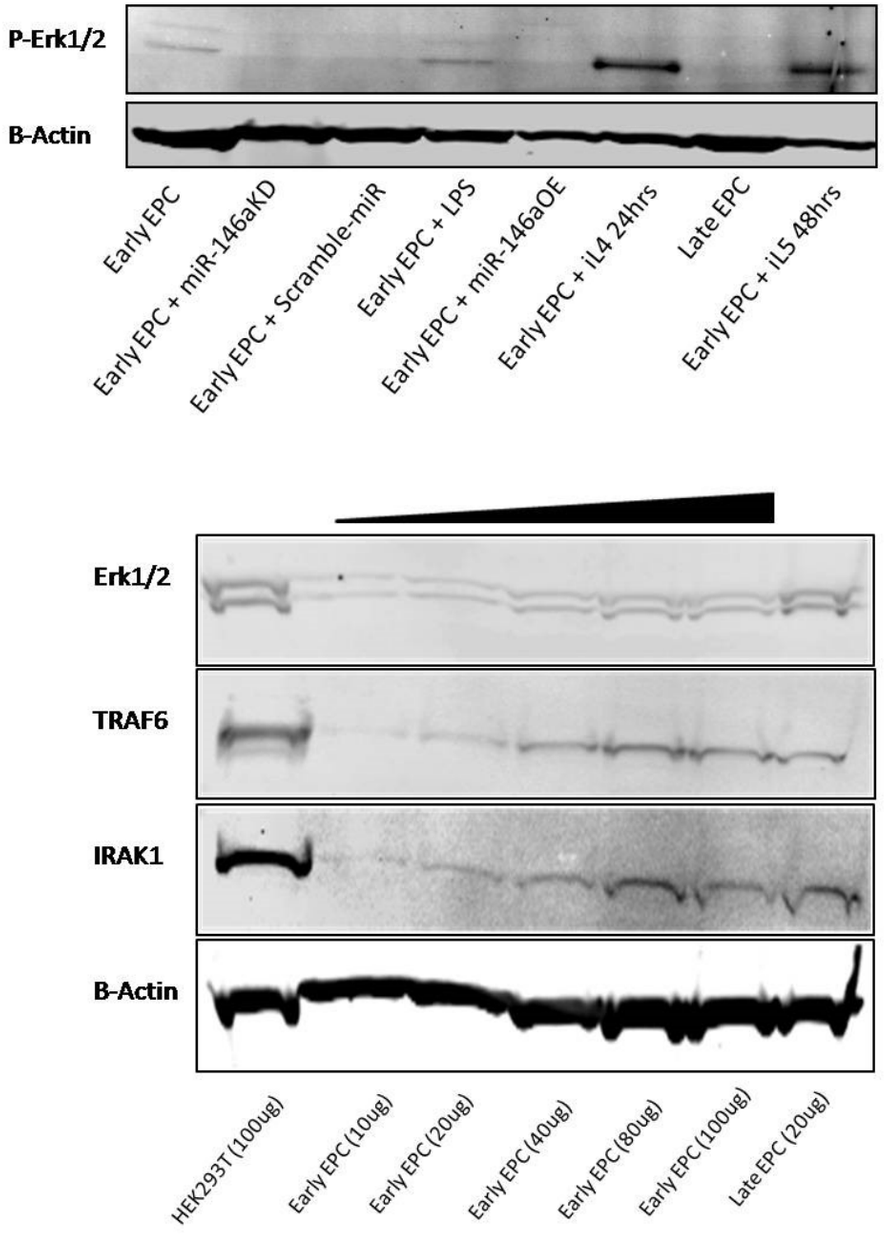

Appendix L: Basal ERK1/2, TRAF6 and IRAK1 in early and late EPCs

(Top) Knockdown of miR-146a in early EPCs does not affect phosphorylated ERK1/2. (Bottom) Representative blot of TRAF6 and IRAK1 protein expression in early and late EPC for comparison in expression.

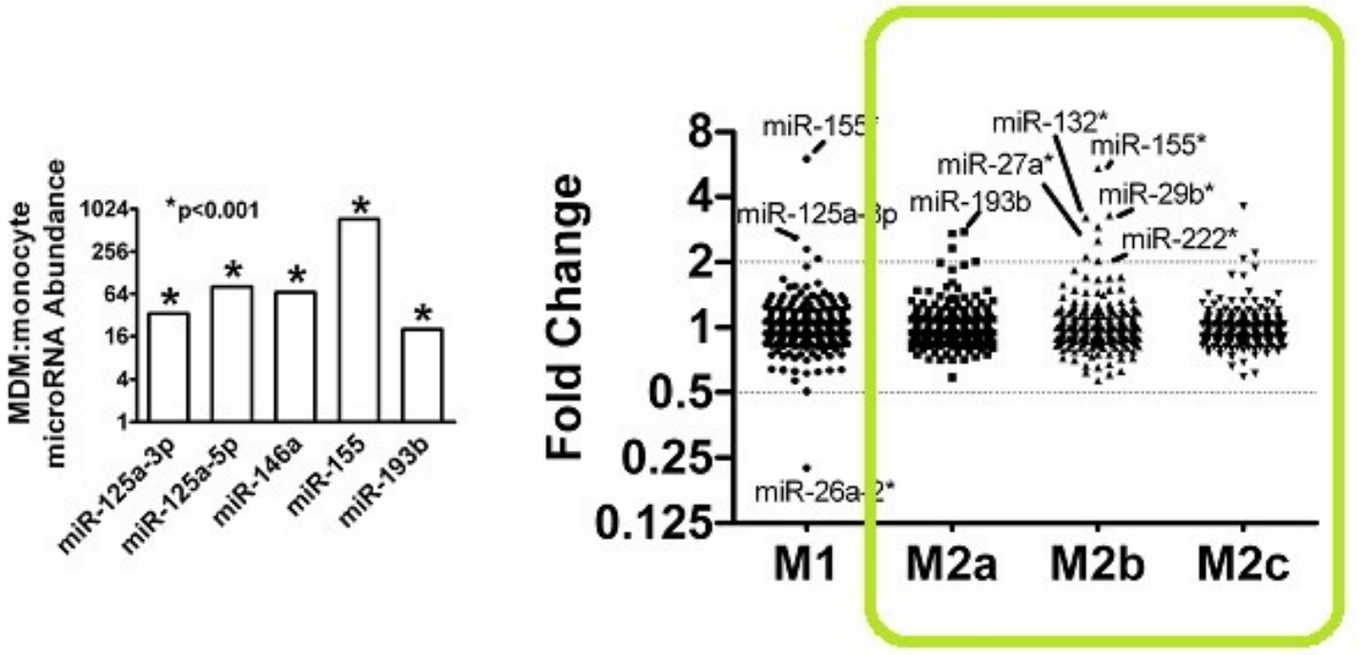

Appendix M: High abundance of miR-146a, miR-132* and miR-155*

Monocyte-derived macrophages (MDM) express progressively increased levels of miR-146a during transdifferentiation. Passenger strands miR-132* and miR-155* are highly expressed in anti-inflammatory M2b macrophages. Image modified from Graff et al. (2012)

Appendix N: Appended Chapter - A robust protocol for efficiently generating late EPCs using MCAM^{+} MNCs

Preamble

Since this chapter covers an area which is outside of the central focus of this thesis, yet has important relevance to the findings presented within this thesis, we have placed it within the appendices. Over the course of this project, we have compiled experimental evidence to uncover the originating fraction of cells from adult peripheral blood, which yield endothelial-like colony forming cells (ELCCs) and late EPCs. Of key importance to this chapter is that late EPCs are typically grown from cord blood, since their generation from adult peripheral blood is often challenging and inefficient, mostly due to the fact that the origin of late EPCs within the mononuclear cell fraction is entirely unknown. Though far less efficient than generating late EPCs from cord blood, late EPCs can be generated either from adult whole blood or from leukapheresis. However, the generation of late EPCs from adult whole blood is often inconsistent and prone to contamination due to low enrichment of the starting cell population, and therefore leukapheresis is often used. In parallel to our experiments covered in this thesis, we devised a reliable protocol to efficiently generate late EPCs using only a fraction of the original protocol's starting leukocyte cell population. This chapter will describe how to isolate the starting fraction of cells from adult peripheral blood, which ultimately yield late EPCs, and how to grow the resultant cell population in order to minimize contamination of non-late EPC ELCCs. For this chapter, the term MCAM is often used instead of CD146 to minimize confusion with miR-146a from previous chapters.

Introduction

a) Identifying the origin of late EPCs

In the past few decades, many studies have been conducted to investigate the origin of human adult late EPCs. It has been suggested that late EPCs arise from very rare precursor cells which likely decrease in abundance with age and co-morbidities (184). This highly proliferative cell population has been demonstrated to have potential therapeutic applications in cell therapy, tissue engineering, as well as being particularly amenable for induction to a pluripotent state (iPS cells) (156, 185). The generation of late EPCs from adult blood is enhanced through leukapheresis since this process eliminates much of the debris and non-specific cell populations from peripheral blood, while providing a larger number of mononuclear cells that can be cultured under typical conditions for the derivation of early EPCs, while reducing the risk of circulating endothelial cell (CEC) contamination. However, leukapheresis requires hours of collection causing discomfort for volunteers, and the uncertain origin of the precise cell fraction from the collected blood needed for late EPCs generation makes it often cumbersome and poses additional costs. Therefore, the ability to identify the precise fraction of the mononuclear cell population that gives rise to late EPCs would allow for increased efficiency for sample collection, isolation, and may enhance their potential use for therapeutic applications.

b) MCAM and Circulating Endothelial Cells

MCAM (aka MCAM MUC18, P1H12, S-Endo 1 or CD146) is an endothelial marker found on late EPCs and is commonly used for identifying CECs (186). It is a constitutively expressed, trans-membrane glycoprotein found in endothelial cells as well as pericytes, activated T lymphocytes, trophoblasts and malignant melanoma tumours

(187, 188). MCAM is also expressed on another known late EPC-like cell population called colony forming unit-hill (or CFU-Hill) cells. CFU-Hill cells are colony forming cells that emerge within a week of culture, expressing the endothelial cell marker CD31, in addition to the monocyte marker CD14 and panleukocyte marker CD45. As such, it is common for researchers to test for CD14 and CD45 in conjunction with CD31 and CD146 when classifying late EPCs. CECs are typically isolated from adult whole blood using antibodies to the CD146 antigen conjugated to paramagnetic beads (176). Unlike late EPCs, CECs emerge within days of plating and have limited proliferation. Magnetic selection of $CD146^+$ cells has also been shown to be effective for isolation of cord blood-derived MNCs destined to become late EPCs. Delorme et al. showed that elimination of CECs, followed by selection for $CD146^+$ MNCs from cord blood yielded late EPCs which lacked the leukocyte marker CD45 (179). To date no study has implicated microRNAs in the regulation of MCAM expression in the derivation of adult late EPCs.

c) Selecting a more reliable method for generating adult late EPCs using MCAM selection

As noted earlier, the classical protocol for the generation of late EPCs from leukapheresis is based on a protocol optimized for the generation of early EPCs. Since it unknown whether late EPCs are transdifferentiated early EPCs or whether these originate from another rare stem cell precursor or "pre-late EPC", combined with the existing consensus that generation of late EPCs from adult leukapheresis is largely inefficient and cumbersome, we pondered whether a more efficient protocol could be achieved for this isolation process using our present understanding.

In optimizing and refining a consistent protocol for the generation of late EPCs, we tested five different approaches to varying MCAM selection based on time of selection and cell enrichment using Ficoll-Paque

(Appendix R). In Appendix R, we present a table comparing generation of ELCCs based on MCAM sorting on day 1 (in green) versus day 7 (in purple) and our original protocol (pink). Our results revealed that the time of MCAM selection (post plating) and the use of Ficoll centrifugation greatly impacted the yield of ELCCs and true late EPCs. However, though MCAM+ MNCs consistently generate colonies which include late EPCs, cell number, longevity and robustness of endothelial phenotype vary depending on donor, and culture conditions[1].

Hypothesis and Aim

Hypothesis: A rare population of angiogenic endothelial progenitor cell precursor cells (i.e. pre-late EPCs) can be identified and isolated from circulating leukocytes or early outgrowth EPCs through MCAM expression; and possibly, the presence of pro-angiogenic miR-126.

Aim: Compare late EPC generation from adult leukocytes using varied approaches for MCAM selection.

Generating Late EPCs using MCAM$^+$ MNCs

[1] Variations based on donor are attributed to health and physiological state, which we identified, is reflected in miR-126 expression (i.e.: donors with cardiovascular complications have MCAM$^+$MNCs with reduced miR-126; which later become late EPCs with reduced longevity). Refer to chapter V.

NOTE: It is crucial to reiterate that ideal culture conditions are essential for generation of true late EPCs. Otherwise, "pre-late EPCs" grown under varying conditions yield endothelial-like colony forming cells that do not express late EPCs markers despite having similar morphology (Appendix P). For this reason, we have used the term "endothelial-like colony cells" or ELCCs instead of late EPCs for the protocol below. For this purpose, late EPCs represent endothelial-like cells cultured normally, possessing classical late EPCs features (i.e.: $CD31^+$ $CD14^-$ and $CD45^-$); while the term ELCCs is less specific, referring to all endothelial-like colony forming cells including those lacking classical late EPCs features e.g. CFU-Hill cells.

Reagents and solutions

MACs Buffer (PBS + 5% BSA)

CD146 MACs beads

MACs separation column

EBM-2 media (Lonza Cat. No. CC-3156)

EGM-2mv bullet kit SingleQuots (Lonza Cat. No. CC-4147)

-Consists of hEGF, Hydrocortisone, GA-1000 (Gentamicin Amphotericin-B), FBS (2mL not used), VEGF, hFGF-B, R3, IGF-1 and Ascorbic Acid

Human Serum (Wisent Cat. No. 022-210)

Human Fibronectin (Roche Cat. No. 11080938001)

Corning $75cm^2$(T75) Flask

3% Acetic Acid with Methylene blue (for initial cell counting Stem Cell Technologies Cat. No. 07060)

LAL reagent water

PBS (Ca^{2+} and Mg^{2+} free)

TrypLE

Ficoll Paque PLUS (GE 17-1440-02)

Human leukapheresis sample

- Collected on a Optima using monocyte enrichment protocol
- 2 total blood volumes cycled, resulting in 150-200 mL collected apheresis
- 60-80 $x10^6$ leukocytes/mL
- 10-25 % monocytes

1. Prior to the start of the experiment, begin by removing 100 mL from the 500 mL EBM-2 media, and replace by adding 100 mL of human serum to obtain EBM-2 consisting of 20% human serum. To this media, add the entire contents of the of the EGM-2MV bullet kits (omitting the addition of fetal bovine serum).

2. To the 5 mg of human fibronectin, add 5 mL of LAL reagent water. The 1 mg/mL concentrated solution is allowed to incubate for 30 minutes to1hour for complete reconstitution at 37ºC with occasional swirling. Add 100 µL of the fibronectin solution into 100 mL of PBS to produce a 10 µg/mL working fibronectin solution. Coat each T75 flask with 12 mL of diluted fibronectin (4 mL per T25, 12 mL per T75, 28 mL per T175). Incubate fibronectin coating for 45 minutes, then replace with PBS to prevent drying of substrate while experiment commences.

Processing and enriching leukapheresis product

For this stage, it is essential that the following steps are completed as quickly as possible and that the media used at each step is pre-warmed to 37ºC to achieve the best results.

1. Dilution: Upon reception, the collected leukapheresis is diluted four fold in 1xDPBS.

2. Pre-plate counting: Aliquot a small portion of the apheresis into prepared media, adjust the initial diluted product concentration based on the initial cell density obtained from apheresis to $2.5x10^6$ cells/mL making note of the total volume for later calculations. From this aliquot, create a 1:1 dilution with methylene blue and perform a cell count.

3. Sorting: Once cell numbers are confirmed, $CD146^+$ cells are sorted using the Mylteni MACs separation system following manufacturer's protocol. Following cell sorting, $CD146^+$ cell fraction is counted again prior to plating; ensure minimal time between cell sorting and plating. Note: A greater total number of $CD31^+$ ELCCs can be achieved by plating non-ficolled leukapheresis on day 0 and sorting for $CD146^+$ cells on day 7 (refer to step C4).

4. Plating: For adequate EPC outgrowth, plate the cells at a density of $0.3\text{-}0.5x10^6$ cells/cm^2. This seeding density accounts for total $CD146^+$ cell population to be counted on day 7 while minimizing competing proliferative cell populations which may have been accidentally plated that could eliminate or reduce ELCC generation.

5. Volume adjustment: Calculate the volume of leukapheresis required to achieve the desired cell number for selected flasks. Remove desired volume from the leukapheresis product with an additional 25% adjusted volume to account for cell loss during washes.

6. Wash: Split the sample volume into 50 mL conical tubes containing 25 mL DPBS per conical tube for washes. Spin cells for 7 minutes at 350 g.

7. Following the wash, remove the supernatant without disturbing the pellet. Resuspend the pellet into the appropriate pre-calculated volume of pre-warmed EGM-2MV media while gently dissolving the pellet. Note: the volume of media used per flask depends on the experimenter; generally, 15 mL is used per T75 (5 mL for T25, and 30 mL for T175).

Early endothelial progenitor cell outgrowth

1. After initial plating and incubation, cells should be left undisturbed for a minimum of 36 hours for full adhesion to fibronectin substrate. Until emergence of colony forming cells, it is critical to minimize disturbance of plated cells as $CD146^+$ have low adherence to fibronectin until colony formation.

2. The first media change should occur after 48 hours of cell plating. It is acceptable to observe a lot of cell debris in the first week of plating. For the generation of ELCC, it is imperative that the media changes are completed with minimal agitation of the flask; using pre-warmed EGM-2MV media. No washes are

necessary. Partial media changes are appropriate but should be adjusted for occurrence to account for freshness.

3. Typical rod-shaped EPCs will emerge in the non-$CD146^+$ sorted cells after the first media change and will continue to emerge 48-72 hours post-plating. For the first week, a reduction of 94% cell leukocyte cell density is expected. This will be accommodated on day 7.

4. Consolidation (NOTE: $CD146^+$ cells sorted on day 0 should not be consolidated on day 7): On day 7, begin by pre-coating half of the total number of plated flasks from day 1, following the same procedures as day 1. Gently remove media from flasks. Apply pre-warmed TrypLE dissociation enzymatic solution to the flasks containing adherent cells and place into the incubator for 10 minutes (use the same volumes used for fibronectin coating). Agitate the flasks every 2 minutes during incubation. Remove TrypLE cell suspensions and place into 50mL conical tubes. Scrape the emptied flasks and rinse with PBS to detach any remaining cells. Add this to the existing cell suspension. Add 20 mL EGM-2MV media to neutralize

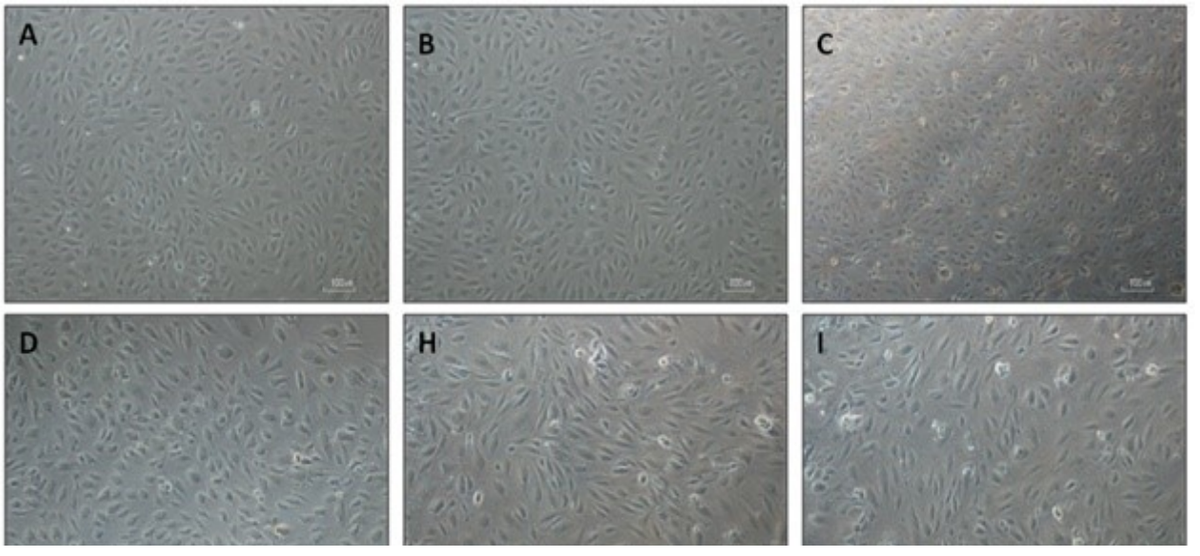

Appendix O: Variations in ELCC morphology from one participant's $MCAM^+$ cells

Representative images of cultured colony forming cells. Cells in groups H and I formed elongated ECFC-like cells which lacked endothelial marker, CD31. A difference in morphology can be noted between cells of group B and D, which differ only in non-ficolled and pre-ficolled conditions, respectively.

TryPLE. Centrifuge cell suspensions at 350 g for 7 minutes. Gently remove the supernatant and resuspend the cell pellets into 5mL EGM-2MV. At this point, each conical tube contains one flask worth of plated cells. Combine every two flasks into one conical tube to consolidate the cell suspension two fold. Re-plate each cell suspension onto a fibronectin pre-coated flask. Place flasks immediately into the cell incubator. Cells should be undisturbed for 12-24 hours.

5. *Plating cells for the generation of ELCCs:* Once cells are detached from their respective flasks in step 4 above, count cells, spin cells at 300 g for 10 minutes and resuspend cells in 60 μL of MACs buffer per 10^7 cells.

6. From step 5, add 20 μL of CD146 MACs microbeads and 20 μL of FCR human blocking reagent. Store cells in a 4 degree fridge for 15 minutes.

7. After 15 minutes, an addition 1 mL MACs buffer is added per 10^7 cells, and cells are centrifuged at 300 g for 10 minutes. The pellet is resuspended in 500 μL buffer per 10^7 cells and this cells suspension is MACs sorted.

8. Separate the $CD146^-$ cell fraction (these cells can be re-plated on fibronectin to form EPCs after 24 hours). Spin down the $CD146^+$ cells at 300 g for 10 minutes. Resuspend the $CD146^+$ cell fraction in appropriate EGM-2MV media, and count cells. Plate the $CD146^+$ cell fraction at 7500 cells per cm^2 on fibronectin-coated flasks. Place flasks immediately into the incubator. Cells should be undisturbed for a minimum of 36 hours with gentle media changes until ELCCs emerge. As ELCCs emerge, floating cell debris will subside.

9. IMPORTANT NOTE: The $CD146^+$ population represents 1-5% of the total EPC cell population after 7 days in culture.

Endothelial colony forming cell outgrowth

1. As early as day 9, ELCCs colonies will begin to emerge within the EPCs.

2. Starting from day 8, begin to scan each flask of plated cells systematically starting from one edge of the flask and working across each high powered field.

3. Once a colony of ELCCs is identified, mark the top of the flask to indicate the location of ELCCs colony for later inspection.

4. Colonies of ELCCs will emerge as small clusters and will proliferate rapidly (the doubling time of ELCCs will vary from donor to donor). Once colonies emerge, ELCCs will expand detaching neighbouring EPCs. Cell debris will emerge above the flask until the heterogeneous EPC/ELCC population becomes a homogeneous ELCC population (after expansion).

IMPORTANT NOTE: During the isolation of $CD146^+$ cells (on day 1 or day 7), a small fraction of $CD146^+$ cells can by lysed for RNA extraction. Compared to typical early EPCs, a high miR-126 expressing $MCAM^+$ cell population will yield more proliferative ELCCs with late EPC characteristics (i.e.: $CD31^+$, $CD14^-$, $CD45^-$).

5. At this time it is essential that a complete media change is performed every 48 hours until expansion is performed.

6. Continue to monitor ELCC growth until multiple ~640 mm^2 sized colonies emerge.

7. Monitor the rate of ELCC proliferation as it will vary from participant to participant. This information will be valuable during expansion.

Appendix P: MNCs, EPCs and ELCCs showing typical cell morphology

Mononuclear Cells (left), EPCs at day 5 (middle) and ELCCs (right) are represented. Images taken at 100x magnification. Scale bar = 100 μm. Purified MCAM expressing cells typically do not undergo differentiation into rod morphology; instead progress directly into colony forming cells.

Endothelial colony forming cell expansion and harvest

1. Typical ELCC proliferation doubling time is 3-4 days. Media changes should be performed every other day.

2. Once multiple ELCC colonies emerge, gently remove media from each flask. Apply TrypLE in the same volume and manner as step 4 of C. Incubate for 5 minutes. The shortened incubation time reflects the adhesion of ELCCs compared to EPCs. ELCCs lift readily with TrypLE compared to EPCs. As such, a shortened incubation time allows for selectivity of ELCCs for expansion. Agitate the flasks every minute during incubation.

3. Carefully remove the TrypLE suspension, and place into a 50 mL conical tube. Add 20 mL EGM-2MV to neutralize TrypLE. Spin cell suspension at 400 g for 7 minutes. Discard adherent EPC from leftover flasks.

4. After spinning, gently remove and discard the supernatant. To the pellet, add 30 mL pre-warmed media while gently disrupting the pellet. At this point, each conical tube represents 1 flask of cells. Split the total volume of cell media suspension into two flasks to expand the distribution of ELCCs two-fold. Plate non-coated corning flasks with this cell suspension. ELCCs do not require fibronectin coating.

5. ELCC doubling times will decrease with subsequent expansion and passages.

Freezing and thawing endothelial colony forming cells for study

i. Upon reception of leukapheresis, unused portions of leukapheresis product must be frozen unmanipulated in 10% DMSO, undiluted. Upon thawing, leukapheresis product must be warmed for 3 minutes in 37 ºC water bath and added directly to a 50 mL conical tube containing 20 mL pre-warmed EGM-2MV media. This cell suspension can then be centrifuged at 350 g for 7 minutes and replaced with fresh EGM-2MV media to remove DMSO. The same procedures as b) can be followed for the remaining procedure.

ii. ELCCs must be frozen at $1x10^6$ cells/mL in 80% EGM-2MV, 10% human serum and 10% DMSO.

Generation of only early EPCs occurs normally from frozen leukapheresis. But ELCCs generated from frozen leukapheresis are extremely rare, emerging after approximately 17 days and do not survive expansion. Generation of early EPCs from frozen leukapheresis is unaffected by freeze/thaw.

From the above protocol, the following parameters were systematically tested to assess effects on the phenotype of the predominant resultant ELCCs:

- Ficolled versus non-ficolled cell preparation on day 1.

- Day of cell sorting (i.e.: MACs sorting for $MCAM^+$ cells on day 1 versus day 7).

We expected that variations in these parameters would provide insight into variability in: ELCC markers (i.e. late EPC vs CFU-Hill), longevity and total cell yield (on the final day of culture, day 28).

Results

Evidence of late EPC precursor cells

In our studies investigating the generation of late EPCs from human adult leukapheresis, we have made several key observations which provide insight into the origin of late EPCs as well as culture conditions that optimize late EPC outgrowth:

i. Late EPCs are only generated from fresh adult leukapheresis. Once frozen, adult leukapheresis can only generate early EPCs. This finding suggests that early EPCs do not transdifferentiate into late EPCs; instead a possibly sensitive late EPCs precursor cell type with impaired freeze/thaw adaptability may exist within the mononuclear cell fraction. As well, late EPCs can be generated directly from MNCs using MCAM selection and proper culture conditions and that these cells become late EPCs *without* first becoming early EPCs. This also suggests that early EPCs are not precursors to late EPCs.

ii. Using Ficoll Paque for enrichment of isolated mononuclear cell buffy coat substantially *reduces* $MCAM^+$ selection, while removal of CECs using an adhesion step did not reduce the generation of late EPCs. Typically, Ficoll improves early EPC generation by increasing the total mononuclear cell fraction and thereby the monocyte population for generation of early EPCs. However, our finding

suggests that a rare precursor cell population which yield late EPCs is not fully represented in the same cell density as mononuclear cells. $MCAM^+$ precursor late EPCs are possibly lost in the ficoll pellet.

iii. ELCCs (including late EPCs) emerge *only* within the $MCAM^+$ cell fraction of human adult leukapheresis. In all conducted experiments involving separation of $MCAM^+$ cells, $MCAM^-$ cell population never yielded colony forming cells (group I in Appendix R was the rare exception). However, only a small fraction of $MCAM^+$ cells yield colony forming cells, not the entire $MCAM^+$ fraction. These rare colony forming cells exist as rounded cells for the initial 7 days in culture and can grow into various cell types when grown under different culture conditions. As such, $MCAM^+$ cells must be cultured under proper conditions to yield late EPCs possessing appropriate characterization. Additionally, late EPCs generated from $MCAM^+$ mononuclear cells from day 1 do *not* take on rod-shaped morphology prior to emerging as colony forming cells. We have not investigated these findings from human adult whole blood and have not reproduced these results with cord blood.

iv. $MCAM^+$ cells isolated from human adult *leukapheresis* are >90% $CD45^+$ on day 1. This number reflects only hemocytometric counts following magnetic activated cell (MACs) sorting. Due to low cell numbers in isolating $MCAM^+$ cells on day 1, flow cytometric analysis was done on day 28 (after the cells had expanded). During passages, cultures were split into triplicates prior to flow cytometry.

v. $MCAM^+$ mononuclear cells represent 1-5% of total human adult leukocytes (measured on day 1 in leukapheresis). However, as mononuclear cells are grown under EPC conditions, total number of $MCAM^+$ cells increase within the first week in culture especially in *non-ficolled* leukapheresis product (Appendix Q). This finding suggests that MCAM expression is not static and can be modified under

appropriate culture conditions. Likewise, MCAM expression is lost gradually with prolonged culture.

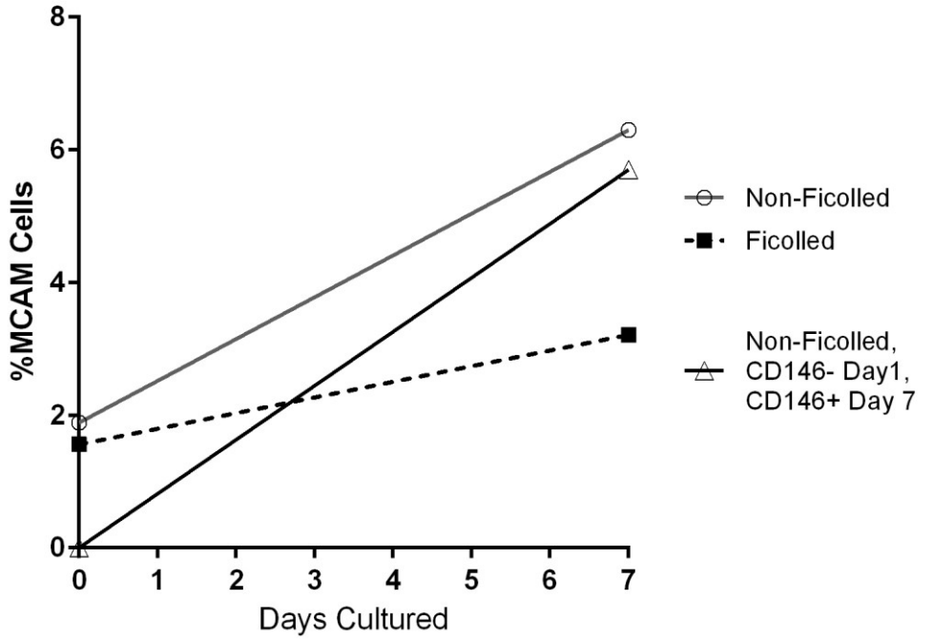

Appendix Q: MCAM expression increases under endothelial-promoting culture conditions

Total percentage of MCAM expressing cells plotted from day of seeding to day 7. All cells were from the same participant sample. The population initially depleted of MCAM cells (white triangle) had the largest increase in $MCAM^+$ cells in 7 days, but overall yielded smallest number of total colony forming cells likely due to early senescence.

Protocol Group	Ficolled /non-Ficolled	Day of MCAM selection	Passage number (after colony formation)	Cell count on day 28 (x10^6)	
A	ficolled	Day 1	2	2.4	
H	non-ficolled	Day 1	1+	1.4	
D	ficolled	Day 7 (during consolidation)	4	3.2	
B	non-ficolled	Day 7 (during consolidation)	4+	1.5	
I*	non-ficolled	*CD146*$^-$ sort day 1, CD146$^+$ sorted on day 7	1	0.55	
C (original protocol)	ficolled	N/A	3	1.6	

Appendix R: MCAM$^+$ sorting techniques for generating ELCCs

To narrow down the precise fraction of cells which yield late EPCs after MCAM selection, we varied Ficollation and the day of MCAM selection and recorded how many passages the resultant cells underwent in 28 days as well as the number of remaining cells on day 28. Group C cells were grown using our classic protocol (which was optimized for early EPCs), this was the only group that was not MCAM sorted. Therefore, to show difference in yield, group C was used as the comparison group for statistical analysis. Consolidation refers to re-seeding cells on day 7 based on cell count to maintain consistent cell density (accounting for loss of cell density over time). In all groups, MCAM expression increased under endothelial promoting culture conditions within the first seven days. All cell characterization was performed on day 28; P1 passages were done on day 14; + indicates that cells survived several passages after data collection. *Group I cells were negatively sorted for MCAM on day 1 but had 2% increase in MCAM$^+$ cells by 7; following MCAM$^+$ sort on day 7, colonies emerged. The results seen with group I was unique and unrepeatable. Not shown in the results presented in above table, non-Ficolled and day 7 sorted cells (protocol B) yield highest total ELCCs on average, based on repeated observations.

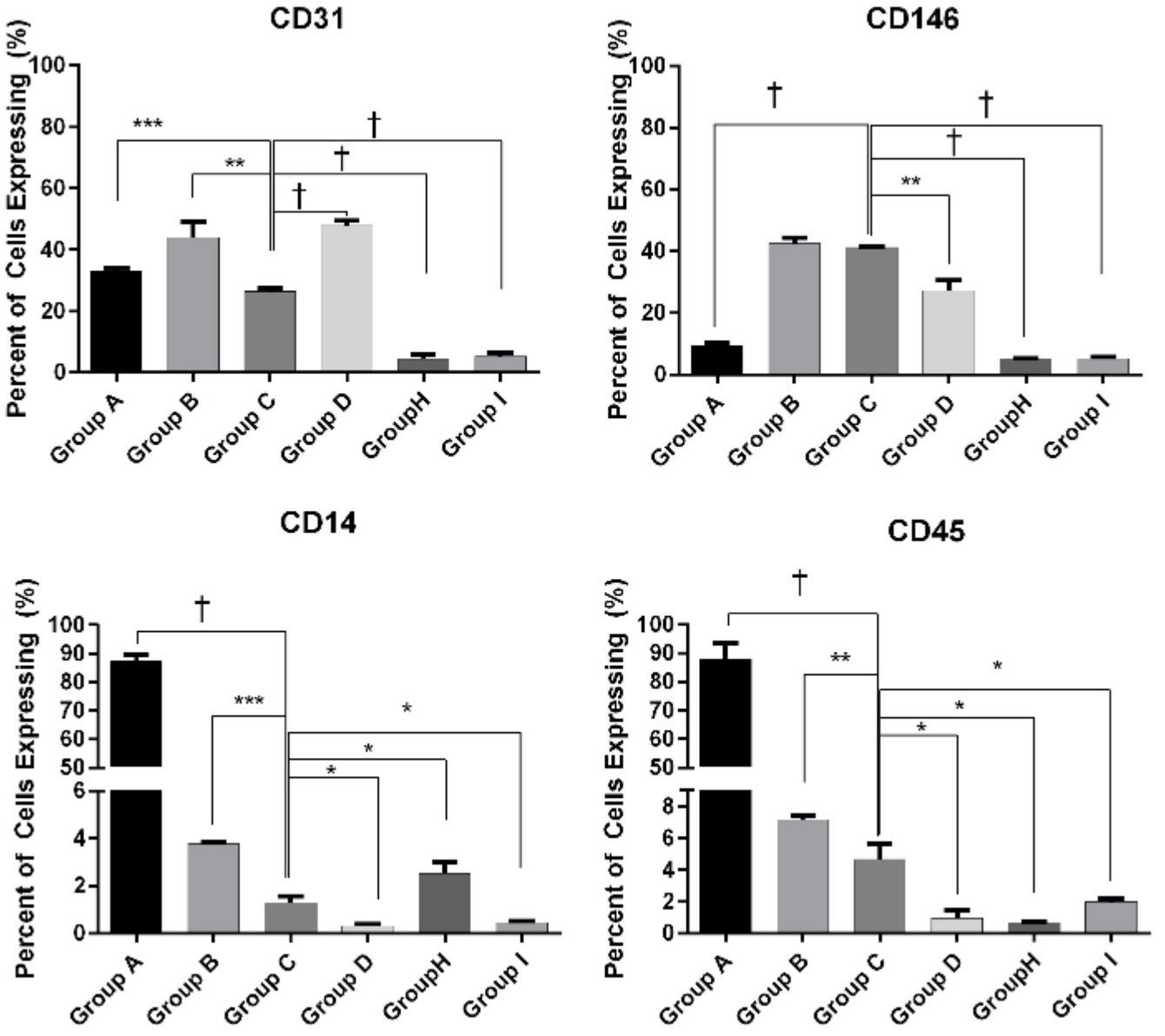

Appendix S: Characterization of ELCCs on day 28

Cell characterization of ELCCs was performed on day 28. Groups B and D expressed highest levels of CD31, but group D expressed less CD146, comparatively. Data represents mean ± SEM; n=3. †p <0.0001, *** p <0.001, **p<0.01, *p<0.05; all groups compared to group C.

Discussion

The expression of α5β1 integrin on monocytes allows for adhesion to fibronectin, which can be exploited in cell culture for their enrichment using a fibronectin substrate. As such, culture of both early and late EPCs on fibronectin is advantageous as it allows for the quick removal of loosely bound ELCCs with a gentle dissociation enzyme like TrypLE without disturbing strongly adherent early EPCs. Consolidation on day 7 allows for exclusion of tightly bound early EPCs, while selecting for loosely bound ELCCs (and late EPCs).

The re-emergence of $CD146^+$ cells after being removed on day 0 (group I) supports existing evidence of endothelial reprogramming of $CD146^-$ cells, due in part, to the presence of endothelial-promoting growth factors such as hFGF, VEGF and IGF-1 which are supplemented with the cell media (29), for a complete list refer to the protocol in the methods section. There is a possibility that MCAM expressing cells may have been missed in the first sorting, which could explain the increased MCAM positive cells after 7 days of culture. However, the overall increased number of MCAM expressing cells when sorted on day 7, was a consistent and reoccurring observation. It should be noted that the week delay before the outgrowth of colonies, combined with a lack of colony forming cells emerging from frozen leukapheresis, strongly supports the theory that these cells are not sloughed endothelial-cells or CECs. If CECs were indeed present during isolation, leukapheresis processing would greatly eliminate CEC presence and the resultant CECs would have limited proliferation. As well, groups sorted for MCAM on day 1, like group A cells (which were selected for MCAM immediately before initial seeding) would most likely be most vulnerable to CEC contamination. Group H would also be prone to CEC contamination for the very same reason. Another explanation for increased MCAM expression could be that a pre-existing population of "true EPCs" (pre-late EPCs) circulating within peripheral blood that may initially lack $CD146^-$ and are later

pushed towards an endothelial phenotype following two weeks in culture. Our results suggest that a "true EPC" population, which is likely reprogrammable, exists within the leukocyte fraction and enrichment with Ficollation reduces the number of such cells and therefore the final ELCC yield. This would explain the reduced yield with Ficoll is used. It is not clear *how much* the initial $CD146^-$ fraction of pre-late EPCs later express CD146 and subsequently become high proliferating true late EPCs (or what these cells may be).

The day of MCAM selection appears to be most critical based on our findings. Our data also shows that cells selected for $CD146^+$ on day 7 as opposed to day 1 (protocol B in Appendix S) produce a larger population of cells expressing the endothelial cell marker CD31 while co-expressing CD146 (and maintaining leukocyte marker CD45 and the monocyte plasticity marker CD14). The presence of CD14 and CD45 in cells from group A is a hallmark feature of CFU-Hill cells (28). Though CFU-Hill cells have been shown to be involved in stimulation and regulation of angiogenesis (55, 189), this cell population is accepted to be of hematopoietic origin and likely never become long term intimal endothelial cells (30, 190). Nonetheless, we were pleased to have identified a new method for the generation of CFU-Hill cells. Cell groups B and D differed only in the Ficoll density centrifugation. This step could account for the decreased CD146 expression in addition to CD14 and CD45 on day 28 (though this difference was marginal).

We observed that the total $MCAM^+$ MNCs from cardiac patients was in the same 1-5% range of total MNCs that we identified in healthy participants. However, Ficolled $CD146^+$ MNCs from cardiac patients (which contain the ELCCs that include the late EPC population) consistently yielded colony-forming cells with reduced longevity, which senesce by passage 3 (Figure 38). Using qRT-PCR, we noted that cardiac patients had significantly reduced expression of miR-126 in their Ficolled $CD146^+$ MNCs when measured on day 1 prior to seeding ($p<0.001$, Figure 38). This finding suggests that $CD146^+$ remains a good predictive marker for colony

forming cell populations, but a high expression of miR-126 is indicative of cardiovascular health and colony forming cell longevity. The explanation for this is found in earlier studies, which indicated that under cardiovascular injury or chronic pathology, decreased miR-126 in endothelial cells (causing increased SDF-1, which promotes healing by recruitment of early EPCs, as noted earlier). Therefore, late EPCs (or similar cells arising from the $CD146^+$ MNC cell fraction) could be undergoing the same or similar process, which causes reduction in miR-126 under cardiovascular injury or chronic pathology. Future experiments could pursue the implications of this.

Since umbilical cord blood typically possesses a richer source of colony forming cells, we postulate a higher fraction of MCAM expressing precursor cells in this sample population. Additionally, cord blood-derived colony forming cells survive higher passaging than adult generated cells, and thus possess greater longevity. To this end, we also postulate that cells from cord blood, which become colony-forming cells likely, possess higher miR-126. It has previously been reported that preeclampsia-derived late EPCs typically express lower miR-126 than their healthy counterpart cells (191). As such, our findings mirror this in adult-generated cells.

Chapter Summary

In summary, our findings from the candidate and global arrays shed light on a number of differences between early and late EPCs, which gave insight into the roles that microRNAs play in these cell types. Our global array inspired us to pursue MCAM while investigating late EPCs. When we pursued the relevance of MCAM in late EPCs and identified that only $CD146^+$ MNCs gave rise to ELCCs and late EPCs. This further inspired to devise a protocol for increasing the efficiency of late EPC generation.

Our findings are the first to identify CD146/MCAM as a *predictive* marker for ELCCs (and late EPCs) from adult leukapheresis. A major difference from our protocol and previous findings is the elimination of Ficoll-Paque for higher generation of colony forming cells (and late EPCs). Cord blood-derived colony forming cells are typically derived following Ficoll density centrifugation (and our findings showed that Ficollation of adult leukapheresis reduced late EPC yield), so it is possible that in human adults MCAM positive precursors are matured and thus possess different density which causes these cells to be lost when adult leukapheresis product is Ficolled.

Using the described protocol, generation of late EPCs can be achieved using less starting material, resulting in an overall greater yield of late EPCs. Identification of high-expressing miR-126 $MCAM^+$ cell population is currently limited by technology, but our protocol allows a unique method for identifying the fraction of mononuclear cells which consistently yield colony-forming cells and late EPCs. It is possible that screening for miR-126 expression using techniques such as qRT-PCR in $MCAM^+$ MNCs on day 1 could further improve our current described protocol.

REFERENCES

1. Micheletti RG, Fishbein GA, Currier JS, Singer EJ, Fishbein MC. Calcification of the internal elastic lamina of coronary arteries. Mod Pathol. 2008;21(8):1019-28.

2. Feletou M. The Endothelium: Part 1: Multiple Functions of the Endothelial Cells-Focus on Endothelium-Derived Vasoactive Mediators. Integrated Systems Physiology: from Molecule to Function to Disease. San Rafael (CA)2011.

3. Radomski MW, Palmer RM, Moncada S. Modulation of platelet aggregation by an L-arginine-nitric oxide pathway. Trends Pharmacol Sci. 1991;12(3):87-8.

4. Freedman JE, Sauter R, Battinelli EM, Ault K, Knowles C, Huang PL, et al. Deficient platelet-derived nitric oxide and enhanced hemostasis in mice lacking the NOSIII gene. Circulation research. 1999;84(12):1416-21.

5. Kubes P, Suzuki M, Granger DN. Nitric oxide: an endogenous modulator of leukocyte adhesion. Proceedings of the National Academy of Sciences of the United States of America. 1991;88(11):4651-5.

6. Lefer AM, Ma XL. Decreased basal nitric oxide release in hypercholesterolemia increases neutrophil adherence to rabbit coronary artery endothelium. Arterioscler Thromb. 1993;13(6):771-6.

7. Lefer DJ, Jones SP, Girod WG, Baines A, Grisham MB, Cockrell AS, et al. Leukocyte-endothelial cell interactions in nitric oxide synthase-deficient mice. Am J Physiol. 1999;276(6 Pt 2):H1943-50.

8. Otrock ZK, Mahfouz RA, Makarem JA, Shamseddine AI. Understanding the biology of angiogenesis: review of the most important molecular mechanisms. Blood Cells Mol Dis. 2007;39(2):212-20.

9. Folkman J, Shing Y. Angiogenesis. The Journal of biological chemistry. 1992;267(16):10931-4.

10. Li S, Huang NF, Hsu S. Mechanotransduction in endothelial cell migration. Journal of cellular biochemistry. 2005;96(6):1110-26.

11. Lamalice L, Le Boeuf F, Huot J. Endothelial cell migration during angiogenesis. Circulation research. 2007;100(6):782-94.

12. Byzova TV, Goldman CK, Pampori N, Thomas KA, Bett A, Shattil SJ, et al. A mechanism for modulation of cellular responses to VEGF: activation of the integrins. Mol Cell. 2000;6(4):851-60.

13. Kuwada SK, Li X. Integrin alpha5/beta1 mediates fibronectin-dependent epithelial cell proliferation through epidermal growth factor receptor activation. Molecular biology of the cell. 2000;11(7):2485-96.

14. Lobov IB, Brooks PC, Lang RA. Angiopoietin-2 displays VEGF-dependent modulation of capillary structure and endothelial cell survival in vivo. Proceedings of the National Academy of Sciences of the United States of America. 2002;99(17):11205-10.

15. Ross R, Bowen-Pope D, Raines EW, Faggiotto A. Endothelial injury: blood-vessel wall interactions. Ann N Y Acad Sci. 1982;401:260-4.

16. Stump MM, Jordan GL, Jr., Debakey ME, Halpert B. Endothelium grown from circulating blood on isolated inteavascular dacron hub. Am J Pathol. 1963;43:361-7.

17. Asahara T, Murohara T, Sullivan A, Silver M, van der Zee R, Li T, et al. Isolation of putative progenitor endothelial cells for angiogenesis. Science. 1997;275(5302):964-7.

18. Shi Q, Rafii S, Wu MH, Wijelath ES, Yu C, Ishida A, et al. Evidence for circulating bone marrow-derived endothelial cells. Blood. 1998;92(2):362-7.

19. Centola M, Capogrossi MC. [Role of G-CSF and GM-CSF therapy in patients with acute myocardial infarction and critical limb ischemia]. G Ital Cardiol (Rome). 2014;15(9):465-74.

20. Kawamoto A, Gwon HC, Iwaguro H, Yamaguchi JI, Uchida S, Masuda H, et al. Therapeutic potential of ex vivo expanded endothelial progenitor cells for myocardial ischemia. Circulation. 2001;103(5):634-7.

21. Orlic D, Kajstura J, Chimenti S, Bodine DM, Leri A, Anversa P. Bone marrow stem cells regenerate infarcted myocardium. Pediatric transplantation. 2003;7 Suppl 3:86-8.

22. Bhattacharya V, McSweeney PA, Shi Q, Bruno B, Ishida A, Nash R, et al. Enhanced endothelialization and microvessel formation in polyester grafts seeded with CD34(+) bone marrow cells. Blood. 2000;95(2):581-5.

23. Sata M, Saiura A, Kunisato A, Tojo A, Okada S, Tokuhisa T, et al. Hematopoietic stem cells differentiate into vascular cells that participate in the pathogenesis of atherosclerosis. Nature medicine. 2002;8(4):403-9.

24. Kim C, Schneider G, Abdel-Latif A, Mierzejewska K, Sunkara M, Borkowska S, et al. Ceramide-1-phosphate regulates migration of multipotent stromal cells and endothelial progenitor cells--implications for tissue regeneration. Stem Cells. 2013;31(3):500-10.

25. Schroder K, Kohnen A, Aicher A, Liehn EA, Buchse T, Stein S, et al. NADPH oxidase Nox2 is required for hypoxia-induced mobilization of endothelial progenitor cells. Circulation research. 2009;105(6):537-44.

26. Rosenzweig A. Endothelial progenitor cells. N Engl J Med. 2003;348(7):581-2.

27. Rehman J, Li J, Orschell CM, March KL. Peripheral blood "endothelial progenitor cells" are derived from monocyte/macrophages and secrete angiogenic growth factors. Circulation. 2003;107(8):1164-9.

28. Yoder MC. Is endothelium the origin of endothelial progenitor cells? Arteriosclerosis, thrombosis, and vascular biology. 2010;30(6):1094-103.

29. Yoder MC, Mead LE, Prater D, Krier TR, Mroueh KN, Li F, et al. Redefining endothelial progenitor cells via clonal analysis and hematopoietic stem/progenitor cell principals. Blood. 2007;109(5):1801-9.

30. Hirschi KK, Ingram DA, Yoder MC. Assessing identity, phenotype, and fate of endothelial progenitor cells. Arteriosclerosis, thrombosis, and vascular biology. 2008;28(9):1584-95.

31. Iba O, Matsubara H, Nozawa Y, Fujiyama S, Amano K, Mori Y, et al. Angiogenesis by implantation of peripheral blood mononuclear cells and platelets into ischemic limbs. Circulation. 2002;106(15):2019-25.

32. Kalka C, Masuda H, Takahashi T, Kalka-Moll WM, Silver M, Kearney M, et al. Transplantation of ex vivo expanded endothelial progenitor cells for therapeutic neovascularization. Proceedings of the National Academy of Sciences of the United States of America. 2000;97(7):3422-7.

33. Itescu S, Kocher AA, Schuster MD. Myocardial neovascularization by adult bone marrow-derived angioblasts: strategies for improvement of cardiomyocyte function. Annals of hematology. 2002;81 Suppl 2:S21-5.

34. Kawamoto A, Tkebuchava T, Yamaguchi J, Nishimura H, Yoon YS, Milliken C, et al. Intramyocardial transplantation of autologous endothelial progenitor cells for therapeutic neovascularization of myocardial ischemia. Circulation. 2003;107(3):461-8.

35. Walter DH, Dimmeler S. Endothelial progenitor cells: regulation and contribution to adult neovascularization. Herz. 2002;27(7):579-88.

36. Li TS, Hamano K, Suzuki K, Ito H, Zempo N, Matsuzaki M. Improved angiogenic potency by implantation of ex vivo hypoxia prestimulated bone marrow cells in rats. American journal of physiology Heart and circulatory physiology. 2002;283(2):H468-73.

37. Herold J, Pipp F, Fernandez B, Xing Z, Heil M, Tillmanns H, et al. Transplantation of monocytes: a novel strategy for in vivo augmentation of collateral vessel growth. Human gene therapy. 2004;15(1):1-12.

38. Ziegelhoeffer T, Fernandez B, Kostin S, Heil M, Voswinckel R, Helisch A, et al. Bone marrow-derived cells do not incorporate into the adult growing vasculature. Circulation research. 2004;94(2):230-8.

39. Kamihata H, Matsubara H, Nishiue T, Fujiyama S, Tsutsumi Y, Ozono R, et al. Implantation of bone marrow mononuclear cells into ischemic myocardium enhances collateral perfusion and regional function via side supply of angioblasts, angiogenic ligands, and cytokines. Circulation. 2001;104(9):1046-52.

40. Fuchs S, Baffour R, Zhou YF, Shou M, Pierre A, Tio FO, et al. Transendocardial delivery of autologous bone marrow enhances collateral perfusion and regional function in pigs with chronic experimental myocardial ischemia. Journal of the American College of Cardiology. 2001;37(6):1726-32.

41. Vicario J, Piva J, Pierini A, Ortega HH, Canal A, Gerardo L, et al. Transcoronary sinus delivery of autologous bone marrow and angiogenesis in pig models with myocardial injury. Cardiovascular radiation medicine. 2002;3(2):91-4.

42. Waksman R, Fournadjiev J, Baffour R, Pakala R, Hellinga D, Leborgne L, et al. Transepicardial autologous bone marrow-derived mononuclear cell therapy in a porcine model of chronically infarcted myocardium. Cardiovascular radiation medicine. 2004;5(3):125-31.

43. Carmeliet P. Mechanisms of angiogenesis and arteriogenesis. Nature medicine. 2000;6(4):389-95.

44. Asahara T, Masuda H, Takahashi T, Kalka C, Pastore C, Silver M, et al. Bone marrow origin of endothelial progenitor cells responsible for postnatal vasculogenesis in physiological and pathological neovascularization. Circulation research. 1999;85(3):221-8.

45. Schatteman GC, Hanlon HD, Jiao C, Dodds SG, Christy BA. Blood-derived angioblasts accelerate blood-flow restoration in diabetic mice. The Journal of clinical investigation. 2000;106(4):571-8.

46. Kocher AA, Schuster MD, Szabolcs MJ, Takuma S, Burkhoff D, Wang J, et al. Neovascularization of ischemic myocardium by human bone-marrow-derived angioblasts prevents cardiomyocyte apoptosis, reduces remodeling and improves cardiac function. Nature medicine. 2001;7(4):430-6.

47. De Falco E, Porcelli D, Torella AR, Straino S, Iachininoto MG, Orlandi A, et al. SDF-1 involvement in endothelial phenotype and ischemia-induced recruitment of bone marrow progenitor cells. Blood. 2004;104(12):3472-82.

48. Shintani S, Murohara T, Ikeda H, Ueno T, Honma T, Katoh A, et al. Mobilization of endothelial progenitor cells in patients with acute myocardial infarction. Circulation. 2001;103(23):2776-9.

49. Urbich C, Aicher A, Heeschen C, Dernbach E, Hofmann WK, Zeiher AM, et al. Soluble factors released by endothelial progenitor cells promote migration of endothelial cells and cardiac resident progenitor cells. Journal of molecular and cellular cardiology. 2005;39(5):733-42.

50. Yamaguchi J, Kusano KF, Masuo O, Kawamoto A, Silver M, Murasawa S, et al. Stromal cell-derived factor-1 effects on ex vivo expanded endothelial progenitor cell recruitment for ischemic neovascularization. Circulation. 2003;107(9):1322-8.

51. Yang C, Zhang ZH, Lu SH, Yang RC, Qian GQ, Han ZC. [Transplantation of cord blood endothelial progenitor cells ameliorates limb ischemia]. Zhonghua yi xue za zhi. 2003;83(16):1437-41.

52. Smadja DM, Bieche I, Uzan G, Bompais H, Muller L, Boisson-Vidal C, et al. PAR-1 activation on human late endothelial progenitor cells enhances angiogenesis in vitro with upregulation of the SDF-1/CXCR4 system. Arteriosclerosis, thrombosis, and vascular biology. 2005;25(11):2321-7.

53. Murohara T, Ikeda H, Duan J, Shintani S, Sasaki K, Eguchi H, et al. Transplanted cord blood-derived endothelial precursor cells augment postnatal neovascularization. The Journal of clinical investigation. 2000;105(11):1527-36.

54. Gulati R, Jevremovic D, Peterson TE, Witt TA, Kleppe LS, Mueske CS, et al. Autologous culture-modified mononuclear cells confer vascular protection after arterial injury. Circulation. 2003;108(12):1520-6.

55. Hur J, Yoon CH, Kim HS, Choi JH, Kang HJ, Hwang KK, et al. Characterization of two types of endothelial progenitor cells and their different contributions to neovasculogenesis. Arteriosclerosis, thrombosis, and vascular biology. 2004;24(2):288-93.

56. Ceradini DJ, Kulkarni AR, Callaghan MJ, Tepper OM, Bastidas N, Kleinman ME, et al. Progenitor cell trafficking is regulated by hypoxic gradients through HIF-1 induction of SDF-1. Nature medicine. 2004;10(8):858-64.

57. Askari AT, Unzek S, Popovic ZB, Goldman CK, Forudi F, Kiedrowski M, et al. Effect of stromal-cell-derived factor 1 on stem-cell homing and tissue regeneration in ischaemic cardiomyopathy. Lancet. 2003;362(9385):697-703.

58. Heeschen C, Lehmann R, Honold J, Assmus B, Aicher A, Walter DH, et al. Profoundly reduced neovascularization capacity of bone marrow mononuclear cells derived from patients with chronic ischemic heart disease. Circulation. 2004;109(13):1615-22.

59. Segal MS, Shah R, Afzal A, Perrault CM, Chang K, Schuler A, et al. Nitric oxide cytoskeletal-induced alterations reverse the endothelial progenitor cell migratory defect associated with diabetes. Diabetes. 2006;55(1):102-9.

60. Walter DH, Rochwalsky U, Reinhold J, Seeger F, Aicher A, Urbich C, et al. Sphingosine-1-phosphate stimulates the functional capacity of progenitor cells by activation of the CXCR4-dependent signaling pathway via the S1P3 receptor. Arteriosclerosis, thrombosis, and vascular biology. 2007;27(2):275-82.

61. Walter DH, Haendeler J, Reinhold J, Rochwalsky U, Seeger F, Honold J, et al. Impaired CXCR4 signaling contributes to the reduced neovascularization capacity of endothelial progenitor cells from patients with coronary artery disease. Circulation research. 2005;97(11):1142-51.

62. Zhang Y, Wittner M, Bouamar H, Jarrier P, Vainchenker W, Louache F. Identification of CXCR4 as a new nitric oxide-regulated gene in human CD34+ cells. Stem Cells. 2007;25(1):211-9.

63. Sbaa E, Dewever J, Martinive P, Bouzin C, Frerart F, Balligand JL, et al. Caveolin plays a central role in endothelial progenitor cell mobilization and homing in SDF-1-driven postischemic vasculogenesis. Circulation research. 2006;98(9):1219-27.

64. Forstermann U, Munzel T. Endothelial nitric oxide synthase in vascular disease: from marvel to menace. Circulation. 2006;113(13):1708-14.

65. Cheng Y, Jiang S, Hu R, Lv L. Potential mechanism for endothelial progenitor cell therapy in acute myocardial infarction: Activation of VEGF- PI3K/Akte-NOS pathway. Ann Clin Lab Sci. 2013;43(4):395-401.

66. Fish JE, Santoro MM, Morton SU, Yu S, Yeh RF, Wythe JD, et al. miR-126 regulates angiogenic signaling and vascular integrity. Developmental cell. 2008;15(2):272-84.

67. Polverini PJ, Cotran PS, Gimbrone MA, Jr., Unanue ER. Activated macrophages induce vascular proliferation. Nature. 1977;269(5631):804-6.

68. Berse B, Brown LF, Van de Water L, Dvorak HF, Senger DR. Vascular permeability factor (vascular endothelial growth factor) gene is expressed differentially in normal tissues, macrophages, and tumors. Molecular biology of the cell. 1992;3(2):211-20.

69. Urbich C, Heeschen C, Aicher A, Dernbach E, Zeiher AM, Dimmeler S. Relevance of monocytic features for neovascularization capacity of circulating endothelial progenitor cells. Circulation. 2003;108(20):2511-6.

70. Ormiston ML, Deng Y, Stewart DJ, Courtman DW. Innate immunity in the therapeutic actions of endothelial progenitor cells in pulmonary hypertension. American journal of respiratory cell and molecular biology. 2010;43(5):546-54.

71. Bitzer M, Ben-Dov IZ, Thum T. Microparticles and microRNAs of endothelial progenitor cells ameliorate acute kidney injury. Kidney international. 2012;82(4):375-7.

72. Mause SF, Weber C. Microparticles: protagonists of a novel communication network for intercellular information exchange. Circulation research. 2010;107(9):1047-57.

73. Lee RC, Feinbaum RL, Ambros V. The C. elegans heterochronic gene lin-4 encodes small RNAs with antisense complementarity to lin-14. Cell. 1993;75(5):843-54.

74. Ambros V. The functions of animal microRNAs. Nature. 2004;431(7006):350-5.

75. Bartel DP. MicroRNAs: Genomics, Biogenesis, Mechanism, and Function. Cell. 2004;116(2):281-97.

76. Fish JE, Srivastava D. MicroRNAs: Opening a new vein in angiogenesis research. Science Signaling. 2009;2(52).

77. Carthew RW, Sontheimer EJ. Origins and Mechanisms of miRNAs and siRNAs. Cell. 2009;136(4):642-55.

78. Czech B, Hannon GJ. Small RNA sorting: matchmaking for Argonautes. Nat Rev Genet. 2011;12(1):19-31.

79. Griffiths-Jones S, Grocock RJ, van Dongen S, Bateman A, Enright AJ. miRBase: microRNA sequences, targets and gene nomenclature. Nucleic acids research. 2006;34(Database issue):D140-4.

80. Liu G, Abraham E. MicroRNAs in immune response and macrophage polarization. Arteriosclerosis, thrombosis, and vascular biology. 2013;33(2):170-7.

81. Rhoades MW, Reinhart BJ, Lim LP, Burge CB, Bartel B, Bartel DP. Prediction of plant microRNA targets. Cell. 2002;110(4):513-20.

82. Tang G, Reinhart BJ, Bartel DP, Zamore PD. A biochemical framework for RNA silencing in plants. Genes & development. 2003;17(1):49-63.

83. Olsen PH, Ambros V. The lin-4 regulatory RNA controls developmental timing in Caenorhabditis elegans by blocking LIN-14 protein synthesis after the initiation of translation. Developmental biology. 1999;216(2):671-80.

84. Zhou B, Wang S, Mayr C, Bartel DP, Lodish HF. miR-150, a microRNA expressed in mature B and T cells, blocks early B cell development when expressed prematurely. Proceedings of the National Academy of Sciences of the United States of America. 2007;104(17):7080-5.

85. Sayed D, Abdellatif M. MicroRNAs in development and disease. Physiological reviews. 2011;91(3):827-87.

86. Poliseno L, Tuccoli A, Mariani L, Evangelista M, Citti L, Woods K, et al. MicroRNAs modulate the angiogenic properties of HUVECs. Blood. 2006;108(9):3068-71.

87. Forrest AR, Kanamori-Katayama M, Tomaru Y, Lassmann T, Ninomiya N, Takahashi Y, et al. Induction of microRNAs, mir-155, mir-222, mir-424 and mir-503, promotes monocytic differentiation through combinatorial regulation. Leukemia. 2010;24(2):460-6.

88. Takeuchi O, Akira S. Pattern recognition receptors and inflammation. Cell. 2010;140(6):805-20.

89. Medzhitov R, Horng T. Transcriptional control of the inflammatory response. Nature reviews Immunology. 2009;9(10):692-703.

90. Jeannin P, Jaillon S, Delneste Y. Pattern recognition receptors in the immune response against dying cells. Current opinion in immunology. 2008;20(5):530-7.

91. Mills KH. TLR-dependent T cell activation in autoimmunity. Nature reviews Immunology. 2011;11(12):807-22.

92. O'Connell RM, Rao DS, Baltimore D. microRNA regulation of inflammatory responses. Annual review of immunology. 2012;30:295-312.

93. Ruland J. Return to homeostasis: downregulation of NF-kappaB responses. Nature immunology. 2011;12(8):709-14.

94. Adhikari A, Xu M, Chen ZJ. Ubiquitin-mediated activation of TAK1 and IKK. Oncogene. 2007;26(22):3214-26.

95. Chen F, Bhatia D, Chang Q, Castranova V. Finding NEMO by K63-linked polyubiquitin chain. Cell Death Differ. 2006;13(11):1835-8.

96. Wang C, Deng L, Hong M, Akkaraju GR, Inoue J, Chen ZJ. TAK1 is a ubiquitin-dependent kinase of MKK and IKK. Nature. 2001;412(6844):346-51.

97. Kawai T, Akira S. Signaling to NF-kappaB by Toll-like receptors. Trends Mol Med. 2007;13(11):460-9.

98. Sun SC. The noncanonical NF-kappaB pathway. Immunol Rev. 2012;246(1):125-40.

99. Alam MM, O'Neill LA. MicroRNAs and the resolution phase of inflammation in macrophages. European journal of immunology. 2011;41(9):2482-5.

100. Contreras J, Rao DS. MicroRNAs in inflammation and immune responses. Leukemia. 2012;26(3):404-13.

101. Dai R, Ahmed SA. MicroRNA, a new paradigm for understanding immunoregulation, inflammation, and autoimmune diseases. Translational research : the journal of laboratory and clinical medicine. 2011;157(4):163-79.

102. O'Neill LA, Sheedy FJ, McCoy CE. MicroRNAs: the fine-tuners of Toll-like receptor signalling. Nature reviews Immunology. 2011;11(3):163-75.

103. Xiao C, Calado DP, Galler G, Thai TH, Patterson HC, Wang J, et al. MiR-150 controls B cell differentiation by targeting the transcription factor c-Myb. Cell. 2007;131(1):146-59.

104. Murray PJ, Wynn TA. Protective and pathogenic functions of macrophage subsets. Nature reviews Immunology. 2011;11(11):723-37.

105. Nahid MA, Satoh M, Chan EK. Mechanistic role of microRNA-146a in endotoxin-induced differential cross-regulation of TLR signaling. J Immunol. 2011;186(3):1723-34.

106. Hou J, Wang P, Lin L, Liu X, Ma F, An H, et al. MicroRNA-146a feedback inhibits RIG-I-dependent Type I IFN production in macrophages by targeting TRAF6, IRAK1, and IRAK2. J Immunol. 2009;183(3):2150-8.

107. Taganov KD, Boldin MP, Chang KJ, Baltimore D. NF-kappaB-dependent induction of microRNA miR-146, an inhibitor targeted to signaling proteins of innate immune responses. Proceedings of the National Academy of Sciences of the United States of America. 2006;103(33):12481-6.

108. Yang L, Boldin MP, Yu Y, Liu CS, Ea CK, Ramakrishnan P, et al. miR-146a controls the resolution of T cell responses in mice. The Journal of experimental medicine. 2012;209(9):1655-70.

109. Nahid MA, Pauley KM, Satoh M, Chan EK. miR-146a is critical for endotoxin-induced tolerance: IMPLICATION IN INNATE IMMUNITY. The Journal of biological chemistry. 2009;284(50):34590-9.

110. Lu LF, Boldin MP, Chaudhry A, Lin LL, Taganov KD, Hanada T, et al. Function of miR-146a in controlling Treg cell-mediated regulation of Th1 responses. Cell. 2010;142(6):914-29.

111. Boldin MP, Taganov KD, Rao DS, Yang L, Zhao JL, Kalwani M, et al. miR-146a is a significant brake on autoimmunity, myeloproliferation, and cancer in mice. The Journal of experimental medicine. 2011;208(6):1189-201.

112. Zhang Q, Kandic I, Kutryk MJ. Dysregulation of angiogenesis-related microRNAs in endothelial progenitor cells from patients with coronary artery disease. Biochemical and biophysical research communications. 2011;405(1):42-6.

113. Minami Y, Satoh M, Maesawa C, Takahashi Y, Tabuchi T, Itoh T, et al. Effect of atorvastatin on microRNA 221 / 222 expression in endothelial progenitor cells obtained from patients with coronary artery disease. Eur J Clin Invest. 2009;39(5):359-67.

114. Zhang X, Mao H, Chen JY, Wen S, Li D, Ye M, et al. Increased expression of microRNA-221 inhibits PAK1 in endothelial progenitor cells and impairs its function via c-Raf/MEK/ERK pathway. Biochemical and biophysical research communications. 2013;431(3):404-8.

115. Meng S, Cao J, Zhang X, Fan Y, Fang L, Wang C, et al. Downregulation of microRNA-130a contributes to endothelial progenitor cell dysfunction in diabetic patients via its target Runx3. PloS one. 2013;8(7):e68611.

116. Meng S, Cao JT, Zhang B, Zhou Q, Shen CX, Wang CQ. Downregulation of microRNA-126 in endothelial progenitor cells from diabetes patients, impairs their functional properties, via target gene Spred-1. Journal of molecular and cellular cardiology. 2012;53(1):64-72.

117. Yan T, Liu Y, Cui K, Hu B, Wang F, Zou L. MicroRNA-126 regulates EPCs function: implications for a role of miR-126 in preeclampsia. Journal of cellular biochemistry. 2013;114(9):2148-59.

118. Qu K, Wang Z, Lin X-l, Zhang K, He X-l, Zhang H. MicroRNAs: Key regulators of endothelial progenitor cell functions. Clinica Chimica Acta. 2015;448(0):65-73.

119. Bijkerk R, van Solingen C, de Boer HC, de Vries DK, Monge M, van Oeveren-Rietdijk A, et al. Silencing of miRNA-126 in kidney ischemia reperfusion is associated with elevated SDF-1 levels and mobilization of Sca-1+/Lin- progenitor cells. Microrna. 2014;3(3):144-9.

120. Shen L, Gao Y, Qian J, Wu Y, Zhou M, Sun A, et al. The role of SDF-1alpha/Rac pathway in the regulation of endothelial progenitor cell polarity; homing and expression of Rac1, Rac2 during endothelial repair. Molecular and cellular biochemistry. 2012;365(1-2):1-7.

121. Zhao X, Qian D, Wu N, Yin Y, Chen J, Cui B, et al. The spleen recruits endothelial progenitor cell via SDF-1/CXCR4 axis in mice. Journal of receptor and signal transduction research. 2010;30(4):246-54.

122. Grunewald M, Avraham I, Dor Y, Bachar-Lustig E, Itin A, Jung S, et al. VEGF-induced adult neovascularization: recruitment, retention, and role of accessory cells. Cell. 2006;124(1):175-89.

123. Rolland-Turner M, Goretti E, Bousquenaud M, Leonard F, Nicolas C, Zhang L, et al. Adenosine stimulates the migration of human endothelial progenitor cells. Role of CXCR4 and microRNA-150. PloS one. 2013;8(1):e54135.

124. Tano N, Kim HW, Ashraf M. microRNA-150 regulates mobilization and migration of bone marrow-derived mononuclear cells by targeting Cxcr4. PloS one. 2011;6(10):e23114.

125. Qu K, Wang Z, Lin XL, Zhang K, He XL, Zhang H. MicroRNAs: Key regulators of endothelial progenitor cell functions. Clinica chimica acta; international journal of clinical chemistry. 2015.

126. Deregibus MC, Cantaluppi V, Calogero R, Lo Iacono M, Tetta C, Biancone L, et al. Endothelial progenitor cell derived microvesicles activate an angiogenic program in endothelial cells by a horizontal transfer of mRNA. Blood. 2007;110(7):2440-8.

127. Cantaluppi V, Biancone L, Figliolini F, Beltramo S, Medica D, Deregibus MC, et al. Microvesicles derived from endothelial progenitor cells enhance neoangiogenesis of human pancreatic islets. Cell transplantation. 2012;21(6):1305-20.

128. Ishizaki T, Tamiya T, Taniguchi K, Morita R, Kato R, Okamoto F, et al. miR126 positively regulates mast cell proliferation and cytokine production through suppressing Spred1. Genes to cells : devoted to molecular & cellular mechanisms. 2011;16(7):803-14.

129. Wakioka T, Sasaki A, Kato R, Shouda T, Matsumoto A, Miyoshi K, et al. Spred is a Sprouty-related suppressor of Ras signalling. Nature. 2001;412(6847):647-51.

130. Cheng CC, Chang SJ, Chueh YN, Huang TS, Huang PH, Cheng SM, et al. Distinct angiogenesis roles and surface markers of early and late endothelial progenitor cells revealed by functional group analyses. BMC genomics. 2013;14:182.

131. Yuan Y, Altalhi WA, Ng JJ, Courtman DW. Derivation of human peripheral blood derived endothelial progenitor cells and the role of osteopontin surface modification and eNOS transfection. Biomaterials. 2013;34(30):7292-301.

132. Zhao T, Li J, Chen AF. MicroRNA-34a induces endothelial progenitor cell senescence and impedes its angiogenesis via suppressing silent information regulator 1. American journal of physiology Endocrinology and metabolism. 2010;299(1):E110-6.

133. Livak KJ, Schmittgen TD. Analysis of relative gene expression data using real-time quantitative PCR and the 2(-Delta Delta C(T)) Method. Methods. 2001;25(4):402-8.

134. Zhang X, Lenburg ME, Spira A. Comparison of nasal epithelial smoking-induced gene expression on Affymetrix Exon 1.0 and Gene 1.0 ST arrays. TheScientificWorldJournal. 2013;2013:951416.

135. Bahar B, O'Doherty JV, Sweeney T. Assessment of RNA integrity in the postmortem pig colonic tissue ex vivo. Journal of animal science. 2012;90 Suppl 4:22-4.

136. Auer H, Newsom DL, Kornacker K. Expression Profiling Using Affymetrix GeneChip Microarrays. Methods Mol Biol. 2009;509:35-46.

137. Fong JE, Le Nihouannen D, Tiedemann K, Sadvakassova G, Barralet JE, Komarova SV. Moderate excess of pyruvate augments osteoclastogenesis. Biology open. 2013;2(4):387-95.

138. Lavoie JR, Ormiston ML, Perez-Iratxeta C, Courtman DW, Jiang B, Ferrer E, et al. Proteomic analysis implicates translationally controlled tumor protein as a novel mediator of occlusive vascular remodeling in pulmonary arterial hypertension. Circulation. 2014;129(21):2125-35.

139. Fujita K, Matsui N, Takahashi Y, Iwasaki Y, Yoshida M, Yuasa T, et al. Increased interleukin-17 in the cerebrospinal fluid in sporadic Creutzfeldt-Jakob disease: a case-control study of rapidly progressive dementia. Journal of neuroinflammation. 2013;10:135.

140. Alvarez-Saavedra M, Antoun G, Yanagiya A, Oliva-Hernandez R, Cornejo-Palma D, Perez-Iratxeta C, et al. miRNA-132 orchestrates chromatin remodeling and translational control of the circadian clock. Human molecular genetics. 2011;20(4):731-51.

141. Kuliszewski MA, Ward MR, Kowalewski JW, Smith AH, Stewart DJ, Kutryk MJ, et al. A direct comparison of endothelial progenitor cell dysfunction in rat metabolic syndrome and diabetes. Atherosclerosis. 2013;226(1):58-66.

142. Wang XX, Zhang FR, Shang YP, Zhu JH, Xie XD, Tao QM, et al. Transplantation of autologous endothelial progenitor cells may be beneficial in patients with idiopathic pulmonary arterial hypertension: a pilot randomized controlled trial. Journal of the American College of Cardiology. 2007;49(14):1566-71.

143. Zhu JH, Wang XX, Zhang FR, Shang YP, Tao QM, Chen JZ. Safety and efficacy of autologous endothelial progenitor cells transplantation in children with idiopathic pulmonary arterial hypertension: open-label pilot study. Pediatric transplantation. 2008;12(6):650-5.

144. Ladage D, Brixius K, Steingen C, Mehlhorn U, Schwinger RH, Bloch W, et al. Mesenchymal stem cells induce endothelial activation via paracine mechanisms. Endothelium : journal of endothelial cell research. 2007;14(2):53-63.

145. Gnecchi M, He H, Liang OD, Melo LG, Morello F, Mu H, et al. Paracrine action accounts for marked protection of ischemic heart by Akt-modified mesenchymal stem cells. Nature medicine. 2005;11(4):367-8.

146. Cho HJ, Lee N, Lee JY, Choi YJ, Ii M, Wecker A, et al. Role of host tissues for sustained humoral effects after endothelial progenitor cell transplantation into the ischemic heart. The Journal of experimental medicine. 2007;204(13):3257-69.

147. Yoon CH, Hur J, Park KW, Kim JH, Lee CS, Oh IY, et al. Synergistic neovascularization by mixed transplantation of early endothelial progenitor cells and late outgrowth endothelial cells: the role of angiogenic cytokines and matrix metalloproteinases. Circulation. 2005;112(11):1618-27.

148. Asahara T, Takahashi T, Masuda H, Kalka C, Chen D, Iwaguro H, et al. VEGF contributes to postnatal neovascularization by mobilizing bone marrow-derived endothelial progenitor cells. The EMBO journal. 1999;18(14):3964-72.

149. Takahashi T, Kalka C, Masuda H, Chen D, Silver M, Kearney M, et al. Ischemia- and cytokine-induced mobilization of bone marrow-derived endothelial progenitor cells for neovascularization. Nature medicine. 1999;5(4):434-8.

150. Spring H, Schuler T, Arnold B, Hammerling GJ, Ganss R. Chemokines direct endothelial progenitors into tumor neovessels. Proceedings of the National Academy of Sciences of the United States of America. 2005;102(50):18111-6.

151. Asakage M, Tsuno NH, Kitayama J, Kawai K, Okaji Y, Yazawa K, et al. Early-outgrowth of endothelial progenitor cells can function as antigen-presenting cells. Cancer immunology, immunotherapy : CII. 2006;55(6):708-16.

152. Li Calzi S, Neu MB, Shaw LC, Grant MB. Endothelial progenitor dysfunction in the pathogenesis of diabetic retinopathy: treatment concept to correct diabetes-associated deficits. The EPMA journal. 2010;1(1):88-100.

153. Ward MR, Stewart DJ, Kutryk MJ. Endothelial progenitor cell therapy for the treatment of coronary disease, acute MI, and pulmonary arterial hypertension: current perspectives. Catheterization and cardiovascular interventions : official journal of the Society for Cardiac Angiography & Interventions. 2007;70(7):983-98.

154. Das Gupta M, Fliesser M, Springer J, Breitschopf T, Schlossnagel H, Schmitt AL, et al. Aspergillus fumigatus induces microRNA-132 in human monocytes and dendritic cells. International journal of medical microbiology : IJMM. 2014;304(5-6):592-6.

155. Graff JW, Dickson AM, Clay G, McCaffrey AP, Wilson ME. Identifying functional microRNAs in macrophages with polarized phenotypes. The Journal of biological chemistry. 2012;287(26):21816-25.

156. Chang WY, Lavoie JR, Kwon SY, Chen Z, Manias JL, Behbahani J, et al. Feeder-independent derivation of induced-pluripotent stem cells from peripheral blood endothelial progenitor cells. Stem cell research. 2013;10(2):195-202.

157. Zhang Q, Kandic I, Kutryk MJ. Dysregulation of angiogenesis-related microRNAs in endothelial progenitor cells from patients with coronary artery disease. Biochemical and biophysical research communications. 2010.

158. Goerke SM, Kiefer LS, Stark GB, Simunovic F, Finkenzeller G. miR-126 modulates angiogenic growth parameters of peripheral blood endothelial progenitor cells. Biological chemistry. 2015;396(3):245-52.

159. Bonauer A, Carmona G, Iwasaki M, Mione M, Koyanagi M, Fischer A, et al. MicroRNA-92a controls angiogenesis and functional recovery of ischemic tissues in mice. Science. 2009;324(5935):1710-3.

160. Zhang Z, Vuori K, Reed JC, Ruoslahti E. The alpha 5 beta 1 integrin supports survival of cells on fibronectin and up-regulates Bcl-2 expression. Proceedings of the National Academy of Sciences of the United States of America. 1995;92(13):6161-5.

161. Park H, Huang X, Lu C, Cairo MS, Zhou X. MicroRNA-146a and microRNA-146b regulate human dendritic cell apoptosis and cytokine production by targeting TRAF6 and IRAK1 proteins. The Journal of biological chemistry. 2015;290(5):2831-41.

162. Wang S, Aurora AB, Johnson BA, Qi X, McAnally J, Hill JA, et al. The endothelial-specific microRNA miR-126 governs vascular integrity and angiogenesis. Developmental cell. 2008;15(2):261-71.

163. Nicoli S, Standley C, Walker P, Hurlstone A, Fogarty KE, Lawson ND. MicroRNA-mediated integration of haemodynamics and Vegf signalling during angiogenesis. Nature. 2010;464(7292):1196-200.

164. Penna E, Orso F, Cimino D, Tenaglia E, Lembo A, Quaglino E, et al. microRNA-214 contributes to melanoma tumour progression through suppression of TFAP2C. The EMBO journal. 2011;30(10):1990-2007.

165. O'Connell RM, Zhao JL, Rao DS. MicroRNA function in myeloid biology. Blood. 2011;118(11):2960-9.

166. Tolar J, Wang X, Braunlin E, McElmurry RT, Nakamura Y, Bell S, et al. The host immune response is essential for the beneficial effect of adult stem cells after myocardial ischemia. Experimental hematology. 2007;35(4):682-90.

167. Thum T, Bauersachs J, Poole-Wilson PA, Volk HD, Anker SD. The dying stem cell hypothesis: immune modulation as a novel mechanism for progenitor cell therapy in cardiac muscle. Journal of the American College of Cardiology. 2005;46(10):1799-802.

168. Eigsti RL, Sudan B, Wilson ME, Graff JW. Regulation of activation-associated microRNA accumulation rates during monocyte-to-macrophage differentiation. The Journal of biological chemistry. 2014;289(41):28433-47.

169. Branzei D, Foiani M. The checkpoint response to replication stress. DNA repair. 2009;8(9):1038-46.

170. Bertoli C, Skotheim JM, de Bruin RA. Control of cell cycle transcription during G1 and S phases. Nature reviews Molecular cell biology. 2013;14(8):518-28.

171. Harris TA, Yamakuchi M, Ferlito M, Mendell JT, Lowenstein CJ. MicroRNA-126 regulates endothelial expression of vascular cell adhesion molecule 1. Proceedings of the National Academy of Sciences of the United States of America. 2008;105(5):1516-21.

172. Schober A, Nazari-Jahantigh M, Wei Y, Bidzhekov K, Gremse F, Grommes J, et al. MicroRNA-126-5p promotes endothelial proliferation and limits atherosclerosis by suppressing Dlk1. Nature medicine. 2014;20(4):368-76.

173. Pitzler L, Auler M, Probst K, Frie C, Bergmeier V, Holzer T, et al. miR-126-3p promotes matrix-dependent perivascular cell attachment, migration and intercellular interaction. Stem Cells. 2016.

174. Chen L, Wang J, Wang B, Yang J, Gong Z, Zhao X, et al. MiR-126 inhibits vascular endothelial cell apoptosis through targeting PI3K/Akt signaling. Annals of hematology. 2016;95(3):365-74.

175. Schweitzer CM, van der Schoot CE, Drager AM, van der Valk P, Zevenbergen A, Hooibrink B, et al. Isolation and culture of human bone marrow endothelial cells. Experimental hematology. 1995;23(1):41-8.

176. George F, Brisson C, Poncelet P, Laurent JC, Massot O, Arnoux D, et al. Rapid isolation of human endothelial cells from whole blood using S-Endo1 monoclonal antibody coupled to immuno-magnetic beads: demonstration of endothelial injury after angioplasty. Thrombosis and haemostasis. 1992;67(1):147-53.

177. Stopp S, Bornhauser M, Ugarte F, Wobus M, Kuhn M, Brenner S, et al. Expression of the melanoma cell adhesion molecule in human mesenchymal stromal cells regulates proliferation, differentiation, and maintenance of hematopoietic stem and progenitor cells. Haematologica. 2013;98(4):505-13.

178. Kebir A, Harhouri K, Guillet B, Liu JW, Foucault-Bertaud A, Lamy E, et al. CD146 short isoform increases the proangiogenic potential of endothelial progenitor cells in vitro and in vivo. Circulation research. 2010;107(1):66-75.

179. Delorme B, Basire A, Gentile C, Sabatier F, Monsonis F, Desouches C, et al. Presence of endothelial progenitor cells, distinct from mature endothelial cells, within human CD146+ blood cells. Thrombosis and haemostasis. 2005;94(6):1270-9.

180. Yoder MC. Endothelial progenitor cell: a blood cell by many other names may serve similar functions. J Mol Med (Berl). 2013;91(3):285-95.

181. Chen H, Li L, Wang S, Lei Y, Ge Q, Lv N, et al. Reduced miR-126 expression facilitates angiogenesis of gastric cancer through its regulation on VEGF-A. Oncotarget. 2014;5(23):11873-85.

182. Du C, Lv Z, Cao L, Ding C, Gyabaah OA, Xie H, et al. MiR-126-3p suppresses tumor metastasis and angiogenesis of hepatocellular carcinoma by targeting LRP6 and PIK3R2. Journal of translational medicine. 2014;12:259.

183. Meister J, Schmidt MH. miR-126 and miR-126*: new players in cancer. TheScientificWorldJournal. 2010;10:2090-100.

184. Hill JM, Zalos G, Halcox JP, Schenke WH, Waclawiw MA, Quyyumi AA, et al. Circulating endothelial progenitor cells, vascular function, and cardiovascular risk. N Engl J Med. 2003;348(7):593-600.

185. Chavakis E, Koyanagi M, Dimmeler S. Enhancing the outcome of cell therapy for cardiac repair: progress from bench to bedside and back. Circulation. 2010;121(2):325-35.

186. Najjar F, Alammar M, Bachour M, Al-Massarani G. Circulating endothelial cells as a biomarker in non-small cell lung cancer patients: correlation with clinical outcome. The International journal of biological markers. 2014;29(4):e337-44.

187. Goon PK, Boos CJ, Lip GY. Circulating endothelial cells: markers of vascular dysfunction. Clinical laboratory. 2005;51(9-10):531-8.

188. Khan SS, Solomon MA, McCoy JP, Jr. Detection of circulating endothelial cells and endothelial progenitor cells by flow cytometry. Cytometry Part B, Clinical cytometry. 2005;64(1):1-8.

189. Asosingh K, Aldred MA, Vasanji A, Drazba J, Sharp J, Farver C, et al. Circulating angiogenic precursors in idiopathic pulmonary arterial hypertension. Am J Pathol. 2008;172(3):615-27.

190. Critser PJ, Yoder MC. Endothelial colony-forming cell role in neoangiogenesis and tissue repair. Current opinion in organ transplantation. 2010;15(1):68-72.

191. Hong F, Li Y, Xu Y. Decreased placental miR-126 expression and vascular endothelial growth factor levels in patients with pre-eclampsia. The Journal of international medical research. 2014;42(6):1243-51.